2015

Thermo-Catalytic Upgrading of Pyrolysis Vapors Using Electromagnetic Heating

Pranjali Devidas Muley
Louisiana State University and Agricultural and Mechanical College

THERMO-CATALYTIC UPGRADING OF PYROLYSIS VAPORS USING ELECTROMAGNETIC HEATING

A Dissertation

Submitted to the Graduate Faculty of the
Louisiana State University and
Agricultural and Mechanical College
in partial fulfillment of the
requirements for the degree of
Doctor of Philosophy

in

The Department of Engineering Science

by
Pranjali Devidas Muley
Bachelor of Technology, Dr. Babasaheb Ambedkar Technological University, 2008
December 2015

Acknowledgments

I am thankful to the almighty for his blessings.

Teachers, family and friends have made this journey possible. I owe my success to them. I would like to thank the department of Biological and Agricultural Engineering, Engineering Science and the LSU Graduate School for providing me with this once in a lifetime opportunity. The faculty of this department has provided me with high quality education.

Dr. Dorin Boldor has been a strong and encouraging advisor. He has been extremely supportive throughout the program. He has always given me the freedom to be innovative, irrespective of how naive my ideas were. He has always taken time out of his busy schedule to discuss my research problems. I am thankful to him for being patient whenever I asked him silly questions. Most importantly, he has improved my technical writing skills.

My committee members Dr. Cristina Sabliov, Dr. Cornelis De Hoop, and Dr. Krishnaswamy Nandakumar have been encouraging and have shown faith in me. Dr. Sabliovs grace and confidence have always awed me. Her depth of knowledge and understanding of the subject and of all her willingness to explain concepts in details have helped me throughout my research work. I have been fortunate to have Dr. Nandakumar on my committee. His questions made me think. His simplicity, gesture and attitude towards learning have made a deep impact on me. Dr. De Hoop's suggestions and ideas have always been a great source inspiration. Their time to time priceless inputs have made my work qualitatively better. I owe my gratitude to them.

I would like to thank Dr. Hall for all the encouragement and anecdotes. I am grateful to Dr. Paulo Waltrich for serving as a Dean's representative on my committee. Special thanks to Dr. Klasson, Dr. Lima and Renee Bigner at USDA-ARS for helping me with sample analysis. I extend my gratitude to Jeff at Calligary, Charlie Milan and Mr. Blanchard

(Tommy) of Oceanography, Dr. Cao, Nitin Kumar, Dr. Morikawa at CAMD, Ms. Connie, Diana Coulon, Zhenyu, Zi, Devendra Pakhre for their help during sample analysis. I learned a lot from them. I would like to thank Ms. Donna, Ms. Angie and Mr. Tom for all the help. I thank my lab mates and my friends Charles, Gustavo, Armaan, Mohammad and Candice for helping me with my experiments. I thank all my friends for their love and support.

Last but not the least, I would like to thank my family, for without them this day seems impossible. My wonderful husband, Prasad Kalghatgi for his love and understanding. Discussions with him have always been a learning experience. His well-reasoned opinion on every matter is a reason I respect him so deeply. My parents Dr. Devidas Muley and Mrs. Kalpana Muley for their love and the trust they have shown in me. I extend my gratitude to my dearest mother in law Meera Kalghatgi, for her strength, encouragement and boundless love and my father-in-law Mohan Kalghatgi for showering his love and wisdom on us. Tai and Jiju for making me feel home away from home. You have all inspired me, loved me, cared for me and corrected me. Thank you for everything.

Table of Contents

List of Tables

List of Figures

Abstract

Electromagnetic heating offers several advantages such as rapid heating rates, accurate temperature control and energy efficiency over conventional reactors. The goal of this study was to design an effective and energy efficient catalytic reactor for pyrolysis vapor upgrading. An induction based catalytic reactor was designed for upgrading of pyrolysis vapors. The effect of catalyst bed temperatures (290 °, 330 ° and 370 °C) and biomass to catalyst ratios of 1, 1.5 and 2 was studied. The results were compared to conventional heating reactor. Induction heating reactor performance exceeded that of conventional heater. The biomass to catalyst ratio of 2 in combination with the temperature of 370 °C gave the highest aromatics yield.

A microwave based catalytic reactor was designed for pyrolysis vapor upgrading. Microwave heating had higher product selectivity and energy efficiency compared to conventional and induction heating reactors. Rate of deterioration of catalyst mainly due to coking was lower for microwave heated catalyst. Higher aromatic hydrocarbon yield, lower oxygen content and high heating value value of bio-oil was obtained by microwave heating of catalyst.

A numerical model studying the microwave heating of porous catalyst bed was developed using COMSOL Multiphysics 5.1. The model was validated against the experimental data. The temperature profiles obtained from microwave heating were compared to those obtained from conventional heating. The model was in good agreement with the experimental results. The sample shape, size and position was found to have significant effect on microwave heating of porous catalyst bed.

Chapter 1
Background and Introduction

1.1 Background

In 2011, the total energy consumption of United States alone was 97.7 quads according to Annual Energy Outlook (Outlook et al., 2011). This energy demand is expected to increase to 102.3 quads by 2025. About 80% of this energy is currently derived from fossil fuels. These fossil fuel resources are finite and non-renewable. Consequentially, they cannot be produced in a sufficient time and quantity to meet our growing national energy demands. To meet this increasing demand, and to develop independence from those finite fossil fuels, the need for alternative and renewable energies is apparent. One attractive area of alternative and renewable energy is the conversion of biomass into energy. Biomass is renewable and abundant due to the ample supplies of agricultural and forestry residues as well as the US potential to grow dedicated energy crop. According to the Billion Ton Update (2011), in the United States the annual availability of unused wood residues from both logging residues and thinnings is estimated to be 97 million dry tons (assuming a moderate $ 60 per dry ton at road-side) (Perlack et al., 2011).

Many technologies have been investigated for the purpose of upgrading lignocellulosic biomass into renewable chemicals and fuels since the beginning of the energy crisis in the 1970s (Zhou et al., 2013) even going as far back as the second world war when the Germans and Japanese investigated pyrolysis of coal and wood. These technologies fall within two main methods for the upgrading of biomass to energy: (i) biochemical conversion, such as anaerobic digestion and fermentation, and (ii) thermochemical conversion, such as incineration, gasification, and pyrolysis. Thermochemical conversion technologies are usually preferred for biomass to energy technologies since they are more easily implemented into the current energy infrastructures (Zhang et al., 2010). Among the thermochemical conver-

sion processes, pyrolysis has received considerable attention, not only as a precursor to the combustion and gasification processes, but also as an independent process (McKendry, 2002)

Pyrolysis creates high-energy products with numerous uses, which makes the pyrolysis process energy efficient and self-sustaining. However, since pyrolysis is still in early developmental stages due to technological and economic challenges, more research need to be conducted in order to make pyrolysis competitive with other current renewable energy technologies. Recent studies have explored the unique features of microwave heating as an attempt to resolve the challenges currently associated with pyrolysis (Fernandez et al., 2011).

1.1.1 Overview of Pyrolysis

Biomass pyrolysis is a thermochemical decomposition of biomass at elevated temperatures in the absence of oxygen (Bridgwater et al., 1999). The temperatures of operation vary from 400 $^{\circ}C$ to 1100 $^{\circ}C$ depending on the biomass used, type of pyrolysis and desired products. As the biomass is heated, it is decomposed into volatile vapors, which are then rapidly condensed to form bio-oil. The remaining products are char and non-condensable gases. Each of these pyrolysis products has numerous applications. The char produced can be converted into activated carbon, used a carbon-based catalyst or used as a soil amendment. The excess non-condensable gases are composed of combustible gases such as H_2, CO, C_2H_2, CH_4, etc. These can be redirected to supply the energy to drive the pyrolysis process itself. Finally, the liquid bio-oil can be upgraded via catalysis much like conventional fossil fuel petroleum for use as hydrocarbon fuel or other industrial chemicals (Motasemi and Afzal, 2013).

Liquid bio-oil is the most desirable product of pyrolysis. Bio-oil is the product of the depolymerization and fragmentation of the biomass feedstock components (cellulose, hemicellulose, and lignin) during pyrolysis. It is a complex mixture of different sized (mostly large) organic molecules such as phenols, furans, levoglucosan, and other compounds (Mullen and Boateng, 2010). Nearly all species of oxygenated organics are present in bio-oil including aldehydes, ketones, alcohols, ethers, esters, phenols, and carboxylic acids. The yield and py-

rolysis product characterization are based on feedstock composition and reaction conditions. For example, there is a greater production of non-condensable gases with a higher temperature and longer residence time. Higher production of bio-oil occurs with a high temperature and short residence time and a greater production of char occurs with a low temperature and a short residence time combination (Lam and Chase, 2012). The molecules that compose the bio-oil liquid are highly oxygenated making it difficult to upgrade via simple water removal (Qi et al., 2007)

1.1.2 Bio-oil upgrading

Although bio-oil produced from fast pyrolysis of biomass has a potential to be directly used as a liquid fuel, this fuel has certain limitations such as high viscosity, acidity, high oxygen content etc. The condensate thus produced is thermodynamically unstable. This thermodynamically unstable product tries to attain equilibrium during storage, resulting in polymerization and repolymerization reactions, which leads to an increase in viscosity and a reduction in the heating value of the product (Zhang et al., 2006). Pyrolysis bio-oil also has high oxygen content of about 40% which marks a major difference between pyrolysis fuel and hydrocarbon fuel (which has oxygen content of less than 1%) (Czernik and Bridgwater, 2004). High oxygen content leads to decrease in energy density by 50% compared to HC fuels, it also makes the bio-oil immiscible in HC fuel; (Zhang et al., 2007). Other problems associated with pyrolysis bio-oil are its high acidity, low heating value, high ash content and low stability. An efficient upgrading technique is required to overcome these limitations and make the bio-oil suitable for use as a HC replacement (Zhang et al., 2007).

Some of the most common techniques for bio-oil upgrading are thermo-catalytic cracking, hydrodeoxygentation, emulsification and steam reforming (Zhang et al., 2007). Both thermo-catalytic cracking and hydrodeoxygenation aim to reduce oxygen content of the fuel. Hydrodeoxygenation is performed in pressurized hydrogen or CO conditions and in presence of a catalyst such as Co-Mo over Al_2O_3 (Zhang et al., 2005). Oxygen is removed in the form

of water and carbon dioxide. The reaction in the previously stated study was performed at 360 $^{\circ}C$ and 2 MPa of hydrogen pressure, and the oxygen content was reduced to 3%. NREL researchers carried out hydro catalytic reactions of bio-oil and observed that the conversion was doubled when $NiMo/Al_2O_3$ catalyst was use instead of CoMo/spinel catalyst (Elliott and Neuenschwander, 1997) . However, hydro treatment of bio-oil demands complicated and highly sophisticated instruments which increase the cost of process. Moreover, technical issues such as catalyst deactivation and reactor clogging adds to the already high cost (Zhang et al., 2007).

Another method for upgrading pyrolysis bio-oil is emulsification with diesel. Since bio-oil and hydrocarbon fuel are immiscible, a surfactant is used for the emulsification process. Chiaramonti prepared bio-oil to diesel emulsions by ratio of 25, 50 and 75 wt% and observed that viscosity increased as the amount of bio-oil in the emulsion increased (Chiaramonti et al., 2003). However, the emulsions were more stable than the bio-oil by itself. Ikura et al emulsified lighter bio-oil fractions with diesel using CANMET surfactant with the ratio of 10, 20 and 30 wt%; the viscosity was lower than pure bio-oil but the cost of production was higher (Ikura et al., 2003). Moreover, emulsification does not solve problems such as corrosiveness.

Most recently, catalytic cracking of bio-oil was shown to be of the most effective way to reduce oxygen content of bio-oil (Stefanidis et al., 2013). In this process, pyrolysis vapors produced from thermochemical decomposition of biomass are passed over a heated catalyst bed; the deoxygenation reaction takes place on the catalyst surface, where the higher molecular compounds are broken down to lower molecular hydrocarbons and oxygen is released in the form of water, CO_2, and CO. Adam et al., studied the effect of 3 different catalysts; $Al-MCM-41$, $Cu/Al-MCM-41$ and $Al-MCM-41$ with enlarged pores on bio-oil composition after the upgrading process (Adam et al., 2005). They observed that the composition of bio-oil significantly changed. Levoglucosan was eliminated whereas the yield of furan, aromatics and acetic acid increased. Adjaye and Bakshi studied the effect

of 5 catalysts, namely, HZSM-5, H-Y, H-mordenite, silicate and silica alumina (Adjaye and Bakhshi, 1995). The experiments were carried out at atmospheric pressure and 4 different temperatures, 290 °, 330 °, 370 ° and 410 °C. Highest yield of hydrocarbon was achieved with HZSM-5 catalyst. The reaction pathways drawn by the authors suggest that the bio-oil conversion is a result of two effects, thermal and thermocatalytic. The thermal effect breaks down high molecular weight compounds to lighter fractions and the thermocatalytic effect produces coke, gas and water which leads to increase in composition of aromatic compounds. Aguado et al., studied the effect of in-situ catalytic flash pyrolysis in a conical spouted-bed reactor in the temperature range of 400-500 °C (Aguado et al., 2000). They observed that the use of catalyst resulted in an increase in gas and char yield and a decrease in the liquid yield. Moreover, CO_2 yield decreased and CH_4 yield in the gases increased significantly.

Nyugen et al studied the effect of Faujasite, a zeolite catalyst on biomass pyrolysis at 500 °C (Nguyen et al., 2013). They observed that upgrading of bio-oil vapors produce superior quality fuel compared to in situ catalytic upgrading. The yield of char, water and gas increased and liquid yield decreased, however, the bio-oil formed was richer in aromatic compounds compared to non-upgraded oil. Among the catalyst investigated, Na0.2H0.8-FAU was most effective in oxygen removal. Catalyst based upgrading also reduces aldehydes, ketones and acids, increasing the energy content of the oil. Numerous studies have been performed over the years to study the effect of various catalysts on pyrolysis vapor upgrading with most of them using the 300 °C to 500 °C as the operating temperature range. Zeolites such as HZSM-5 have proved to be one of the most effective catalyst for deoxygenation of bio-oil when operating in the temperature range of 250 °C-400 °C (Adjaye and Bakhshi, 1995). As a general rule, higher operating temperatures result in an increase in the gas yield.

The major disadvantages of catalytic upgrading of pyrolysis bio-oil are non-uniform heating of catalyst in the reactor and the issues associated with the deactivation of catalytic sites via either coke deposition or poisoning (Czernik and Bridgwater, 2004; Zhang et al., 2007).

Cooler temperature zones in catalyst bed cause deposition and repolymerization reaction on the surface of the catalyst which deactivates the catalyst, whereas, hotspots may favor higher gas yield. Moreover, conventional heating methods are not energy efficient, have slower heating and cooling rates and cause temperature gradient. In conventional methods, heat is provided to the catalyst bed using heat carriers such as sand, or using heat exchangers surrounding the catalyst bed. The temperature is maintained by passing cooler fluid, which absorbs excess heat while maintaining a constant catalyst bed temperature. Heat loss during transfer of energy from carrier/heat exchanger to catalyst and to coolant is significant for conventional cooling techniques. RF heating has the potential to overcome many of these issues since RF heating is a has numerous advantages over conventional heating methods such as faster heating rates due to high power densities, higher energy efficiency, and better control of temperature of operation (Tsai et al., 2006a,b).

In the research presented here we explore the application of electromagnetic heating for catalytic upgrading of bio-oil vapors from pyrolysis of biomass. A comparative study of electromagnetic heating and conventional heating is also performed. Quantitative and qualitative analysis of products were performed and process mechanism was investigated. This dissertation is structured in 5 chapters including an introduction chapter 1 and conclusions and future work chapter number 5. Chapter 2, 3, and 4 discuss the following studies.

1.2 Dissertation Layout

Chapter 2. Pyrolysis and upgrading of pinewood sawdust using induction heating reactor: This study explores the effect of induction heating of catalyst for upgrading of pyrolysis vapors using thermo-catalytic technique. A low frequency induction heater was used for pyrolysis of biomass. The vapors thus formed were passed over a hot catalyst bed which was heated in a high frequency induction heater. The bio-oil obtained after condensing the vapors was analyzed both quantitatively and qualitatively. Catalyst, char and gas samples were analyzed. The results were compared with a conventionally heated catalyst bed.

Chapter 3. Thermo-catalytic upgrading of pyrolysis vapors using microwave reactor: Microwave heating is an effective way of heating a material as microwaves impart energy directly to the material. However, factors such as dielectric properties and penetration depth of material, frequency of operation and desired process temperatures play an important role in the geometry and design of a microwave reactor. A 2450 MHz microwave traveling wave applicator was modified to accommodate a catalytic reactor. Experiments were conducted for catalyst to biomass ratio of 2 at three different temperatures (290 °, 330 ° and 370 °C). The qualitative analysis of oil and catalyst was compared with inductively-heated catalyst reactions and conventional heating reactions.

Chapter 4. Numerical modeling of microwave heating of porous catalyst bed: Since microwave heating imparts heat directly to the material under process, it significantly reduces any heat loss as associated with conduction and convection through the media (both under process and ambient). A numerical model was developed using Comsol Multiphysics 5.1 to understand the temperature and flow profiles within a porous catalyst bed when heated with microwave energy and conventional heat source. The model was validated against experimental results and tested for grid independence. The effect of position of catalyst bed, size and shape of catalyst bed on microwave heated catalyst bed was also studied.

Chapter 2
Pyrolysis and Upgrading of Pinewood Sawdust Using Induction Heating Reactor

2.1 Introduction

Research and development in the field of environmental friendly bio-fuel production from renewable resources such as biomass has gained momentum in past few decades due to exhaustion of fossil energy sources and an ever-increasing population with its corresponding ever increasing demand for energy. Among the technologies proposed, thermo-chemical treatment of biomass has gained considerable attention in last few years due to its ability to produce high-energy content fuel, with little or no overall environmental impact. Thermo-chemical conversion involves breaking down of biomass at elevated temperatures, followed eventually by catalytic treatment. Pyrolysis is a thermo-chemical process where dry, ground biomass is heated in the absence of oxygen at elevated temperatures (500-900 $^{\circ}C$) (Bridgwater et al., 1999). The gases thus formed are immediately quenched to obtain bio-oil. This pyrolytic bio-oil is a mixture of water, tar and lighter organic liquid molecules.

Bio-oil produced from fast pyrolysis of biomass is highly unstable in nature. This thermodynamically unstable product tries to attain equilibrium during storage, resulting in polymerization and re-polymerization reactions, which leads to increase in viscosity and reduction in heating value of the product. Other limitations associated with pyrolytic bio-oil are high acidity, oxygen content, and relatively large ash content, making the fuel undesirable. Although the quality and quantity of bio-oil produced depends on biomass type, pyrolysis method generally produces poor quality oil that is highly oxygenated (Zhang et al., 2005, 2007; Bridgwater, 2012). Pyrolysis bio-oil has oxygen content of about 40% which marks

a major difference between pyrolysis fuel and hydrocarbon fuel (which has oxygen content of less than 1%)(Czernik and Bridgwater, 2004). High oxygen content leads to decrease in energy density by 50% compared to HC fuels, it also makes the bio-oil immiscible in HC fuel (Zhang et al., 2007). An efficient bio-oil upgrading technique is required to overcome these limitations (Zhang et al., 2007).

One of the most efficient and cost effective way to reduce oxygen content of bio-oil is by thermo-catalytic cracking (Stefanidis et al., 2013). In this process, pyrolysis vapors produced from thermochemical decomposition of biomass are passed over hot catalyst bed, the de-hydro-oxygenation reaction. Oxygenated bio-oils are decomposed to lighter hydrocarbons over catalysts maintained at high temperatures. Oxygen from bio-oil is removed in the form of water, CO_2 and CO (Mullen and Boateng, 2010).

For in situ upgrading of pyrolysis vapors, rapid and uniform heating of catalyst is crucial for efficiency of the process and to obtain high quality product. If the catalyst bed is not uniformly heated, it may act as a heat sink. Certain unstable components of bio-oil undergo polymerization and condense on the lower temperature regions of the catalyst, thus blocking the active sites, whereas, hotspots may favor higher gas yield. Slow heating of catalyst causes temperature gradient which may lead to catalyst fouling.

Induction heating or RF heating has a potential to overcome these issues since it offers several key features which make it promising as a pyrolysis and catalyst heating source: rapid heating rates, precise temperature control, and energy efficiency (Lucia et al., 2014; Tsai et al., 2006a). Induction heating is a contact less heating method in which an AC power source is used to supply an alternating current to an induction heating coil. Induction heating takes place by two mechanisms: eddy currents and magnetic hysteresis. Eddy currents oppose the applied magnetic field and are the primary source of heat from induction heating; while magnetic hysteresis creates additional heat in ferromagnetic materials. Some studies have explored induction heating for pyrolysis of biomass (Tsai et al., 2006a,b, 2009a,b). However, there has been very little published work on this method, and therefore

this technique needs further study to establish its use and practicality. This study was conducted to test the performance of an induction heating pyrolysis reactors ability to produce bio-oil both with and without a catalytic bed from pine sawdust.

Although induction heating is applied in many industrial fields (furnace, cooking, welding, brazing etc.) those are mostly related to the metal processing. This heating method has not been extensively used in chemical or related industries. Induction heating can be used as an efficient and well controlled heating method for endothermic catalytic reactions such as proposed by (Latifi et al., 2014) that applies induction heating of catalyst in a batch micro reactor. The catalyst was placed in a ceramic crucible with metal rods placed equidistantly inside. The heat was uniformly distributed to the catalyst in shorter time and eliminated hot spots compared to conventional heating reactor (Latifi et al., 2014). Another novel application of induction heater is in the field of pyrolysis. (Tsai et al., 2006b) used a high frequency induction heater to heat a horizontal tubular reactor made of stainless steel. This system was tested at 100 $^{\circ}C$ increments from 400-800 $^{\circ}C$ for four different biomasses, sugarcane bagasse, sewage sludge, Napier grass and coconut shells. The study concludes that optimal yields of greater than 40% could be obtained using temperatures greater than 500 $^{\circ}C$ (Tsai et al., 2006b).

In this study, an induction heating reactor was used for biomass pyrolysis as well as for heating the catalyst bed for catalytic upgrading of pyrolysis vapors. The bio-oil obtained was quantitatively and qualitatively analyzed. The catalyst was also analyzed for its quality and to quantify the coke deposition. The results from inductively heated catalyst bed were compared to conventional heating of catalyst using a heating tape.

2.2 Materials and Methods

2.2.1 Materials

Pine sawdust from scrap wood out of Biological and Agricultural Engineering wood shop at the Louisiana State University Agricultural Center was used for preliminary pyrolysis

experiments. The sawdust was ground and its moisture content was measured **(Figure 2.1)**. Both nitrogen and argon gas was supplied by Air Liquide (Houston, TX). The HZSM-5 catalyst was supplied by Zeolyst International, (PA, USA) and Sigma Aldrich (St. Louis, MO, USA). Pyrolysis and upgrading experiments were conducted in two separate induction heating machines. The biomass was pyrolyzed in a 5 kW RDO induction heater operating at a frequency (frequency range 35-100 kHz) (RDO Induction LLC, Washington, NJ). The reaction tube was a 310-stainless steel tri-clamp tube, which was 419 mm length with inner diameter of 34.4 mm. The system was purged of oxygen using Nitrogen gas at 1 L/m for 20 min. The induction coil used was a ten loop rubber coated copper coil with an overall length of 285 mm and an inner diameter of 59mm. The reaction tube temperature was controlled using a calibrated Omega IR2C series infrared feedback controller (Omega, Stamford, CT) which uses an infrared sensor to monitor the temperature.

Figure 2.1: Pine sawdust biomass for pyrolysis

For upgrading reaction, the catalyst was heated in a 5 kW RDO induction heater operating at higher frequencies (range 135-400 kHz) (RDO Induction LLC, Washington, NJ).

The reaction tube was a 310-stainless steel tri-clamp tube, which was 270 mm length with inner diameter of 25.4 mm. The reaction tube temperature was controlled using a calibrated Raytek M13 series infrared remote temperature sensor (Raytek Corporation 1999-2014) that was coupled with a PID controller (Red Lion Controls Inc. York, PA, USA).

The bio-oil collection system consists of an electrostatic precipitator(ESP) that was built in house and a 500 mL flask suspended in an ice bath. The ESP has a quartz glass frame that is 304.8 mm in length and has an internal diameter of 57 mm with a tapering joint attached to a 24/40 connector that fits inside the glass collector. A 304 L stainless steel hollow cylinder of 152.4 mm length, 50.8 mm internal diameter, and 1.24 mm thick was tightly fitted inside the quartz cylinder. A 304 L stainless steel rod of 0.2 mm thickness was suspended using a rubber stopper (size 13) inside the cylinder such that it was placed at the center of the cylinder **(Figure 2.2)**.

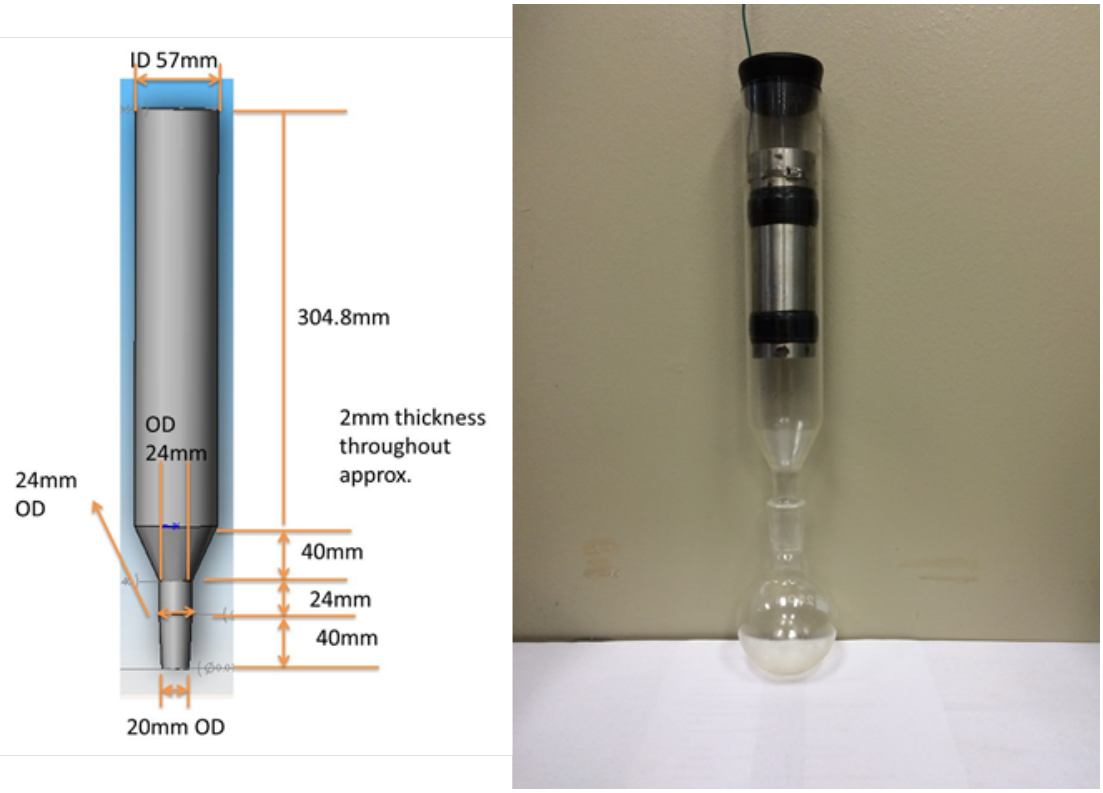

Figure 2.2: Electrostatic precipitator

2.2.2 Procedure

Two sets of experiments were designed and performed. Preliminary experiments were conducted for testing various parameters for pyrolysis in induction heater and setting the basis for secondary upgrading experiments **(Figure 2.3)**. The results from secondary upgrading experiments using induction heater were compared with catalyst heated conventionally.

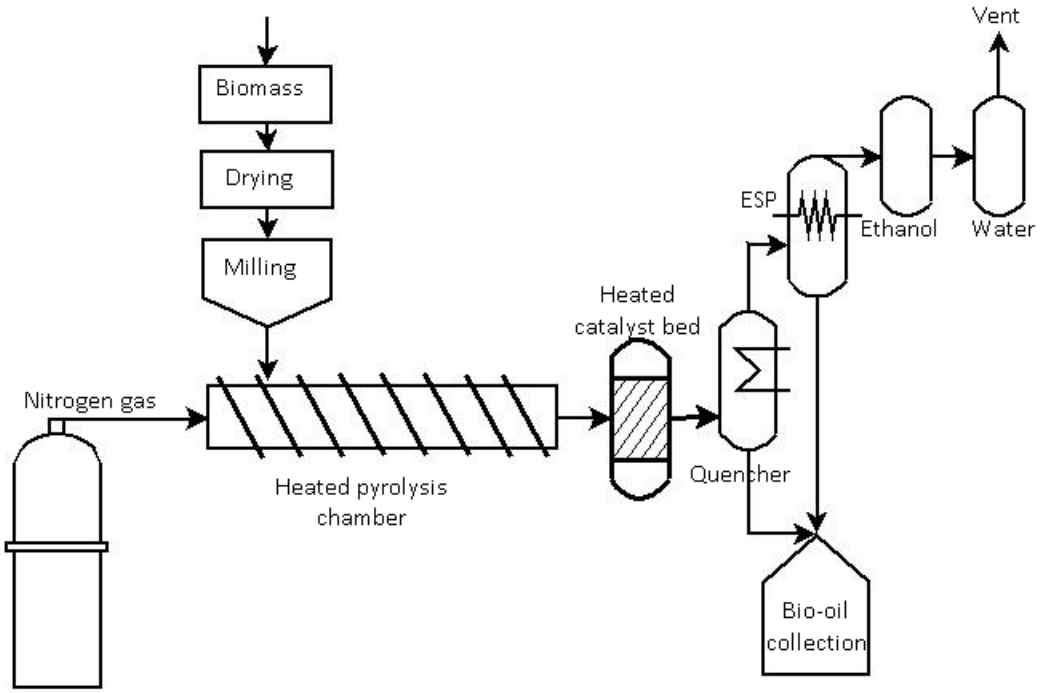

Figure 2.3: Flowchart for pyrolysis upgrading in an induction heater

2.2.2.1 Preliminary experiments

Since the infrared thermocouple measures temperature of the pipe surface, preliminary experiments were conducted in order to determine the true biomass temperature inside the pipe. The pipe was loaded with char from previous runs and the temperature of 500 $^{\circ}C$ was set. Char was used so as to avoid formation of pyrolytic gases at the exit. As soon as the set temperature was achieved, the induction heater was switched off and a regular k-type thermocouple was inserted inside the pipe. The temperature recorded by this k-type thermocouple was recorded using a PicoLog temperature data logger (TC-08 data logger,

Pico Technology, Tyler, TX) and compared to the data from the infrared remote sensor to identify any discrepancies. The difference in the two reading was less that 5 $^{\circ}C$ thus it was assumed for all subsequent experiments that the biomass temperature is same as that of the outside pipe temperature recorded by the infrared remote sensor for the given setup.

Total reaction time at the respective temperatures was determined for the sawdust by performing pyrolysis experiments for different time intervals spanned at 10 min intervals, and weighing the char residue. A 25 g biomass sample was heated in the induction heater at a particular temperature. The temperature was maintained for ten minutes and then the system was allowed to cool down. The weight of the biomass char residue was recorded. This was repeated until the change in weight of the char residue was negligible. The time, at which the char weight remained unchanged from the previous experimental run, was considered as an optimal time required for complete reaction.

2.2.2.2 Pyrolysis of pine sawdust without upgrading

A 30 g of finely grounded sawdust was placed in the induction pyrolysis reactor **(Figure 2.4)**. The system was purged for 20 min with nitrogen gas before heating. Pyrolysis was carried out at five different temperatures from 450 $^{\circ}C$ to 700 $^{\circ}C$ in 50 $^{\circ}C$ increments. The vapors thus produced flowed out of the reaction chamber and into the collection system equipped with the ice bath condensing and electrostatic precipitator.

2.2.2.3 Secondary upgrading experiments

All upgrading experiments were carried out at three different temperatures (290, 330 and 370 $^{\circ}C$) using HZSM-5 catalyst. For catalyst preparation, HZSM-5 catalyst was calcined at 550 $^{\circ}C$ for 5 h, pelletized and broken into smaller particle size. The vapors obtained from reactor 1 (biomass induction pyrolyzer) were passed over HZSM-5 catalyst inside a 25.4 cm ID stainless tube. The tube was heated using the 2nd induction heater. Three catalyst to biomass ratios (C/B) were studied; 1:1, 1:1.5 and 1:2. The same catalyst was

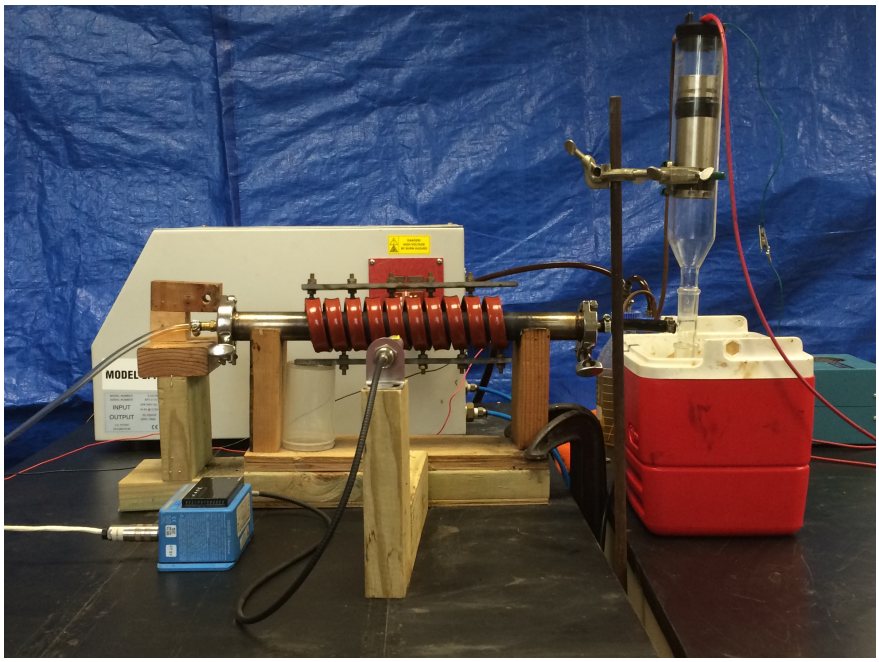

Figure 2.4: Primary pyrolysis experimental setup

used twice for each ratio and temperature combination as two separate experiments to study the extent of deactivation and coke deposition of catalyst. A heating tape was used to maintain the temperature between two induction reactors, so as to avoid inline condensation. The resulting upgraded vapors were condensed in a round bottom flask placed in an ice bath followed by the electrostatic precipitator to collect remaining condensable gases. The system was allowed to cool down for 40-50 min. Liquid was drained in a glass vial, weighed and stored at -20 $°C$ to avoid further polymerization reactions during storage. The incondensable gases were then passed through an ethanol and water trap before being vented **(Figure 2.5)** with samples being collected in gas sample bags. The char and catalyst were also collected, weighed and stored.

The results were compared with conventional catalyst bed heating method using the heating tape wrapped around the tube. Sufficient insulation was provided so as to minimize heat losses. Experiments were carried out for C/B ratio of 1:2 at three different temperatures (290 °, 330 ° and 370 $°C$). Based on the results obtained from induction heating reactor, 1:2 C/B ratio was the most effective, hence, this ratio was chosen for the conventional heating

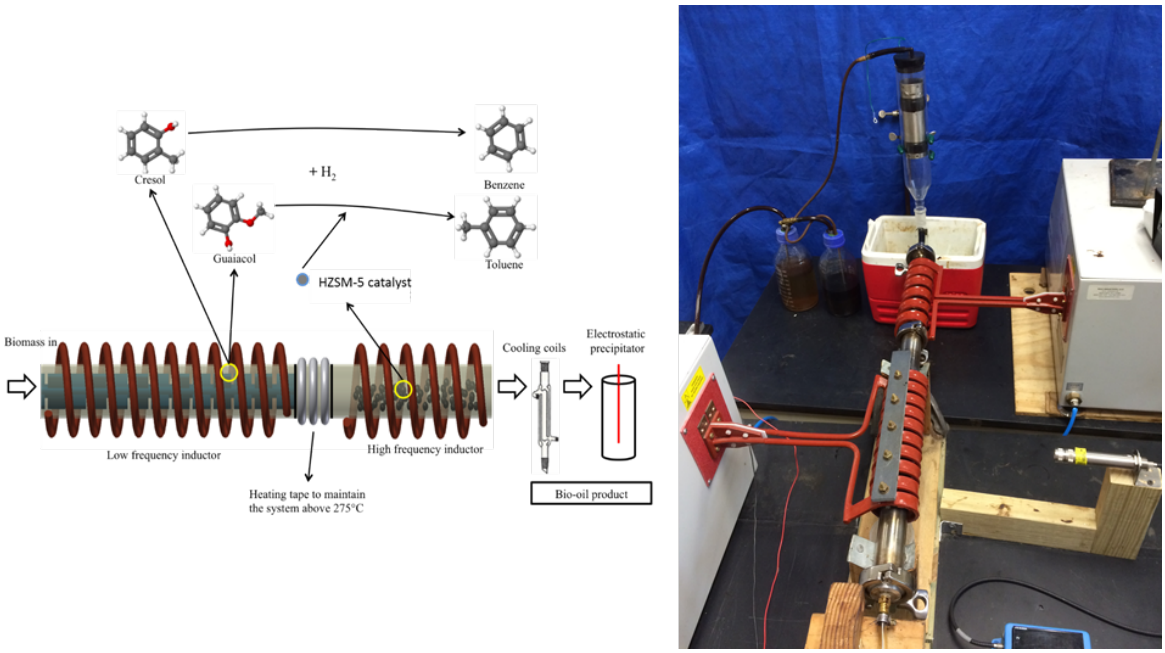

Figure 2.5: Pyrolysis upgrading in induction heater

experiments. The catalyst was rerun in the reactor to study the extent of deactivation. The bio-oil and catalyst quality was compared with the induction heating experiments.

2.2.2.4 Product characterization

Liquid, gas and char yields were quantified for both primary and secondary experiments. Yields were calculated based on initial biomass weight. Oil and char samples were analyzed for CHNO content using Perkin-Elmer 2400 elemental analyzer (Mullen and Boateng, 2010). Karl-Fischer titration was used to determine water content of the pyrolysis bio-oil (Mullen et al., 2010). Gas samples were analyzed for $C_1 - C_5$ and CO_2 and CO composition using a SRI8610c gas chromatograph (SRI Instruments LLC.). Liquid samples were also studied for water content using Karl-Fisher titration, BTEX composition using GC-FID by Shimadzu and BTEX standard, GCMS by Varian 1200 series for product identification. The surface of the catalyst was characterized using different techniques to investigate the extent of coking and deactivation. X-ray diffraction (XRD) was used to determine presence of internal coke in the catalyst using Empyrean X-Ray Diffractometer (PANalytical, Westborough, MA)

(Lin, Fan et al. 2007). X-ray photoelectron spectroscopy (XPS) was used to identify and quantify the different elements present in the catalyst using a Kratos Axis 165 ray photon spectroscope/auger electron spectroscope Operated with Mono-Al Ka X-ray source with beam current at 10 mA and HT at 12 kV. Scanning electron microscope (SEM) images of catalyst were taken both before and after reaction to visualize the changes on catalyst surface using FEI Quanta 3D FEG FIB/SEM dual beam system. Catalyst surface area and pore volumes were measured using BET surface analyzer by NOVA 2200e series Surface area and Pore Size Analyzer using nitrogen adsorption (Quantachrome Instruments Inc.).

Temperature-programmed desorption of ammonia (NH3-TPD) analysis was carried out using Micrometritics 2700 chemisorption apparatus. 0.05 g of prepared sample was loaded in the U-tube, the sample was degasses using He gas at 500 $°C$ for 30 min. The sample was then cooled to 100 $°C$ and ammonia was adsorbed at the flowrate of 5 $°C/min$ from 100 $°C$ to 500 $°C$. TCD signal was recorded (Lee et al., 2012). The coke deposition on catalyst was determined using elemental analyzer CHN (Perkin Elmer series 2400)(Al-Khattaf, D'Agostino et al. 2014). A Fourier transform infrared (FTIR) spectroscopy of catalyst was performed to determine the chemical composition of coke that is deposited on the catalyst surface (Lin et al., 2007).

2.3 Results and Discussion

2.3.1 Biomass properties

Physical and chemical properties of biomass used in pyrolysis has a significant impact on the quality of bio-oil produced (McKendry, 2002). Pinewood sawdust used in our experiments was tested for moisture content determination, elemental analysis to determine carbon, hydrogen and nitrogen (CHN) content, and thermogravimetric analysis (TGA). The moisture content was performed using a Mettler Toledo LD 16, and was determined to be 5.37% $\pm$ 0.12%. Knowing the water content of the biomass is important as it shows partially where water in the liquid product comes from and also as it was shown to act as a stabilizing agent

during the pyrolysis reaction (Demirbas, 2005). The elemental analysis shows the presence of carbon, hydrogen, and nitrogen in the biomass feedstock (section 2.3.4.1). The biomass density obtained from literature was 0.168 g/cm^3 (Briggs, 1994). The TGA of the biomass **(Figure 2.6)** shows the percentage of pine sawdust remaining with respect to change in temperature. This gives a practical idea of which temperature would maximize the biomass decomposition. The majority of the loss of mass occurs at 380 $°C$ and then follows a slight decline until the reaction temperature reaches 800 $°C$. At that temperature the biomass is reduced to its nonreactive ash content. This shows us that a temperature range between 380 - 800 $°C$ allow for the best reduction of biomass, and the range used for the pyrolysis 500 700 $°C$ fits into this range of optimum biomass reduction (Seo et al., 2010).

2.3.2 Pyrolysis yield

Figure 2.6 shows a comparison of gas, char and liquid yield between the non-upgraded and upgraded experiments. All product yields were calculated on mass basis.

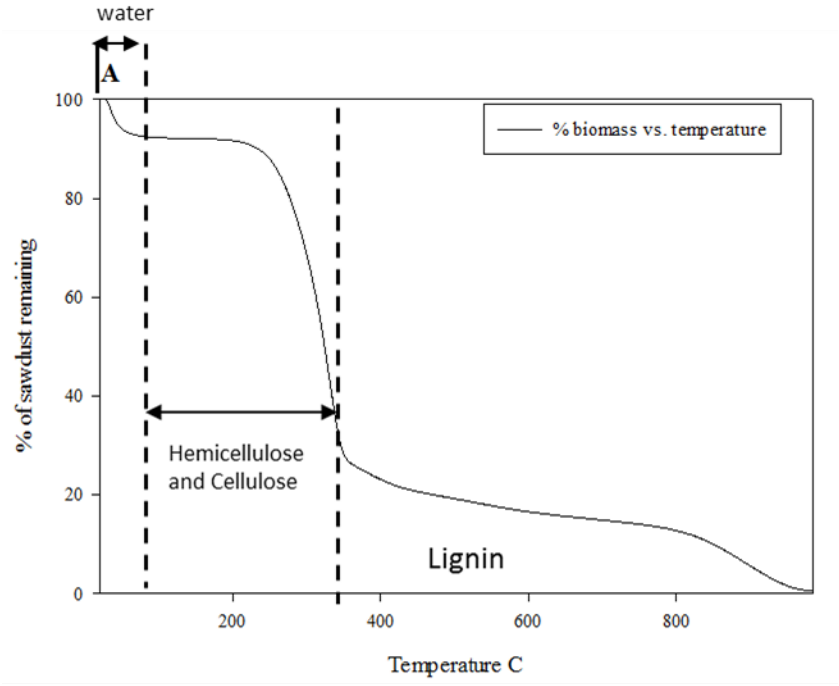

Figure 2.6: TGA analysis showing the loss of mass as temperature rises

2.3.2.1 Non-upgraded bio-oil

The composition of the pyrolysis yields (non-upgraded) followed expected trends shown in numerous works described in literature (Amutio et al., 2012; Bridgwater et al., 1999; Shafizadeh, 1982). Char yields decreased with increased temperatures due to the more complete decomposition of the biomass achieved at higher temperatures. The maximum char yield was 22.86% and it was obtained at the lowest reaction temperature, 500 $^{\circ}C$. The gas yields increased at higher temperatures as a more thorough breakdown of the biomass occurred, yielding lower molecular mass products. The highest gas yield was achieved at 700 $^{\circ}C$ with 28.81% of the biomass converted into non-condensable gases. The liquid yields increased to a maximum and then decreased as the temperature increased, with the maximum yield of 55.28% achieved at 600 $^{\circ}C$ **(Figure 2.7)**.

(Figure 2.7) shows yield of liquid, char, coke and gases for three different ratios of biomass to catalyst namely 1:1, 1:1.5 and 1:2 for three different temperatures 290 °, 330 °, and 370 $^{\circ}C$ respectively. Run 2 represent the experiments with the same catalyst as used in Run 1, without any regeneration. The general observation is that liquid yield decreases when biomass vapors are catalytically upgraded compared to non-upgraded process. The overall decrease in liquid yield was of about 10% when pyrolysis vapors were upgraded over heated catalyst. Liquid yield reduced from 50-55% for no upgrading to 35-45% after catalytic upgrading. It is observed that highest liquid yield was achieved at highest catalyst bed temperature, with maximum yield of 45.43% at 370 $^{\circ}C$ and C/B ratio of 1:1 in run 1. The lowest liquid yield was 27% at 290 $^{\circ}C$ and C/B ratio of 2:1 in run 1. These results were consistent with those reported in the literature (Adjaye and Bakhshi, 1995).

The liquid yield mostly increased when the catalyst was reused for second run with the exception of 330 $^{\circ}C$ C/B with ratio 2 and 370 $^{\circ}C$ with C/B ratio of 1.5. The increase in yield for second run could be due to coke deposition on the catalyst surface partially deactivating the catalyst. This deactivated catalyst does not support the cracking reaction and liquid yield increases which is an observed trend for reactions without catalytic upgrading.

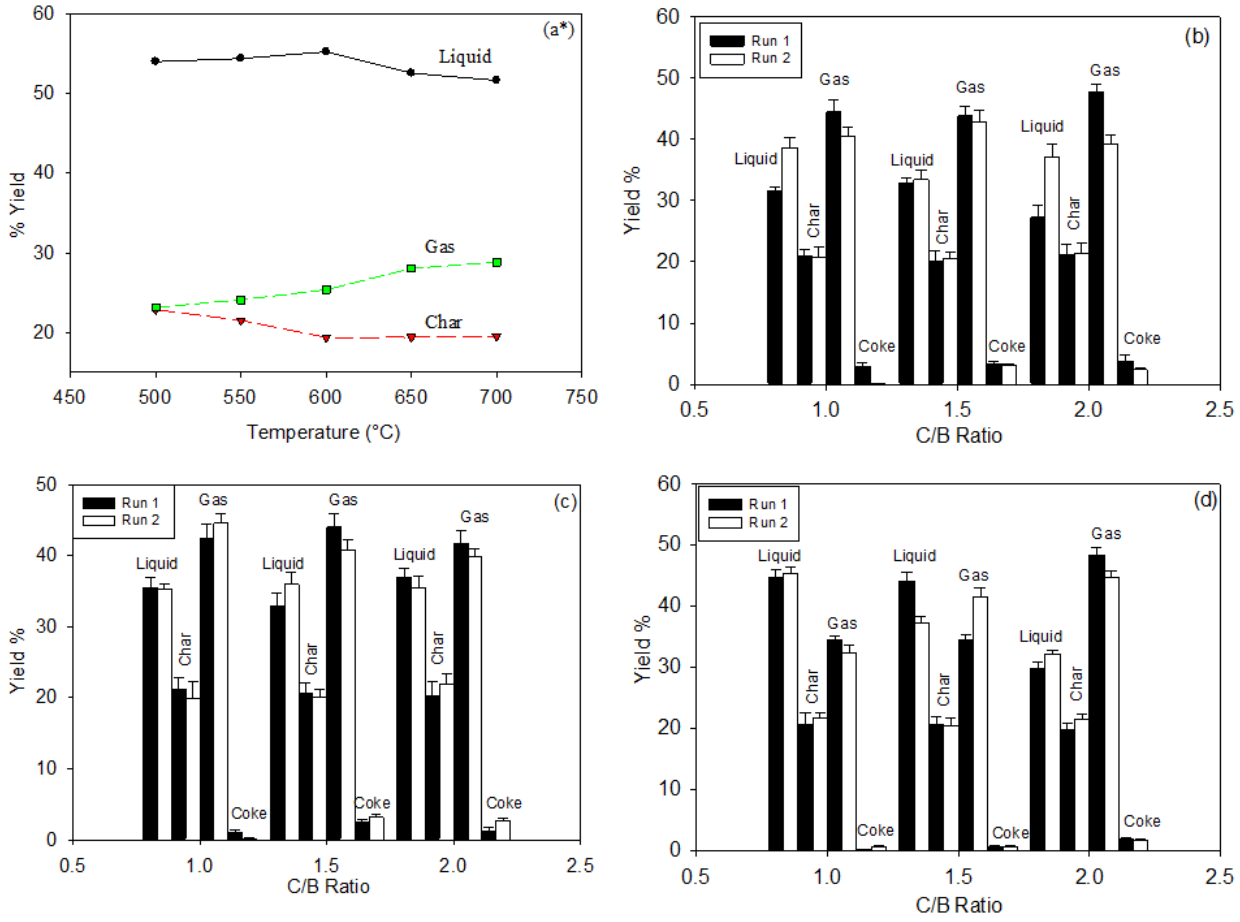

Figure 2.7: Pyrolysis liquid, char, gas and coke yield for (a) without catalyst, (b) 290 $°C$ at different C/B ratio, (c) 330 $°C$ at different C/B ratio and, (d)370 $°C$ at different C/B ratio

2.3.2.2 Upgraded bio-oil

The exception at 370 $°C$ with C/B ratio of 1.5 is rather significant, however the reason is unknown. Liquid yield also decreases as C/B ratio increases at all temperatures. For a higher catalyst to biomass ratio, high molecular weight compounds are broken down to lower fractions and gases more often as more catalyst surface is available for reaction. This also explains the increase in gas yield with increasing C/B ratio. The coke yield was measured from the difference in initial and final weight of catalyst after each run and was consistent with the elemental analysis of catalyst which is discussed elsewhere in this paper (section 2.2 product characterization). Highest coke deposition was observed at highest C/B ratio and

lowest temperature. No significant change in bio-oil yield was observed when the catalyst bed was heated using conventional heating and induction heater.

2.3.3 Water content of bio-oil

2.3.3.1 Non-upgraded bio-oil

Figure 2.8 compares the organic fraction and the water fraction found in the liquid product. The amount of water found in the liquid bio-oil product is consistently between 40-55% for all samples, the lowest water percentage of 32.23% occurring at 700 $°C$ **Figure 2.8,d**; this indicates that while the overall liquid yield may be lower at the higher pyrolysis temperatures the quality of the oil may be slightly improved (Henkel, 2014).

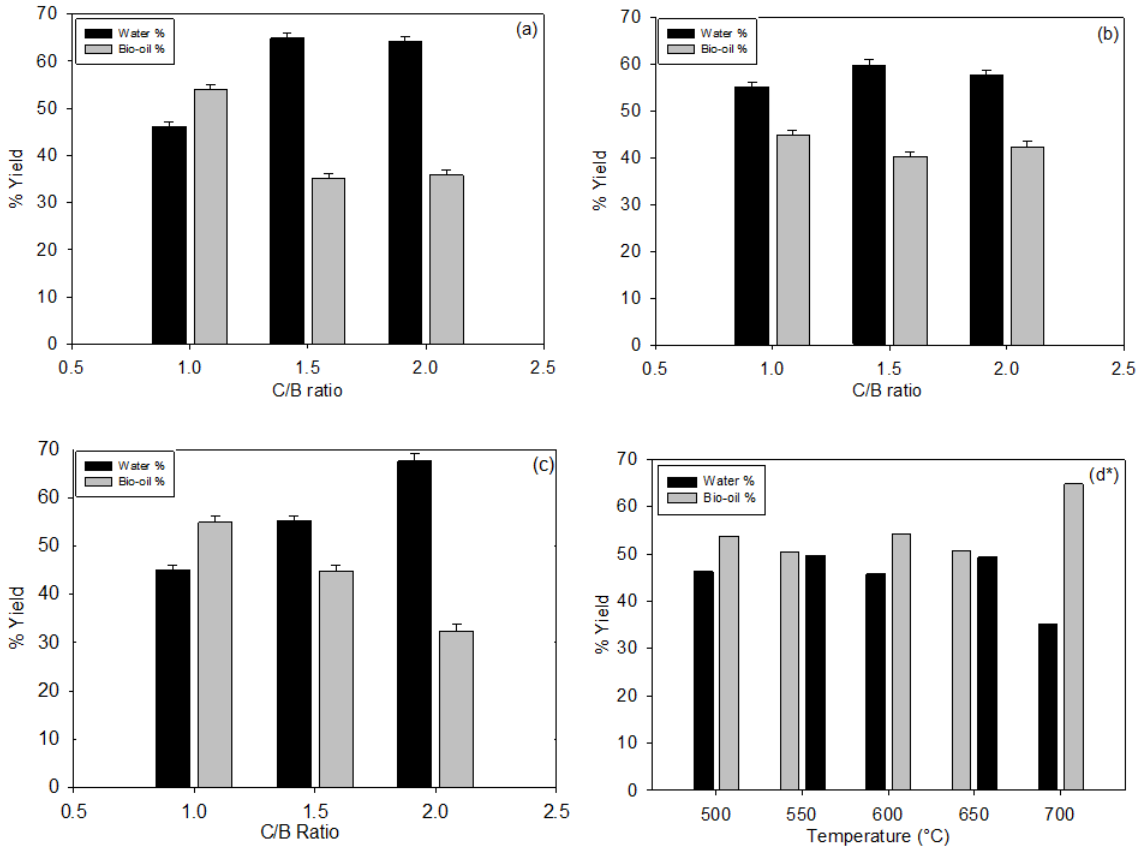

Figure 2.8: Water content and bio-oil yield from pinewood sawdust at (a) 290 $°C$ at different C/B ratio, (b) 330 $°C$ at different C/B ratio and, (c)370 $°C$ at different C/B ratio and,(d) without catalyst

2.3.3.2 Upgraded bio-oil

Catalytic upgrading removes oxygen in the form of water, carbon dioxide and carbon monoxide, which is why water content of upgraded bio-oil is higher than that of non-upgraded bio-oil (Adjaye and Bakhshi, 1995). Amount of water increased as catalyst amount increased for all temperatures as expected, as more oxygen was removed in the form of water. No specific trend was observed between different temperature ranges. The increase in water content for upgraded bio-oil was about 15-20% compared to non-upgraded bio-oil, depending on the catalyst amount. The difference in water content of liquid fraction for the two type of catalyst heating methods, namely, conventional heating and induction heating was less than 5% concluding that neither liquid yield nor water content was significantly affected when the method of heating the catalyst was changed heater.

2.3.4 Elemental analysis

2.3.4.1 Sawdust and char

An elemental analysis was performed on the sawdust and char samples of the pyrolysis reactions. The percent of carbon, hydrogen, and nitrogen were studied **(Table 2.1)**. Nitrogen values were negligible for all samples. Carbon content increased from 46.63% for pure sawdust to 81-86% for char depending on the reaction temperature, whereas, hydrogen content decreased from 6.43% for unpyrolyzed sawdust to 1.89% for char at 700 $^{\circ}C$ pyrolysis temperature. Hydrogen values for char decreased as the pyrolysis temperature increased. The carbon content for char increased with an increase in temperature. This is an indication that the biomass was more thoroughly reduced at the higher temperatures (Ronsse et al., 2013) that is also supported by the char yield data. The pyrolysis reaction itself is a series of reactions that leave behind an increasingly condensed carbon matrix (Ronsse et al., 2013). The removal of the more reactive hydrogen was increased at the higher temperatures, while the more stable carbon was left un-volatized in the absence of oxygen (Henkel, 2014).

Table 2.1: The CHN composition of the char product of the non-catalyzed pyrolysis reaction and the unburned biomass

Reaction Temperature °C	% Carbon	% Hydrogen	% Nitrogen
Unpyrolyzed Sawdust	46.63	6.43	0.20
500	81.19	3.50	0.34
550	86.00	3.09	0.37
600	88.50	2.44	0.53
650	89.70	2.01	0.75
700	88.52	1.89	1.46

2.3.4.2 Non-upgraded bio-oil

Figure 2.9,a shows carbon, hydrogen and oxygen (CHO) content for bio-oil without catalyst treatment. The carbon-content of the bio-oil yield shows little relation to temperature, which could be attributed to the variation in the water content and volatility of bio-oil samples (Henkel, 2014).

2.3.4.3 Upgraded bio-oil

Figure 2.9,b, c, and d also show C, H and O analysis of upgraded bio-oil samples. The oxygen content of bio-oil was reduced from 45-60 % to 25-30 % for almost all temperature and C/B ratio combinations. Some discrepancies could be due to machine error, or error due to mass changes. Many compounds in the bio-oil tend to volatize at room temperature; this fact made it rather difficult to maintain a constant weight for carbon, elemental analysis. A general trend was observed whereby oxygen content decreased as C/B ratio increased. No specific relation was observed with respect to temperature or heating method heater.

2.3.5 Product composition

Gas chromatography was used for identifying the product composition of the bio-oil using integration of area under corresponding peaks. Non-upgraded bio-oil was mostly composed of phenols and aldehydes with some concentration of ketones, alcohols and acids with aromatic

compounds detected in insignificant amounts (Henkel, 2014). This is a typical observation for bio-oil obtained from pyrolysis of biomass. This bio-oil is generally rich in oxygenated hydrocarbons such as phenols (Adjaye and Bakhshi, 1995; Mullen et al., 2010). A clear distinction in the quality of bio-oil through its color can be seen in **Figure 2.10**.

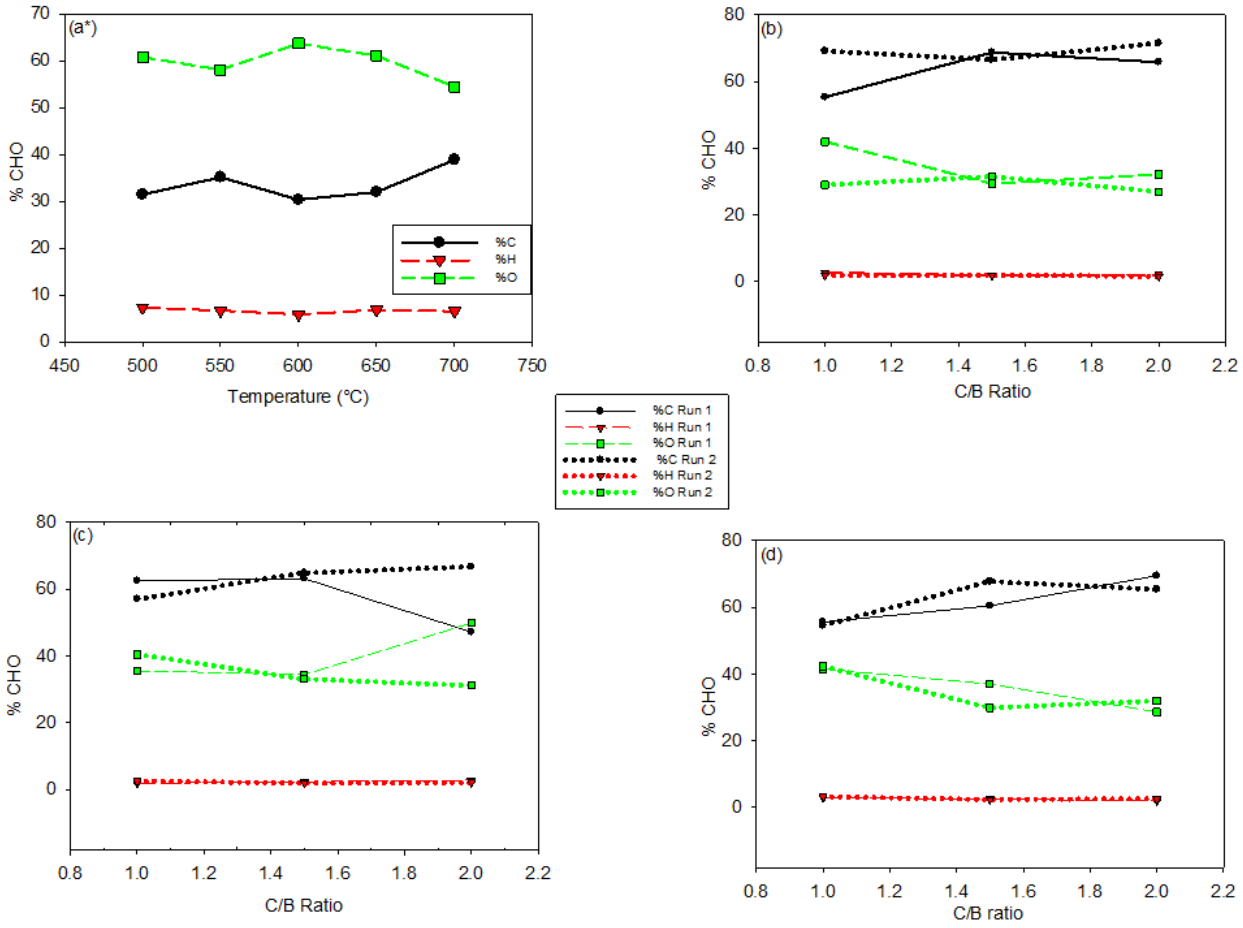

Figure 2.9: Change in % Carbon, Hydrogen and Oxygen for(a) untreated bio-oil, (b) 290 $°C$, (c) 330 $°C$ and, (d)370 $°C$

Use of catalyst produces higher yield of non-oxygenated hydrocarbons such as aromatic hydrocarbons (C5-C10). These hydrocarbons have higher octane number (comparative to those of petroleum fuel) and are of interest for fuel replacement and additives. Moreover, about 32.02% aromatic yield is obtained for induction heated catalyst, whereas for conventional heated catalyst, the aromatic yield was 25%, indicating superior upgrading performance of the inductively heated catalyst **(Table 2.2)**.

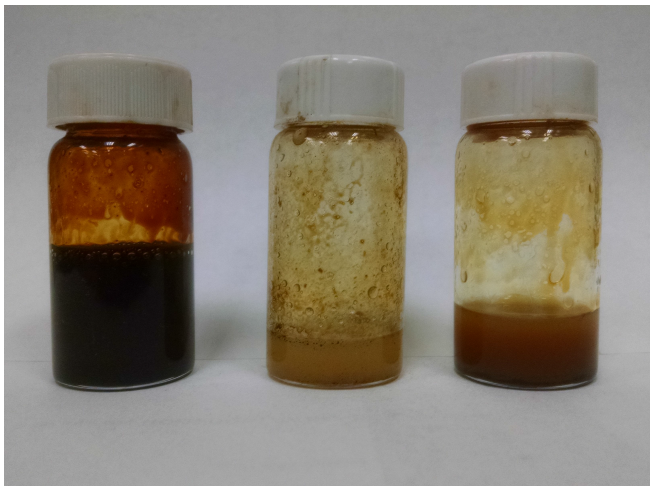

Figure 2.10: Oil sample after pyrolysis for (a) non-upgraded, (b) inductively heated and, (c) conventionally heated catalyst bed

Table 2.2: Product composition and yield for pyrolysis bio-oil with and without upgrading

Compound Group	Without Catalyst		Inductively Heated Catalyst		Conventionally Heated Catalyst	
	Composition	Yield	Composition	Yield	Composition	Yield
Ketones	9.78	3.36	2.79	1.26	0.928	0.292
Aldehydes	13.60	4.67	5.56	2.50	1.55	0.487
Alcohols	3.03	1.04	5.76	2.59	0.56	0.176
Acids	1.38	0.47	1.08	0.49	4.35	1.368
Phenols	53.41	18.33	30.45	13.70	33.1	10.41
Other	8.34	2.86	7.54	3.39	12.5	3.932
Aromatics	-	-	32.02	14.41	25.01	7.868
Benzene	-	-	11.03	4.96	-	-
Methylbenzene	-	-	0.36	0.16	4.05	1.274
Ethyl-benzene	-	-	0.32	0.14	0.684	0.215
Xylenes	4.49	2.02	7.92	2.49	-	-
C9-C10	-	-	14.54	6.54	12.356	3.887
Naphthalenes	-	12.06	5.43	10.4	3.271	-
Olefins	-	0.25	0.11	-	-	-
Unidentified	10.46	0.04	3.77	1.70	11.602	0.06

2.3.6 Catalyst analysis

Since C/B ratio of 2 gave highest yield for aromatic compounds, this set was chosen for analysis. A total of 12 catalyst samples from pinewood sawdust pyrolysis upgrading with C/B ratio of 2 were analyzed. The catalysts in the reactor were heated at three different temperatures; 290 $°C$, 330$°C$ and 370 $°C$. The catalyst samples for run were fresh catalysts, which were reused for the subsequent rerun in run 2. Pure HZSM-5 was also analyzed for comparison. Catalyst heated with conventional heating method was also analyzed for comparison for the same reaction setup.

2.3.6.1 X-Ray diffraction (XRD) analysis

XRD analysis was performed on the catalyst samples to determine if the coke deposition was present inside the catalyst. XRD patterns of coked catalyst were compared to the fresh catalyst. **Figure 2.11** shows XRD pattern for fresh and coked catalyst in the 2θ range of 22-25. The peak for used samples shifted slightly to the left, with the difference in angle being about 0.2. Two adjoining peaks were observed for fresh HZSM-5 at 2θ of 23.5 and 23.7, respectively. These peaks were observed with lower intensity for catalyst samples heated at 290 $°C$ but were not observed for 330 $°C$ and 370 $°C$ samples. An increase in intensity was also observed for all coked catalysts compared to fresh HZSM-5 especially for 330 $°C$ run 2 and 370 $°C$ run 2. Change in peak position was also observed for coked catalyst with peaks at 2θ of 24.3 and 24.7 for fresh catalyst. This change in intensity and position of subsequent peaks is a result of carbon deposition into the catalyst pores, which causes distortion of zeolite lattice structure (Lin et al., 2007).

2.3.6.2 FTIR analysis

In order to study the chemical nature of coke, FTIR analysis of both fresh HZSM-5 and used catalyst was undertaken **(Figure 2.12)**. FTIR analysis is used to study surface chemistry and reactivity of a catalyst. With coke deposited on the surface, FTIR spectra helps deter-

mine the type of carbon bonds in a certain range of wavenumber. Although the wavenumber range studied was 0 to 3500 cm^{-1}, only 1200-3200 cm^{-1} is shown in as it is the most relevant.

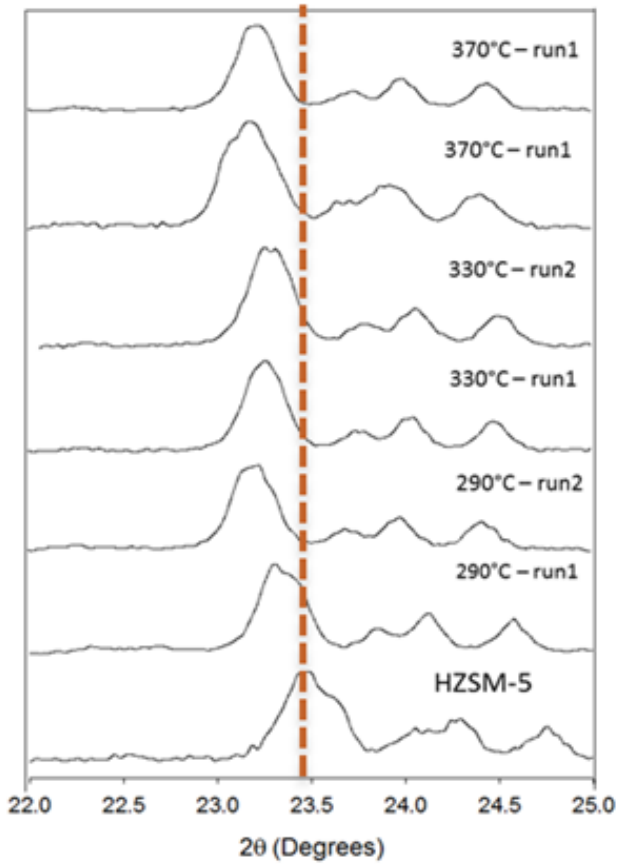

Figure 2.11: XRD pattern for fresh and coked catalyst

Three important bands between 2800 cm^{-1} and 3000 cm^{-1} corresponding to aliphatic compounds $\equiv CH$, $= CH_2$ and $-CH_3$ were observed for all catalyst samples except for the fresh catalyst. The dip is especially sharp for reused catalyst samples at all temperatures **(Figure 2.12)**.

The decrease in intensities for each reused sample could be because the coke turns polyaromatic in nature (Paweewan et al., 1999). With time, the coke becomes more hydrogen deficient that changes its nature from aliphatic to aromatic or polyaromatic. Another sharper dip around 1600 and 1700 cm^{-1} is observed for catalyst samples at 290 $^{\circ}C$ run 1 for both inductively heated and conventionally heated catalyst but is missing from HZSM-5. This is

another characteristic coke band which indicates the presence of polyalkalene or polyaromatic compounds (Lin et al., 2007).

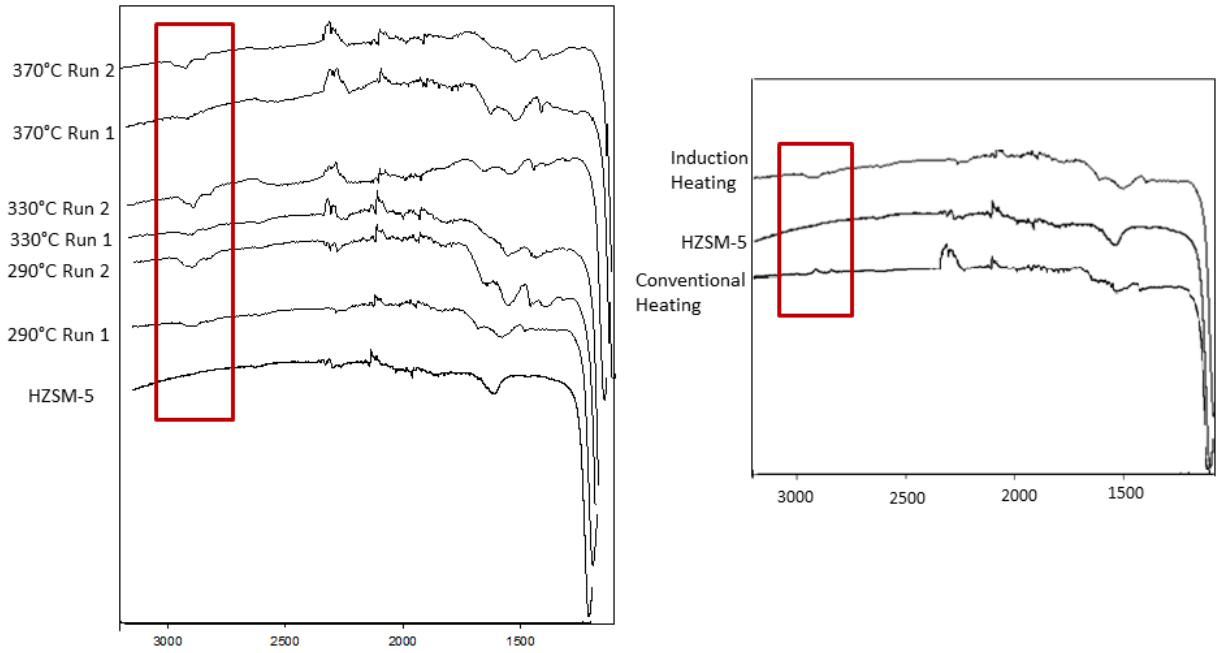

Figure 2.12: FTIR analysis of fresh and coked catalyst

2.3.6.3 Elemental analysis

Elemental analysis was also performed on the catalyst to quantify the carbon, hydrogen, nitrogen, and sulphur (CHNS) content of the samples. All samples were corrected based on CHNS reading from pure HZSM-5 **(Table 2.3)**. The results were consistent with those obtained from XPS. Carbon deposition decreased as upgrading process temperature increased. Higher carbon percent was observed for conventionally heated catalyst (13-20% at 290 $°C$) compared to inductively heated catalyst (7-12% at 330 $°C$). Hydrogen, nitrogen and sulphur values were negligible. These results highlight the improved performance of the inductively heated catalyst over conventional methods.

Table 2.3: Elemental analysis (CHNS) for fresh and coked catalyst

Upgrading Temperature (°C)	Sample	Carbon (%)	Hydrogen (%)	Nitrogen (%)	Sulphur (%)
	HZSM-5	0.2±0.02	0.38±0.09	0.18±0.04	0.00±0.00
Induction Heating					
290°C	Run 1	12.67±0.19	1.09±0.06	0.03±0.00	0.01±0.00
	Run 2	7.89±0.00	0.67±0.11	0.00±0.00	0.00±0.00
330°C	Run 1	5.90±0.08	0.12±0.01	0.1±0.01	0.00±0.00
	Run 2	7.89±0.08	0.30±0.02	0.06±0.00	0.00±0.00
370°C	Run 1	6.12±0.03	0.61±0.01	0.00±0.00	0.00±0.00
	Run 2	6.68±0.02	0.29±0.11	0.13±0.05	0.00±0.00
Conventional Heating					
290°C	Run 1	13.63±0.01	1.98±0.09	0.07±0.00	0.00±0.00
	Run 2	20.25±0.04	1.7±0.10	0.07±0.00	0.00±0.00
330°C	Run 1	13.77±0.38	1.19±0.05	0.06±0.00	0.00±0.00
	Run 2	11.63±0.13	0.7±0.18	0.04±0.01	0.00±0.00
370°C	Run 1	12.83±0.04	0.85±0.09	0.05±0.02	0.00±0.00
	Run 2	8.58±0.05	0.36±0.005	0.03±0.02	0.00±0.00

2.3.6.4 Surface area and pore volume

Table 2.4 shows the surface area and volume for micropores. BET surface area and pore volume of catalyst showed significant decrease in surface area for used catalyst compared to pure HZSM-5 catalyst. Micropore volume also decreased. No specific trend was observed with respect to temperature. The decrease in surface area is consistent with the increase in

coke content of the catalyst. Less surface area is available for Run 2 (reused catalyst) at each temperature. For the temperature of 370 $°C$, more surface area is available when the catalyst is heated using induction heater compared to conventionally heated catalyst.

Table 2.4: BET Surface area and volume of fresh and coked catalyst for C/B ratio of 2:1

Sample	Run no.	BET surface area (m^2/g)	Micropore area (m^2/g)	Micropore volume (cm^3/g)
HZSM-5		247.7	196.4	0.0950
Induction Heating				
290°C	Run1	197.0	0.0	0.00
	Run2	152.5	99.0	0.0490
330°C	Run 1	179.8	120.7	0.0590
	Run 2	25.1	60.0	0.0280
370°C	Run 1	210.7	143.4	0.0700
	Run 2	85.5	156.3	0.0690
Conventional Heating				
370°C	Run 1	177.624	105.203	0.047
	Run 2	91.186	50.00	0.022

2.3.6.5 NH_3-TPD analysis

NH_3-TPD analysis help in determining the extent to which deactivation of catalyst has occurred and helps draw the mechanism of hydrocarbon conversion as the deactivation proceeds. Coking can affect the catalyst activity in two major ways; depending on the nature of the coke deposited on the catalyst, the coke may poison the catalyst. Or coke deposition may simply block the active sites and block the catalyst pores. Ammonia is a smaller sized molecule and can diffuse through smaller pores or partially blocked pores. This NH_3-TPD technique can be useful to determine the effect of coking on the strength of acid sites. Two distinct peaks for fresh HZSM-5 are observed in **Figure 2.13**. The one at lower temperature represents weak acid sites and the one at higher temperature represents strong acid sites. The peak at higher temperature seems to slowly disappear for both samples at 290 $°C$ that means coke deposition occurs mainly on strong acid sites. Weak acid sites are also consumed

but the rate of consumption is lower compared to that of strong acid sites. Slight shift of peak towards left also indicates decrease in the strength of acid sites due to coke deposition.

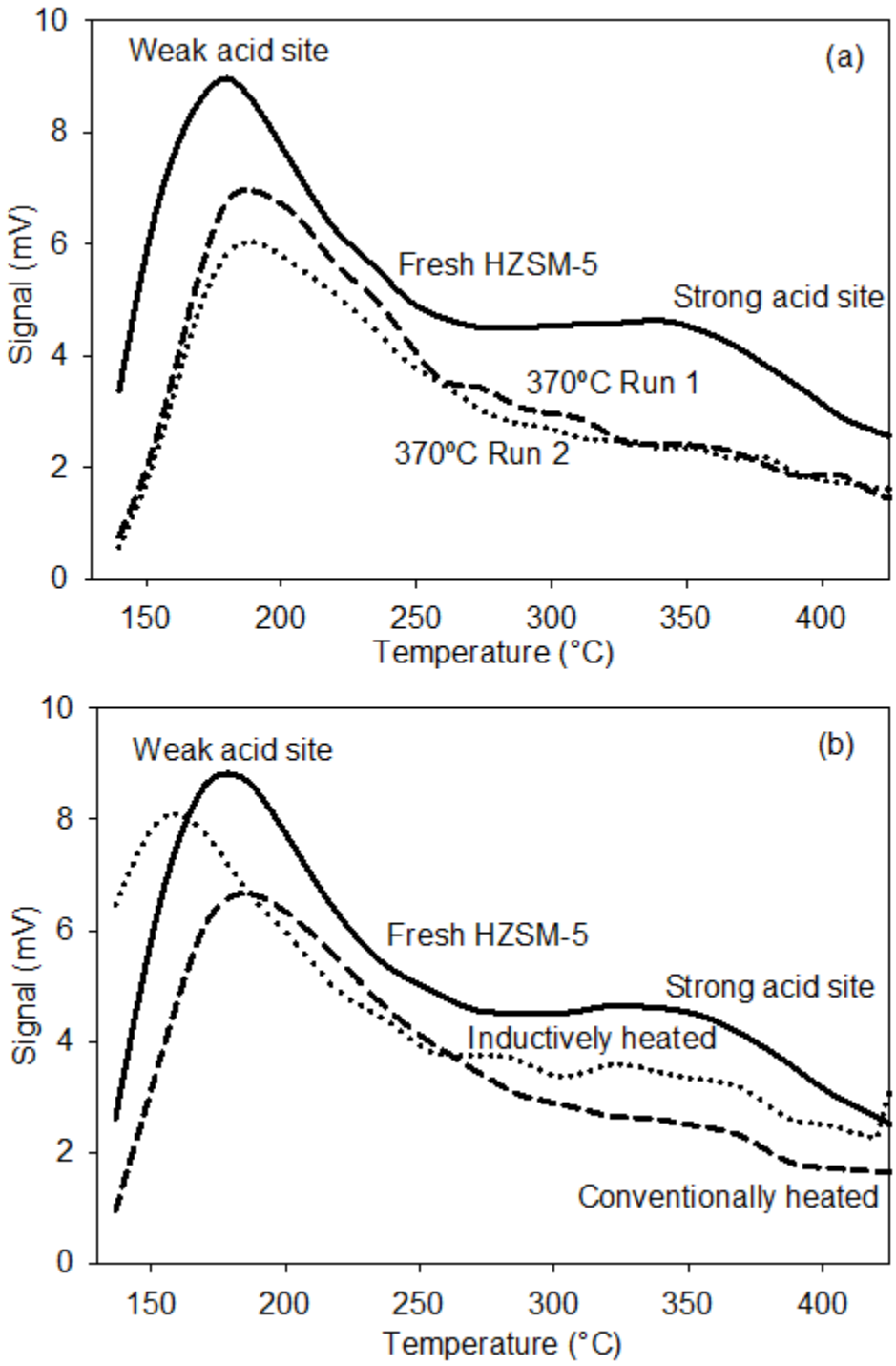

Figure 2.13: NH_3-TPD profile for C/B ratio 2:1 and at 370 $^{\circ}C$ for (a) fresh and inductively heated catalyst , (b) fresh, inductively, and conventionally heated catalyst

The peaks are smaller for reused samples compared to samples from run 1. Overall the higher the coke deposition, the lower the peak area. These results are consistent with other studies reported in the literature for HZSM-5 catalyst behavior in time (Lin et al., 2007). **Figure 2.13** shows the comparison of peak for fresh catalyst to that with conventionally and inductively heated catalyst. Strong acid sites completely disappear for conventionally heated catalyst compared to induction heated catalyst. The weak acid sites also decrease comparitively. These results are consistent with the catalysts aromatization activity. Stronger the acid site, greater is the aromatization and HZSM-5 has higher concentration of strong acid sites (Viswanathan and Pillai, 1992).

2.3.6.6 X-ray photoelectron spectroscopy (XPS) analysis

X-ray photoelectron spectroscopy is a quantitative surface chemical analysis technique that measures the elemental composition of the material (Cimino et al., 1999). All catalyst samples were ground and dried to remove any moisture absorbed. The XPS analysis was represented in Carbon to Silicate ratio (C/Si mass basis). Since the zeolite has a constant Silicate to Aluminum ratio (Si/Al), the amount of silicate does not change. The change in C/Si ratio is only due to occurrence of carbon due to coke deposition on catalyst. The occurrence of carbon peak in XPS measurement is due to coke deposition on the catalyst surface. However, some carbon traces are also observed on pure HZSM-5, which could be due to some cross contamination from other samples. One of the reasons for high amount of carbon obtained on conventionally heated catalyst could be a result of condensation of molecules on the cooler sections of the catalyst surface due to non-uniform heating.

Figure 2.14 shows C/Si ratio for fresh and used catalyst. The C/Si ratio was higher for catalyst heated in conventional heater; also, a higher ratio was observed at lower temperatures. For inductively heated catalyst, the ratio did not vary significantly ($R^2 = 0.9$). Coke formation on acid catalysts like that of HZSM-5 is strongly governed by dehydrogenation, and cracking reactions. These reactions break the long chain polymers to form aromatic

compounds (Appleby et al., 1962). However, at lower temperatures, some organic molecules may condense on the cooler catalyst surface; this phenomenon is more prominent for non-uniformly heated catalyst surface, where the molecules may condense on cooler zones.

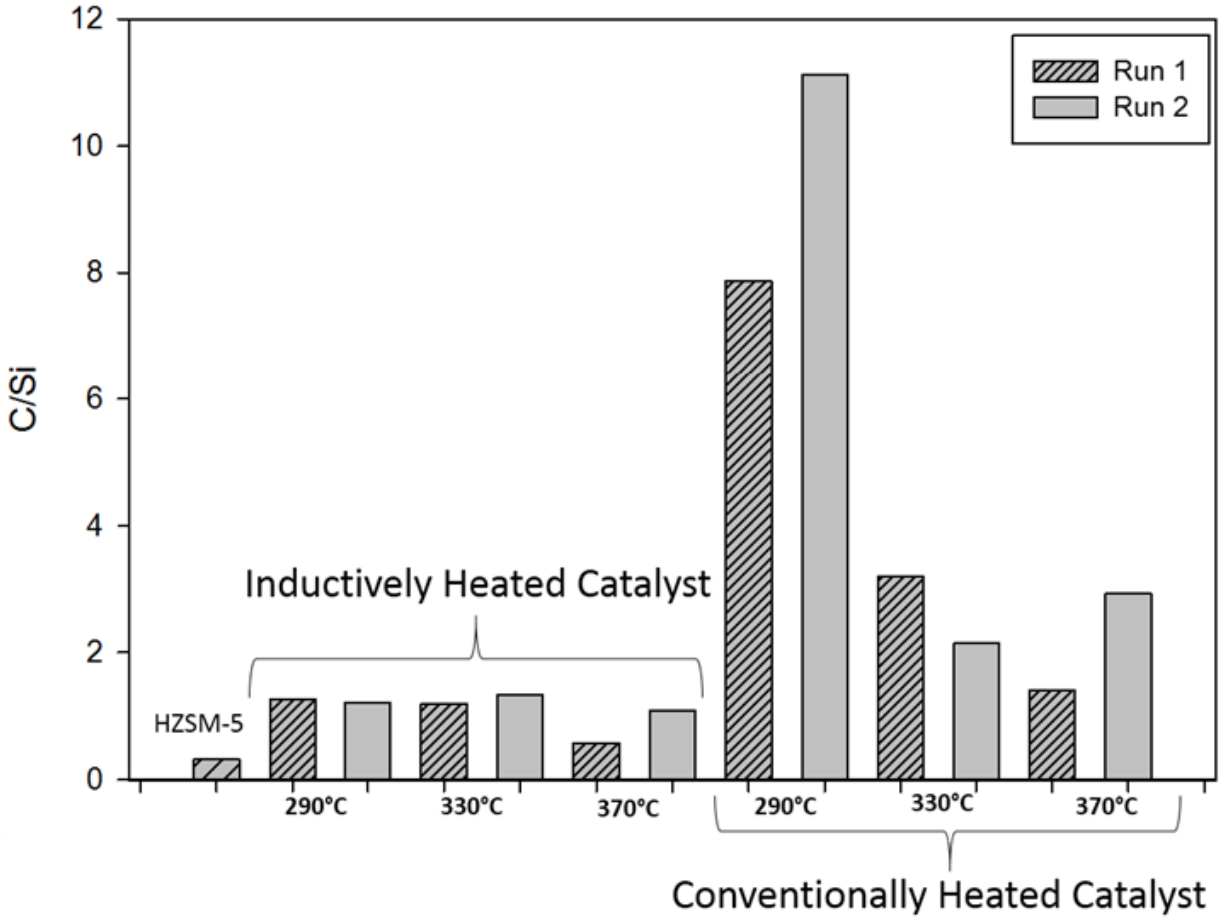

Figure 2.14: C/Si ratio for catalyst samples by XPS analysis

2.3.7 SEM analysis of catalyst

SEM images of fresh and used catalyst surface were acquired at 35,000X magnification **(Figure 2.15)** and **(Figure 2.16)**. A sharp crystalline structure of catalyst is observed for fresh catalyst image **(Figure 2.15)**. The image becomes more granular and loses its crystallinity for inductively heated catalyst at 370 $°C$ (run 1 and run 2). The effect is higher for run 2 corresponding to 370 $°C$ run 2 compared to run 1 as run 2 is a reused catalyst from run 1. This granular structure could be due to coke deposition on the surface

of the catalyst. SEM images were also aquired for fresh catalyst, conventionally heated catalyst and inductively heated catalyst at 10,000X magnification **(Figure 2.16)**. Again, a sharp crystalline structure is observed for fresh catalyst. This crystallinity decreases for the inductively heated catalyst, but does not decrease significantly for conventionally heated catalyst. The catalyst appears more broken for run 2 in each case.

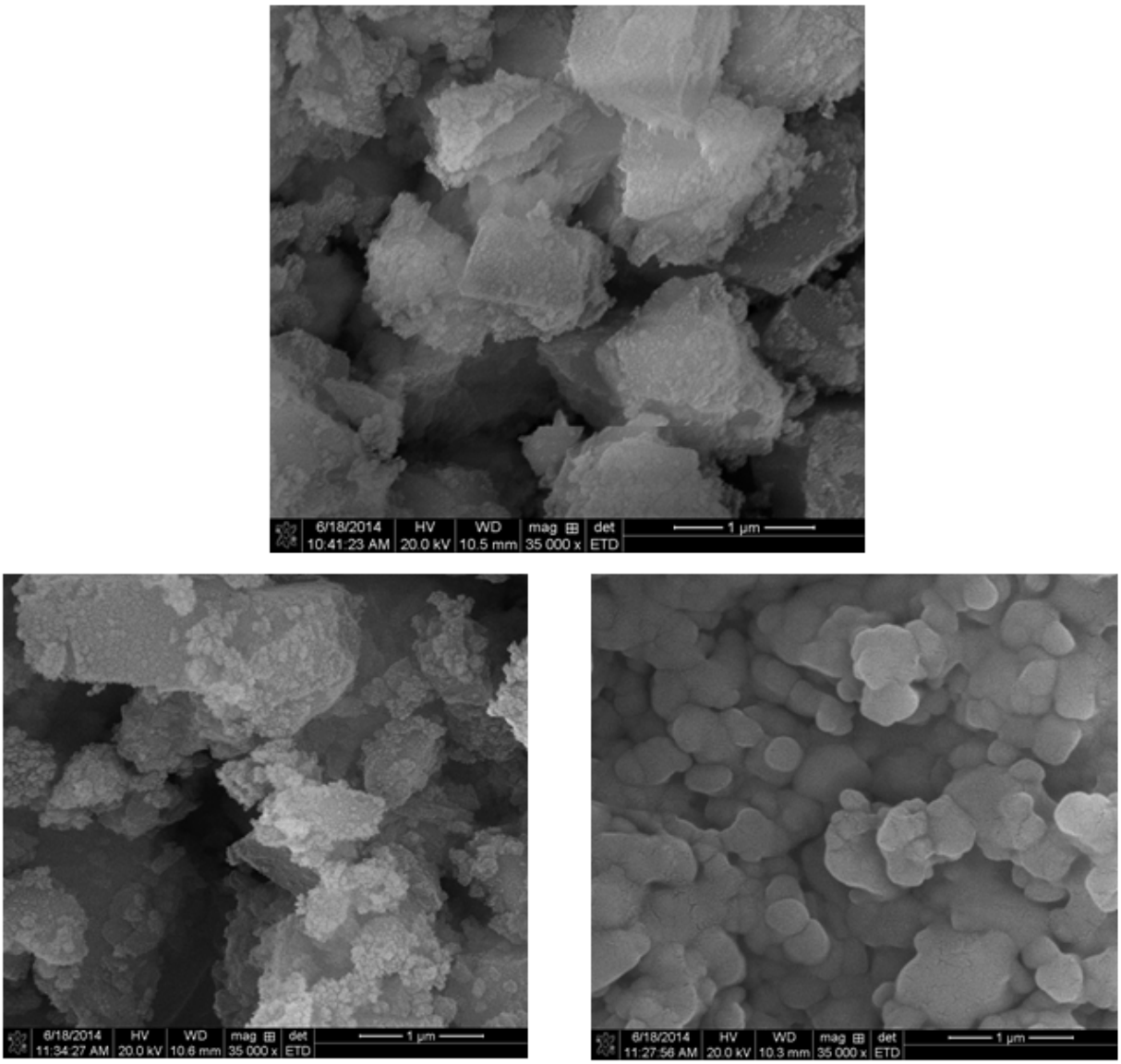

Figure 2.15: SEM images of fresh, and inductively heated catalysts at 370 $^{\circ}C$ at run 1 and run 2

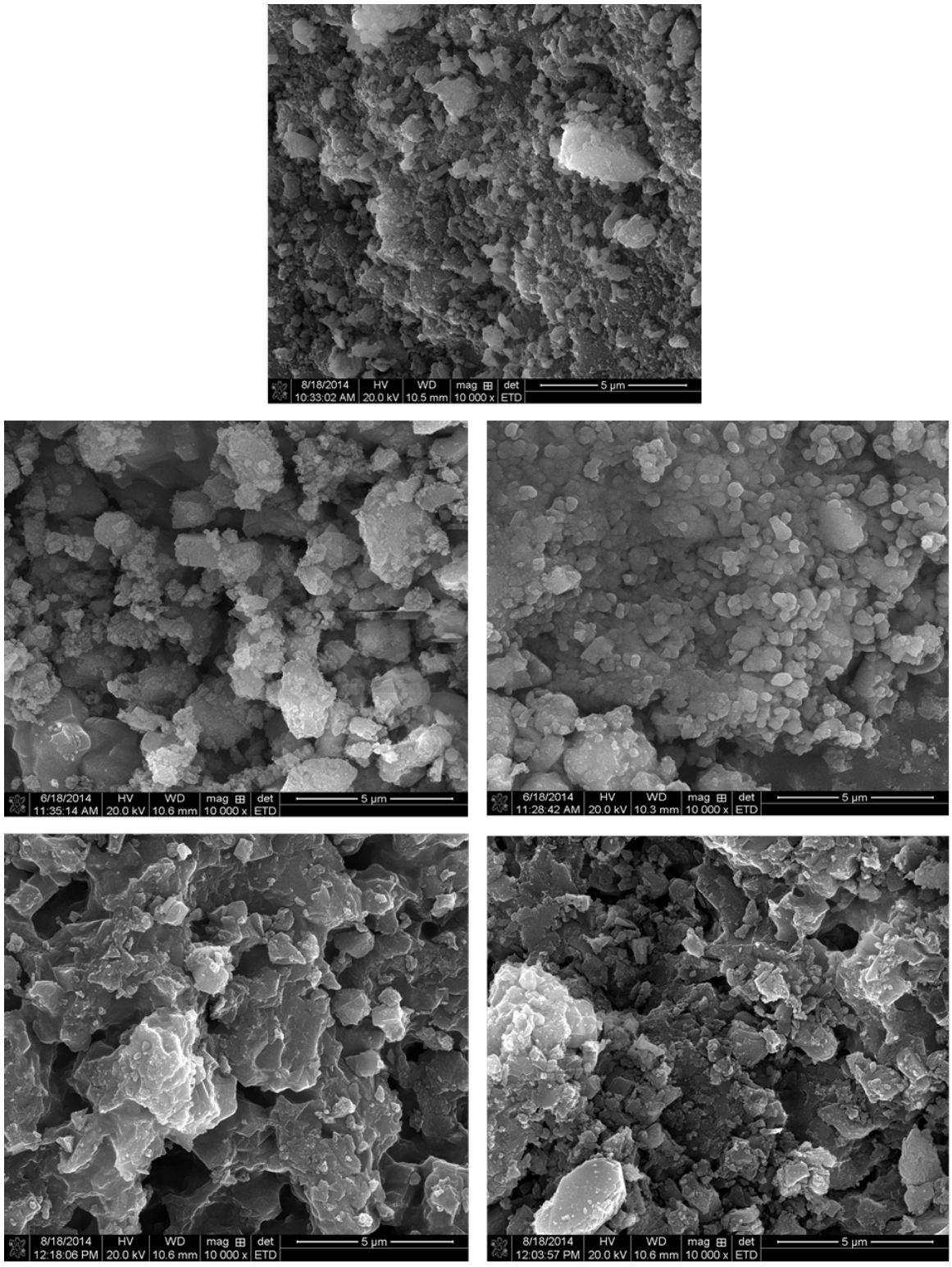

Figure 2.16: SEM images of fresh, and inductively heated catalysts at 370 $^{\circ}C$ at run 1 and run 2

2.3.8 Energy requirement and process scale-up

The induction heater employed for both pyrolysis and upgrading had a maximum power input of $5kW$. To maintain the catalyst bed temperature of 290°, 330 ° and 370 °C, total power input for the heater was 8%, 10% and 14% respectively, corresponding to 400, 500, and 700 W. The total energy input for biomass pyrolysis at 600°C was 24% of $5kW$ corresponding to $1200W$. Induction heating in general has a high efficiency of about 85% compared to other heating techniques, as only 15% of the energy is lost as heat energy to surrounding (Al-Khattaf et al., 2014; Amutio et al., 2012), but these values are listed for insulated systems, which was not the case in these experiments. The associated convective and radiative heat losses are estimated in the following paragraphs. In any case, as indicated by the results above, the power requirement for induction heating is also high **(Table 2.5)**. We determined the HHV of char, gas and liquid samples to calculate the energy recovery of the overall process, including upgrading. The radiative and convective heat losses for reaction and catalyst tube was calculated from the following equation,

$$P = \epsilon\sigma A[{T_\mathrm{t}}^4 - {T_\mathrm{a}}^4] + hA[T_t - T_\infty] \tag{2.1}$$

Where, P is the total power (W), ϵ is the emissivity of the reaction tube (measured as 0.76), σ is the Stefan Boltzmann constant ($56.7e^{-9}$ W/m^2K^4), T_t is the tube temperature, T_a is the room temperature, A is the area of the reaction tube, and h is the convective heat transfer coefficient (28 W/m^2K). The first term on the right hand side of the equation represents the radiative heat transfer and the second term is the convective heat transfer. Controlling 70% of these heat losses by insulation, the actual energy input reduces and the overall energy ratio ≥ 3.0 are obtained for all operating temperatures, with the highest being obtained at the lowest temperature of 290 °C. This energy ratio is sufficient to operate a generator with a thermal efficiency of 33%, indicating the feasibility of using this approach. In the present study, much of the energy inputs is coming from the the induction systems.

Table 2.5: Energy balance for induction heating applied to biomass pyrolysis and upgrading

Temp. -Run ($^\circ C$)		E_b[a] (kJ/h)	E_c[b] (kJ/h)	E_g[c] (kJ/h)	E_T[d] (kJ/h)	E_{Induc}[e] (kJ/h)		Total E_{induc}[f]	E_{bal}[g] (kJ/h)	Heat Loss (kJ/h)		Est. E_{ind}[h] (KJ/h)	E_{ratio}[i]	Est. E_{ratio}
						Biomass Heating	Catalyst Heating			Reaction Tube	Catalyst Tube			
290	1	5916	3190	2193	11299	4320	1440	5760	5540	3261.1	580.5	3070.88	1.96	3.67
290	2	11421	3213	1783	16417	4320	1440	5760	10658	3261.1	580.1	3070.8	2.85	5.34
330	1	4079	3055	1076	8210	4320	1800	6120	2090	3261.1	638.55	3390.24	1.34	2.42
330	2	8606	3099	1543	13249	4320	1800	6120	7129	3261.1	638.55	3390.24	2.16	3.90
370	1	6515	2920	2439	11874	4320	2520	6840	5035	3261.1	774.0	4015.43	1.73	2.95
370	2	10567	3103	1476	15416	4320	2520	6840	8308	3261.1	774.0	4015.43	2.21	3.77

[a]Energy in bio-oil obtained from pyrolysis after upgrading
[b]Energy in char obtained from pyrolysis after upgrading
[c]Energy in gas obtained from pyrolysis after upgrading
[d]Total output energy
[e]Electrical energy consumed during pyrolysis and upgrading
[f]Total electrical energy consumed
[g]Energy balance defined as output energy energy consumed
[h]Estimated electrical energy consumed during pyrolysis and upgrading after controlling 70% of heat losses
[i]Energy ratio defined as energy content of products over electrical energy consumed

As the system is scaled up and converted into a continuous system, these energy costs can be lowered, with a corresponding increase in overall efficiency. In other studies, Fuji Electric has demonstrated pyrolysis with an induction heater without catalytic upgrading (Al-Khattaf et al., 2014). The feed rate for their study was 100 kg/h with an electrical power input of 100 kW/h (Al-Khattaf et al., 2014). The total output energy of 1940 MJ/h was achieved, distributed as 750, 640 and 550 MJ/h for oil, char and gas respectively. The power input for the process was 360 MJ/h corresponding to 18% of the total energy output, demonstrating good efficiency at higher scales. The experimental set-up presented herein was not optimized for efficiency but for higher yield, with its main objective being to demonstrate that catalytic upgrading can be carried out using a fast and relatively easy induction heating method, with better results for catalyst upgrading compared to conventional heating. Further studies to optimize the process and increase the efficiency are required and will be reported in further studies.

Scale up of induction heating based process for different applications have been attempted in the past. For example, Fuji Electric Company built an induction based kiln for continuous pyrolysis of industrial waste; mainly plastics for demonstration (Al-Khattaf et al., 2014). Since induction heating directly heats the metal and transfers heat to biomass, heat losses associated with heating the heat carrier are eliminated. A number of designs can be implemented to increase the efficiency of the process by reducing the temperature gradient. For instance, biomass can be mixed with metal balls for direct heating. Metallic fins or baffles can be inserted inside the reactor to increase temperature uniformity. Accumulation of soot does not affect the efficiency of induction heating and hence the startup and shut down times for induction based processes are shorter (Al-Khattaf et al., 2014; Amutio et al., 2012).

2.4 Conclusion

Pyrolysis upgrading is an important process for obtaining stable high quality bio-oil. Pyrolysis vapor upgrading was performed using thermo-catalytic cracking using HZSM-5 catalyst.

The catalyst bed was heated using an advanced high frequency induction heating technology for efficient and uniform heating. The results were compared with conventionally heated catalyst bed reactor. Different biomass to catalyst ratios was studied and the effect of different catalyst bed temperatures was also investigated. The quality of bio-oil was compared to that obtained without upgrading reaction. It was observed that (a) As the temperature and B/C ratio increases, the quality of oil gets better with more aromatic compounds. However, the water content of the bio-oil also increases. (b) High gas yield is achieved with higher catalyst bed temperatures. (c) Higher amount of aromatic compounds are obtained with induction heated catalyst due to more uniform and rapid heating which in turn improves catalyst performance. (d) From the catalyst characterization, high coke deposition, lower BET surface area and lower acid sites are observed for conventionally heated catalyst compared to induction heated catalyst which can be attributed to high thermal gradient which causes condensation of molecules on catalyst surface and incomplete reactions due to uneven heating.

Chapter 3
Thermo-Catalytic Upgrading of Pyrolysis Vapors Using Microwave Reactor

3.1 Introduction

Biomass conversion to biofuels offers economic and environmental benefits in the wake of the lingering energy crisis and the concerns related to greenhouse emissions from fossil fuels. Among the thermochemical processes used for conversion of biomass to liquid fuels, pyrolysis has received considerable attention, not only as the precursor to the combustion and gasification, but also as an independent process (McKendry, 2002).

Pyrolysis (thermochemical decomposition without oxygen) creates high-energy products with numerous uses, including those that can be used for self-sustaining the pyrolysis process, which makes it an energy efficient process. Pyrolytic bio-oil is a complex mixture of different sized organic molecules such as phenols, furans, levoglucosan, and other compounds (Zhang et al., 2007) formed as a result of the depolymerization and fragmentation of the biomass feedstock components (cellulose, hemicellulose, and lignin) during pyrolysis. Nearly all species of oxygenated organics are present in bio-oil including aldehydes, ketones, alcohols, ethers, esters, phenols, and carboxylic acids (Zhang et al., 2007).

Although bio-oil produced from fast pyrolysis of biomass has a potential to be directly used as a liquid fuel, this fuel has certain limitations such as high viscosity, acidity, low heating value, high ash content etc. Pyrolysis bio-oil also has high oxygen content of about 40% which marks a major difference between pyrolysis fuel and hydrocarbon fuel (which has oxygen content of less than 1%) (Czernik and Bridgwater, 2004). High oxygen content leads to a 50% decrease in energy density compared to HC fuels (Zhang et al., 2007) and catalytic

cracking of bio-oil is the most effective way to reduce oxygen content of bio-oil (Stefanidis et al., 2013). In this process, pyrolysis vapors produced from thermochemical decomposition of biomass are passed over a heated catalyst bed; the deoxygenation reaction takes place on the catalyst surface, where higher molecular compounds are broken down to lower molecular hydrocarbons and oxygen is released in the form of water, CO_2, and CO.

Numerous studies have been performed over the years to study the effect of various catalysts on pyrolysis vapor upgrading, with most of them using the 300 ° to 500 °C as the operating temperature range (Adam et al., 2005; Adjaye and Bakhshi, 1995; Bridgwater, 2012; Foster et al., 2012; Karanjkar et al., 2014; Qi et al., 2007). Zeolites such as HZSM-5 have proved to be one of the most effective catalyst for deoxygenation of bio-oil when operating in the temperature range of 250 ° - 400 °C (Adjaye and Bakhshi, 1995). The major disadvantages of catalytic upgrading of pyrolysis bio-oil are non-uniform heating of catalyst in externally heated reactors and the issues associated with the deactivation of catalytic sites via either coke deposition or poisoning (Czernik and Bridgwater, 2004; Zhang et al., 2007). In spite of smart heat- transfer designs, conventional heating technologies lack a rationally designed method for efficient and optimum use of imparted energy to achieve a desired temperature distribution.

Use of electromagnetic energy in the microwave region (300 to 6000 MHz) is an effective heating mechanism as microwaves impart energy directly to the material as heat. However, factors such as dielectric properties and penetration depth of material, frequency of operation and desired process temperatures play an important role in the design of a microwave reactor (Metaxas and Meredith, 1983). These properties of microwave heating make it a more efficient heating method compared to conventional heating, with a conversion efficiency of electrical energy to heat of 80-85% (Lam and Chase, 2012). While microwave heating has been used for pyrolysis of biomass, dedicated microwave catalytic upgrading has not been reported (Borges et al., 2014; Wan et al., 2009; Xie et al., 2014). Apart from increased heating efficiency, microwave heating of catalyst may improve catalyst performance compared to

conventional heating, mainly due to an increase in rate of reaction as described by Arrhenius equation (Lidstrom et al., 2001).

$$K = Ae^{-\mathrm{Ea/RT}} \tag{3.1}$$

Where, K is the rate constant, Ea is the activation energy, R is the gas constant, T is temperature and, A pre exponential factor. The frequency factor A represents molecular mobility and depends on the frequency of vibration of reacting molecules at the reaction interface which is directly affected by the microwave irradiation. An increase in frequency factor indicates increased rate of collision, thus, increases the rate of reaction (Lidstrom et al., 2001). Another theory put forth is that the microwave energy affects the activation energy thus affecting the exponential factor increasing the rate of reaction (Lidstrom et al., 2001). Moreover, microwave heating of catalyst is known to reduce coke deposition on the surface due to self-gasification of coke peculiar to microwave reactions only (Menendez et al., 2007). Microwave irradiated coke tend to desorb from the surface of the catalyst as microwave heating is also an effective means of desorption of polar molecules (Reub et al., 2002). These advantages of microwave make it a viable option for catalyst heating.

Literature review Due to the advantages of microwave technology applied to chemistry, it is now extensively studied to investigate the effect of microwave heating of catalyst in endothermic reactions. (Perry et al., 2002) evaluated the effect of microwave heating of catalyst in methanol steam reforming reaction both experimentally and numerically (Perry et al., 2002). The numerical model showed elimination of radial heat transfer effects, of space gradients, and of hot spot formation. The experimental results showed improved performance of the catalyst, which can be related to uniform heating. Other reports show improvements in catalyst performance for heterogeneously catalyzed reactions such as conversion of methane (Ioffe et al., 1995). Microwave heating in catalyzed oxidation of gas phase toluene was shown to have certain advantages such as rapid heating and steady bed temperature and uniform heating compared to conventional heating (Bo et al., 2013). In comparing catalytic oxygenation of benzene by microwave heating and electric furnace (Zhang et al., 2012),

it was noted that the catalyst had better catalytic activity under microwave irradiation than with electric furnace. (Gopalakrishnan et al., 2006) studied the effect of microwave irradiation on oxidation of benzene to phenol over Fe-ZSM-5 catalyst and concluded that microwave increases phenol selectivity and decreases catalyst deactivation (Gopalakrishnan et al., 2006). These advantages greatly reduce the cost of operation. This present study was conducted to examine the effect of microwave heating of catalyst bed for upgrading of pyrolysis vapors to produce bio-oil. The pyrolysis of biomass was carried in an induction heater and, the exiting bio-oil vapors were passed over a hot catalyst bed heated using a traveling wave microwave reactor. The performance of microwave process was compared with conventionally and inductively heated catalyst bed processes in terms of yield and quality of the produced bio-oil, and to evaluate catalyst performance under repeat utilization.

3.2 Materials and methods

3.2.1 Materials

Pine sawdust was obtained from scrap wood at Biological and Agricultural Engineering wood shop at the Louisiana State University Agricultural Center. The sawdust was grinded and its moisture content was measured. Nitrogen gas cylinder was supplied by Air Liquide (Houston, TX, USA). The HZSM-5 catalyst was supplied by Sigma Aldrich (St. Louis, MO, USA). The biomass pyrolysis reactor was a 5 kW RDO induction heater operating at a frequency range of 35-100 kHz (RDO Induction LLC, Washington, NJ). The reaction tube was a 310-stainless steel tri-clamp tube, 419 mm in length with an inner diameter of 34.4 mm. The reaction tube temperature was controlled using a calibrated Omega IR2C series infrared feedback controller (Omega, Stamford, CT) and an IR sensor to monitor the temperature. For upgrading reaction, the catalyst was heated by three different methods;

1. Conventional heating using a 13 mm x 1220 mm high temperature heavy insulated heating tape with 313 W output operating at 120 V (Briskheat Corporation, Columbus OH, USA) surrounding the reaction tube. The temperature was measured using a k-type thermo-

couple and controlled using a bench top temperature controlled from Briskheat Corporation (Columbus, OH).

2. Induction heating using a 5 kW RDO induction heater operating at frequency range of 135-400 kHz (RDO Induction LLC, Washington, NJ) to heat the catalyst bed. The reaction tube temperature was controlled using a calibrated Raytek MI3 series infrared remote temperature sensor (Raytek Corporation 1999-2014) that was coupled with a PID controller (Red Lion P-1641100, Red Lion Controls Inc. York, PA, USA). For both conventional and induction heating methods, the reaction tube was a 310-stainless steel tri-clamp tube, which was 270 mm length with inner diameter of 25.4 mm (P. D. Muley, 2015).

3. Microwave heating using a 1.2 kW, 2450 MHz microwave system. A 2450 MHz microwave traveling wave applicator was modified to accommodate the catalytic bed. The reaction tube was made of quartz with 71 mm inner diameter and 472.7 mm in length. The tube was designed to meet the microwave waveguide requirement, whereas a hole in the waveguide is less than 1/3 of the wavelength. The length of the tube was selected so that two IR thermocouples in the center measured the catalyst temperature at two different points and a thermal camera measured the temperature of the catalyst through a metallic mesh region of the waveguide **(Figure 3.1)**.

In addition to the microwave safety criteria described above, the dimensions and configuration of the tube were selected considering the ease of loading and unloading of the catalyst and cleaning the tube. Catalyst bed temperature was controlled by using a PID controller (Red Lion P-1641100, Red Lion Controls Inc. York, PA, USA) which adjusted the anode current of the microwave generator depending on the desired set temperature. The controlled variable was the temperature from the IR sensor fitted over the waveguide, focused on the catalyst bed. The emissivity and transmittance values of the tube were measured and accounted for in the calibration of the non-contact IR sensor (Raytek M13, Raytek Corporation, Wilmington, NC).

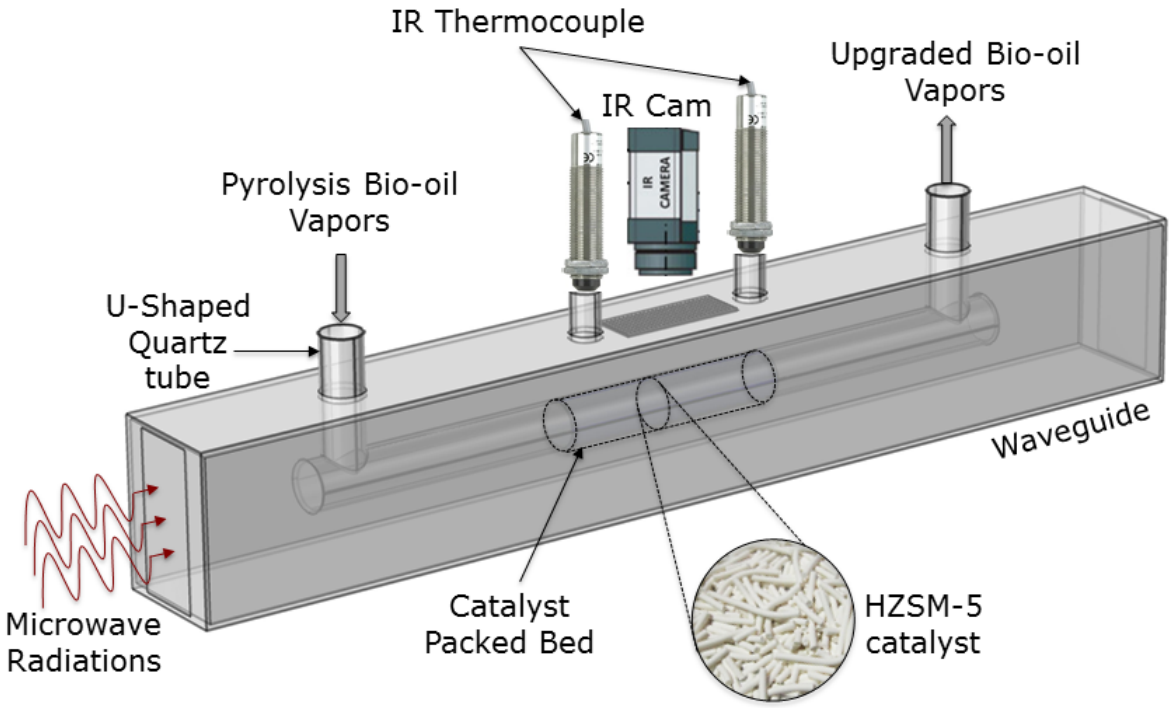

Figure 3.1: Microwave catalytic reactor for pyrolysis vapor upgrading

The temperature was continuously cross-verified using two other temperature sensors (Omega OS137 series, Omega Engineering, Stamford, CT) and a thermal camera (FLIR A40, FLIR Systems, Wilsonville, OR) focused on the catalyst bed.

3.2.2 Procedure

Three sets of experiments were performed to compare the effect of different heating mechanisms on bio-oil product composition and on catalyst activity for the ex-situ upgrading reaction. For all experiment groups, the initial pyrolysis was performed in the induction pyrolysis reactor **(Figure 3.2)**. Thirty grams of finely ground sawdust was placed in the pyrolysis reactor and decomposed at 600 $^{\circ}C$. The system was purged of Oxygen using Nitrogen gas at 1 L/m for 20 min to remove any oxygen present in the system. The vapors obtained from pyrolyzing reactor were passed over HZSM-5 catalyst in the three systems described above. Quantitative and qualitative analysis results of produced bio-oil and catalyst were compared with inductively heated and conventionally heated catalyzed reactions.

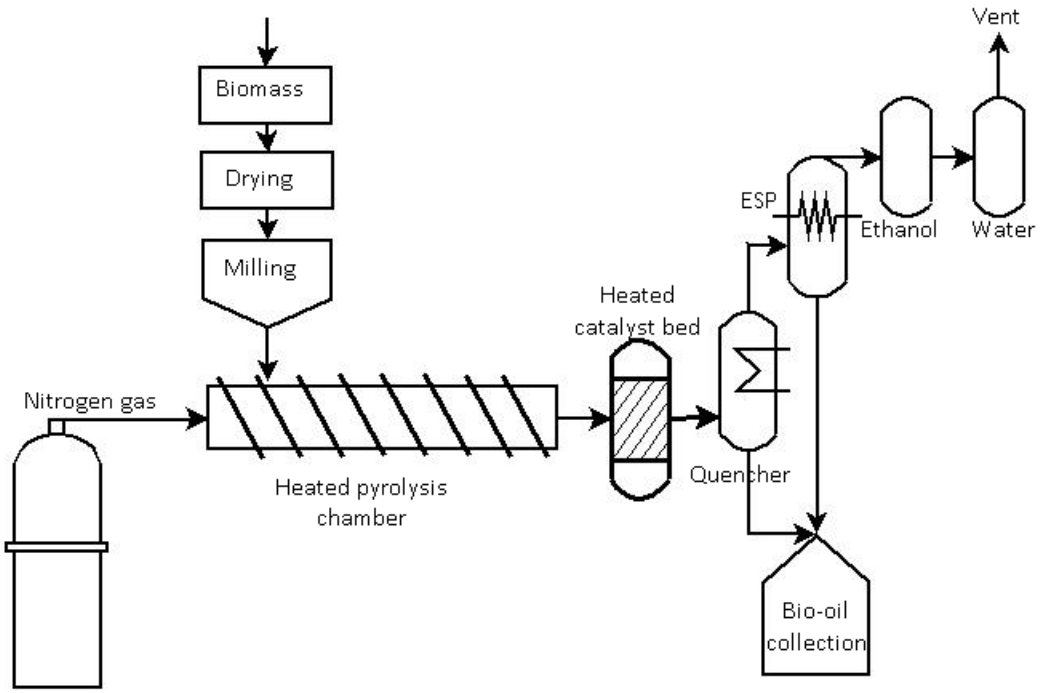

Figure 3.2: Flowchart for pyrolysis upgrading in an induction heater

All upgrading experiments were carried out at three different temperatures (290 °, 330 ° and 370 °C) using HZSM-5 catalyst. Based on the results obtained from our earlier studies (P. D. Muley, 2015) for different catalyst to biomass ratios (1:1, 1:1.5 and 1:2), 1:2 B/C ratio was the most effective, hence, this ratio was chosen to study the effect of different heating mechanisms. The same catalyst was used twice for each ratio and temperature combination as two separate experiments to study the extent of deactivation and coke deposition of catalyst in repeat conditions. A heating tape was used to maintain the gas line temperature above 275 °C between the pyrolyzer and the catalytic reactor, so as to avoid inline condensation and minimize secondary reactions. All experiments were performed in duplicated for reproducibility. The bio-oil collection system consists of an electrostatic precipitator (ESP) that was built in house and a 500 mL flask suspended in an ice bath where the resulting upgraded vapors were condensed **(Figure 3.2)**. The incondensable gases were passed through an ethanol and water trap before being vented with samples being collected in gas sample bags. The system was allowed to cool down for 40-50 min. Liquid was drained in a glass

vial, weighed and stored at -20 $^{\circ}C$ to avoid further polymerization reactions during storage. The char and catalyst were also collected, weighed and stored.

3.2.2.1 Product characterization

Liquid, gas and char yields were quantified. Yields were calculated based on initial biomass weight. Water content of liquid samples was determined using Karl-Fischer titration as described in literature (Mullen and Boateng, 2010). Composition of liquid samples was determined via GCMS (Varian 1200 series, Agilent Technologies, Santa Clara, CA) for product identification. Elemental analysis of oil, char and catalyst samples was conducted using Perkin-Elmer 2400 (PerkinElmer Inc. Waltham, MA) elemental analyzer as previously described (Mullen and Boateng, 2010). High heating values of the liquid samples were measured using bomb calorimeter (Parr Instrument Company, Moline, IL.) according to the procedure described in literature (International, 2009).

3.2.2.2 Catalyst characterization

The surface of the catalyst was characterized using different techniques to investigate the extent of coking and deactivation. X-ray photoelectron spectroscopy (XPS) was used to identify and quantify the different elements present in the catalyst using a Kratos Axis 165 ray photon spectroscope/auger electron spectroscope operated with Mono-Al Ka X-ray source with beam current at 10 mA and HT at 12 kV (Kratos Analytical Ltd. Manchester, UK). Catalyst surface area and pore volumes were measured using BET surface analyzer via a NOVA 2200e series Surface area and Pore Size Analyzer using nitrogen adsorption (Quantachrome Instruments Inc., Boynton Beach, FL). Temperature-programmed desorption of ammonia (NH3-TPD) analysis was carried out using Micrometritics 2700 chemisorption apparatus (Micromeritrics Corporation, Norcross, GA). Briefly, 0.05 g of prepared sample was loaded in the U-tube, the sample was degasses using He gas at 500 $^{\circ}C$ for 30 min. The sample was then cooled to 100 $^{\circ}C$ and ammonia was adsorbed at the flowrate of 5 $^{\circ}C/min$

from 100 $^{\circ}C$ to 500 $^{\circ}C$. TCD signal was recorded (Lee et al., 2012). The coke deposition on catalyst was determined using elemental analyzer CHN (Perkin Elmer series 2400, Waltham, MA) as previously described (Al-Khattaf et al., 2014). Scanning electron microscope (SEM) images of catalyst were taken both before and after reaction to visualize the changes on catalyst surface using FEI Quanta 3D FEG FIB/SEM dual beam system (FEI inc. Hillsboro, OR).

3.3 Results and discussion

3.3.1 Effect of catalyst bed temperature

3.3.1.1 Product yield

The product yield was quantified based on initial mass of biomass. The char yield for all experiments ranged between 20-22 % **(Tables 3.1,3.2,3.3)**. Since the pyrolysis temperature for all experiments was 600 $^{\circ}C$, char yield was not affected by catalyst bed temperature. Elemental analysis (CHNO) of all char samples indicated a composition of 85-88% carbon, 3-6% hydrogen and traces of nitrogen and sulphur based on total char yield (with the difference as Oxygen). The char was rich in carbon compared to fresh biomass, which had 46% carbon, 6.43% hydrogen and traces of nitrogen. Pyrolysis and catalyst bed temperatures play an important role in the quality and quantity of oil (Jae et al., 2014). The gas yield was calculated from the difference in biomass input and liquid and char yield. Gas yield increased as the catalyst bed temperature increased; higher catalyst bed temperatures increased the cracking reaction rate which encouraged the formation of non-condensable gases. The gas samples were analyzed for composition and were found to be rich in carbon monoxide (20-23% wt) and carbon dioxide (9-10 wt %) with lower yield of methane (4-6% wt) and other C_2 - C_5 gases (1-3% wt). About 20-30 wt % of gas composition was unidentified. Gas samples could not be analyzed for H_2 content due to equipment limitations. Amount of methane and C_2 - C_5 gases increased as the catalyst bed temperature increased from $290 - 370^{\circ}C$.

Table 3.1: Yield values for upgraded products for three heating methods at 290 $^{\circ}C$

Temperature	Non-upgraded bio-oil	Conventional heating		Induction heating		Microwave heating	
290 $^{\circ}C$		% Composition		% Composition		% Composition	
		Run 1	Run 2	Run 1	Run 2	Run 1	Run 2
Char	19.36	21.33	20.43	21.13	21.37	24.87	21.07
Gas	25.37	47.20	46.23	51.63	41.50	39.53	44.77
Water	25.28	21.08	20.23	17.47	24.21	20.12	18.21
Bio-oil	29.98	10.37	13.11	9.76	12.92	15.48	15.95
Total	100	100	100	100	100	100	100
CHN analysis of liquid fraction							
Carbon	30.37	62.35	60.33	65.8	61.49	60.17	61.92
Hydrogen	5.85	3.004	3.35	2.067	1.57	3.126	4.667
Nitrogen				traces			
Oxygen[a]	63.71	34.64	36.32	32.13	36.94	36.7	33.42
Total	100	100	100	100	100	100	100
Organic Liquid Fraction Composition (wt % of bio-oil)							
Furfural	8.34	1.455	0.16	0.452	-	0.538	-
Ketones	9.78	3.919	12.95	7.365	6.951	18.4	18.76
Alcohols	3.03	8.506	3.531	4.235	5.208	9.776	5.964
Aldehyde	13.60	13.75	9.838	10.25	12.67	-	1.508
Acids	1.38	-	-	-	-	-	2.382
Phenols	53.41	33.93	37.8	30.63	33.67	15.55	34.95
Aliphatic HC	-	1.707	3.68	7.958	4.958	14.45	1.478
Aromatic HC	-	28.08	26.22	27.06	25.5	34.12	28.56
Benzene	-	4.44	1.41	1.32	1.226	1.16	-
Methylbenzene	-	19.49	17.75	12.25	11.29	7.225	5.803
Ethyl-benzene	-	2.256	0.119	1.98	-	1.484	2.687
Toluene	-	0.708	0.42	0.66	0.86	0.343	1.179
Xylenes	-	0.279	4.627	6.54	5.668	22.77	11.45
C9-C10	-	0.944	1.886	4.31	6.457	1.142	7.437
Unidentified[b]	10.56	8.649	5.823	12.05	11.05	7.167	6.438
Total	100	100	100	100	100	100	100

[a]Determined by difference
[b]Determined by difference

Table 3.2: Yield values for upgraded products for three heating methods at 330 $^{\circ}C$

Temperature	Conventional heating		Induction heating		Microwave heating	
330 $^{\circ}C$	% Composition		% Composition		% Composition	
	Run 1	Run 2	Run 1	Run 2	Run 1	Run 2
Char	20.93	22.7	20.17	21.97	26.97	22.50
Gas	48.33	44.23	42.90	42.60	37.57	45.47
Water	20.29	17.59	15.65	21.36	20.76	20.64
Bio-oil	10.44	15.48	21.29	14.08	14.71	11.39
Total	100	100	100	100	100	100
CHN analysis of liquid fraction						
Carbon	69.18	62.82	67.2	66.71	67.11	68.16
Hydrogen	3.15	3.65	2.88	2.13	3.45	6.61
Nitrogen	traces					
Oxygen[a]	27.67	33.52	30.92	31.16	29.45	25.22
Total	100	100	100	100	100	100
Organic Liquid Fraction Composition (wt % of bio-oil)						
Furfural	0.45	0.74	0.49	1.69	-	-
Ketones	2.22	5.13	3.43	2.86	9.75	8.41
Alcohols	5.17	1.62	4.85	5.24	4.58	1.95
Aldehyde	9.27	12.95	1.74	6.45	1.03	14.75
Acids	-	0.41	-	-	1.33	4.37
Phenols	26.48	33.47	19.7	21.18	29.8	22.57
Aliphatic HC	1.48	3.25	11.59	19.1	2.32	1.67
Aromatic HC	42.55	32.56	45.13	37.03	45.47	40.77
Benzene	0.93	5.98	2.13	2.49	0.46	7.15
Methylbenzene	30.8	8.98	10.26	15.63	31.49	17.44
Ethyl-benzene	2.79	0.38	9.94	2.02	6.94	1.15
Toluene	-	0.54	1.751	0.09	0.65	0.25
Xylenes	7.03	13.84	5.82	2.3	12.87	13.58
C9-C10	0.99	2.82	16.81	16.99	0.88	1.19
Unidentified[b]	9.34	9.85	13.06	1.73	0.90	5.45
Total	100	100	100	100	100	100

[a]Determined by difference
[b]Determined by difference

Liquid yield is lower for the catalytic upgrading process compared to the non-upgraded products. Liquid yield also slightly decreased as the catalyst bed temperature increased. Elemental analysis was used to quantify the composition of carbon, hydrogen, nitrogen and oxygen (C, H, N and O) in the liquid samples.

Table 3.3: Yield values for upgraded products for three heating methods at 370 $^{\circ}C$

Temperature	Conventional heating		Induction heating		Microwave heating	
370 $^{\circ}C$	% Composition		% Composition		% Composition	
	Run 1	Run 2	Run 1	Run 2	Run 1	Run 2
Char	22.7	23.57	16.87	21.4	22.30	20.26
Gas	47.97	50.07	50.23	46.47	43.03	49.06
Water	19.41	15.37	20.21	18.41	22.43	18.34
Bio-oil	9.91	11.00	9.69	13.72	12.24	12.32
Total	100	100	100	100	100	100
CHN analysis of liquid fraction						
Carbon	69.16	68.41	69.46	65.4	69.02	67.12
Hydrogen	2.4	3.93	1.93	2.624	3.2	7.93
Nitrogen	traces					
Oxygen[a]	28.38	27.66	28.6	31.97	27.68	24.95
Total	100	100	100	100	100	100
Organic Liquid Fraction Composition (wt % of bio-oil)						
Furfural	0.28	1.94	-	1.14	-	-
Ketones	2.82	5.2	5.29	4.91	10.80	6.41
Alcohols	1.13	2.87	-	0.9	2.03	2.27
Aldehyde	5.54	9.44	-	2.57	-	9.78
Acids	1.74	-	-	2.2	0.80	1.55
Phenols	5.53	13.46	25.03	32.54	5.08	6.10
Aliphatic HC	4.44	-	-	3.09	1.73	0.13
Aromatic HC	64.76	57.59	63.79	48.76	69.64	64.67
Benzene	2.28	11.28	1.72	0.96	1.36	1.21
Methylbenzene	39.97	31.3	41.46	16.74	32.10	38.73
Ethyl-benzene	2.43	0.16	4.01	0.02	1.08	2.68
Toluene	0.15	0.87	0.66	1.08	5.25	3.34
Xylenes	13.31	8.53	3.33	-	25.10	11.88
C9-C10	6.61	5.45	12.61	29.96	4.75	6.84
Unidentified[b]	13.76	9.43	9.22	3.82	10.00	9.01
Total	100	100	100	100	100	100

[a]Determined by difference
[b]Determined by difference

During catalytic cracking oxygen is removed in the form of water, CO and CO_2 thus reducing the oxygen content of upgraded bio-oil by 40-50% compared to non-upgraded bio-oil. Low oxygen and higher carbon content was observed as the catalyst bed temperature increased **(Tables 3.1, 3.2, 3.3)**.While overall higher carbon values were obtained for bio-oil upgraded over fresh catalyst compared to reused catalyst in conventional and induction heating, for the microwave-based process the carbon content slightly increased for the second run, with much higher hydrogen and lower oxygen compared to the other two heating methods. Highest oxygen content of 36% was observed at 290 $^{\circ}C$ with run 2 conventional method **(Table 3.1)** and lowest oxygen content of 24% was obtained at 370 $^{\circ}C$ microwave heating **(Table 3.3)**.

3.3.1.2 Water Content

Catalytic upgrading removes oxygen in the form of water, carbon dioxide and carbon monoxide which is why water content of upgraded bio-oil is higher than that of non-upgraded bio-oil (Adjaye and Bakhshi, 1995). No specific trend was observed between different temperature ranges. Lower water content was observed for 2nd run for both conventional and microwave heating. This could be because the catalyst activity reduces with reuse and less reaction results in lower water yield. The difference in water content of liquid fraction for the different type of catalyst heating methods, namely, conventional heating, induction heating and microwave heating was less than 5% concluding that both liquid yield and water content were not significantly affected by the method of catalyst heating.

3.3.1.3 Product composition

Non-upgraded bio-oil is generally rich in oxygenated hydrocarbons such as phenols, ketones, alcohol and aldehydes and acids with aromatic compounds detected in insignificant amounts (Adjaye and Bakhshi, 1995; Mullen and Boateng, 2010). Catalytic upgrading significantly affects these groups. Use of catalyst produces higher yield of non-oxygenate hydrocarbons

such as aromatic and aliphatic hydrocarbons which can be blended with gasoline. These hydrocarbons have higher octane number (comparable to those of petroleum fuel) and are of interest as fuel replacement and additives. Composition of aromatic hydrocarbons increased as the catalyst bed temperature increased. The aromatic hydrocarbon yield increased from 26-28% at 290 $^{\circ}C$ **(Table 3.1)** to 55-65% at 370 $^{\circ}C$ **(Table 3.3)**. At all temperatures, the aromatic HC yield decreased when the catalyst was reused in the second run, marking the decrease in catalyst activity either due to coke deposition, active site poisoning, or both. At lower temperatures, yield of phenol, ketones and alcohols was higher followed by aliphatic hydrocarbons. However, as the temperature rose to 370 $^{\circ}C$, the composition of these compounds decreased significantly. Traces of aldehydes, acids and furfurals were noted at lower temperatures which vanished at 370 $^{\circ}C$ **(Table 3.3)**. These results are in agreement with those noted in literature (Adjaye and Bakhshi, 1995).

3.3.2 Effect of heating method

No change in yield with respect to the heating method used for catalyst heating was observed for gas or char. As stated above the difference in water content of liquid fraction for the type of catalyst heating methods, namely, conventional heating, microwave heating and induction heating was less than 5% concluding that neither liquid yield nor water content was significantly affected when the method of heating the catalyst was changed. From the elemental analysis of liquid samples, microwave heating had the lowest oxygen content compared to conventional and induction heating at higher temperatures (330 $^{\circ}C$ and 370 $^{\circ}C$) **(Tables 3.2, 3.3)**.

Higher hydrogen content was also observed in all liquid samples after microwave heating compared to other heating methods showing that production of a higher grade fuel with microwave reactor.

From the perspective of obtained compounds, high yields of non-oxygenates such as aliphatic or aromatic hydrocarbons is desirable for better quality fuel. Aliphatic hydrocarbon

yield was no more than 19 wt% for any combination and decreased as the catalyst bed temperature increased. Microwave heating yielded highest aromatic hydrocarbon yield for all temperature with aromatic HC yield consistently higher by 5-7% in the initial run with microwave heating. Even when the catalyst was reused without regeneration, the aromatics yield was consistently higher with microwave heating. The lowest aromatic HC yield was 25.5% at 290 $^{\circ}C$ obtained by induction heating for reused catalyst.

Aromatic hydrocarbons mainly contained of benzene, ethyl benzene, methyl benzene, toluene, xylene and $C_9 - C_{10}$; with the highest composition of methyl benzene and xylene. Benzene content was low at all temperatures and heating methods except for induction heating. The low concentration of benzene is probably due to alkylation reaction on acid cites of the catalyst (Adjaye and Bakhshi, 1995). Toluene and ethyl benzene composition was also found to be negligible. $C_9 - C_{10}$ concentration varied for samples and was greater at higher temperatures but did not follow a specific trend for the type of heating method employed.

3.3.3 Catalyst characterization

3.3.3.1 X-ray phototelectron spectroscopy (XPS) analysis

X-ray photoelectron spectroscopy is used to study the quantity of carbonaceous material present on the catalyst surface on of the material. The most distinct peaks observed on the catalyst were aluminum, silicon, carbon, oxygen and traces of nitrogen, sulphur and hydrogen. Chemical formula for HZSM-5 contains all of the above compounds except carbon, sulphur and nitrogen. **Figure 3.3** shows the variation in the C/Al peak for catalyst sample at different temperatures and heating method. Occurrence of carbon peak is due to coke deposition on the catalyst surface; in this case, a lower value indicates a better performance. At 290 $^{\circ}C$, it was observed that the coke formation was highest for catalyst heated with conventional heating techniques (C/Al = 3.0583) compared to that of induction heating or microwave heating. Coke formation on acid catalysts like that of HZSM-5 is strongly

governed by dehydrogenation and cracking reactions. These reactions break the long chain polymers and form aromatic compounds (Appleby et al., 1962). These reactions are highly temperature dependent and favor higher temperatures, which can explain higher coke deposition at higher temperatures in the microwave heating method. However, carbon deposition could also occur due to condensation of molecules on cooler catalyst surface.

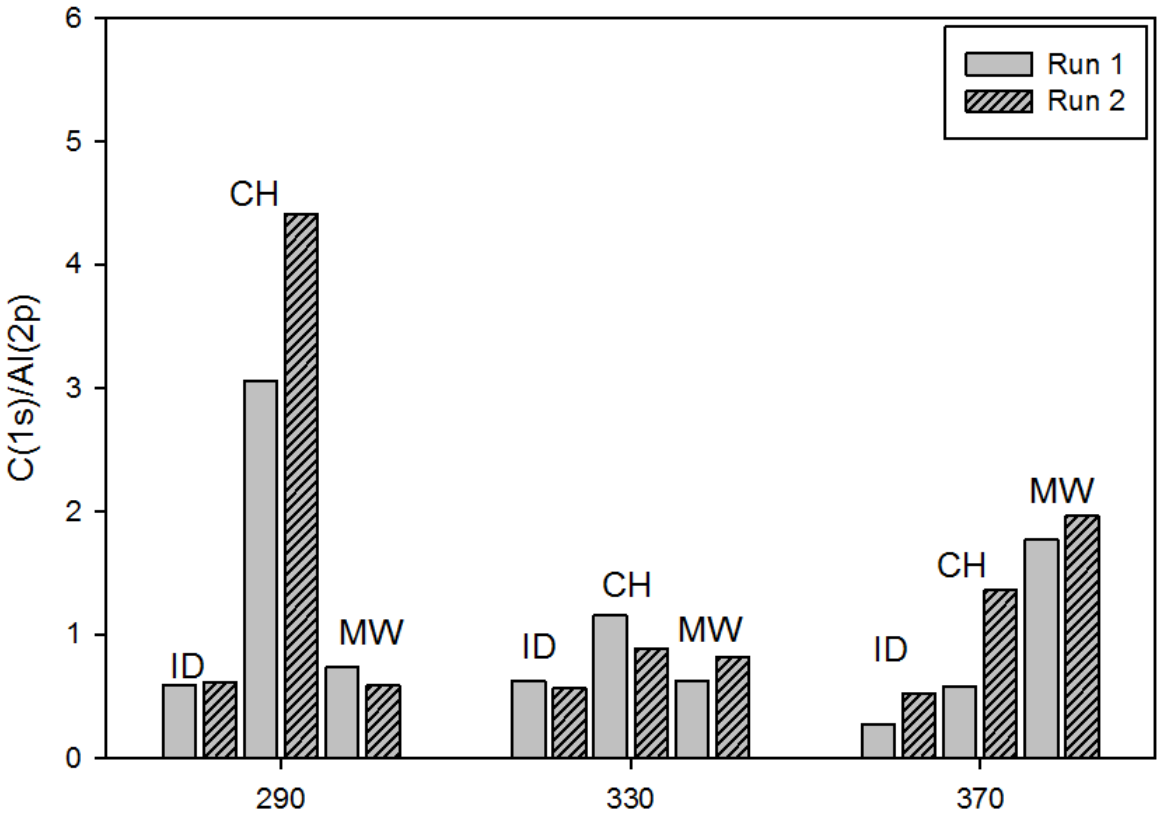

Figure 3.3: XPS analysis (C/Al) of catalyst after reaction at different temperatures and heating methods (CH conventional heating, ID induction heating, MW microwave heating)

This phenomenon occurs when the catalyst surface is not uniformly heated and cooler spots on the catalyst surface may encourage vapor condensation on the surface and leads to catalyst poisoning and deactivation. Higher coke deposition for lower temperature samples with heating tape (CH conventional heating) could be attributed to this phenomenon. As explained further in the section on surface area, lower coke deposition in microwave could be due by self-gasification of carbon deposited on the catalyst (Menendez et al., 2007).

3.3.3.2 Elemental analysis

Since XPS study is mainly used for surface analysis, even though the samples were finely ground, the results can still be interpreted as surface analysis. Hence we performed elemental analysis of catalyst by combustion to give CHNS data that can be considered as bulk analysis. The observations made for surface analysis were confirmed by the elemental analysis of catalyst **(Table 3.4)**. High amounts of carbon were obtained at all catalyst temperatures for the conventional heating method. Higher C/H mole ratio also suggests that the coke present is aromatic in nature. For microwave upgrading, the C/H mole ratio was observed to increase with temperature. These results were in agreement with the product composition of bio-oil obtained after upgrading. Nitrogen and sulphur values were negligible for all samples.

3.3.3.3 Surface area analysis

BET surface area and micropore area available after reaction was investigated and compared to fresh catalyst. Total surface area available after reaction directly corresponds to the amount of coke deposited on the catalyst surface. The fresh catalyst surface area as provided by the vendor was 250 m^2/g; our own measurements showed a surface area 247.7 m^2/g **(Table 3.5)**. More surface area is available for microwave-heated catalyst, followed by induction heating, and lastly by conventionally heated catalyst. Higher surface area after the runs corresponds to lower coke deposition on the catalyst surface. Evidence of self-gasification of coke on catalyst inside a microwave reactor has been established in the past (Menendez et al., 2007). This self-gasification leads to reaction of coke with CO_2 in the presence of steam to form CO and H_2 gases thus reducing the amount of coke deposited on the catalyst (Menendez et al., 2007). The reason for self-gasification process might lie in the fact that both catalyst and coke respond to microwave radiations. It is an established fact that coke deposition on zeolite surface is a result of adsorption of coke on catalyst surface (Guisnet and Magnoux, 2001).

Table 3.4: Elemental analysis (CHNS) for fresh and coked catalyst

Upgrading Temperature (°C)	Sample	Carbon (%)	Hydrogen (%)	Nitrogen (%)	Sulphur (%)	C/H mole ratio
HZSM-5		0.2±0.02	0.38±0.09	0.18±0.04	0.00±0.00	0.96±0.06
Induction Heating						
290°C	Run 1	12.67±0.19	1.09±0.06	0.03±0.00	0.01±0.00	0.93±0.08
	Run 2	7.89±0.00	0.67±0.11	0.00±0.00	0.00±0.00	0.98±0.05
330°C	Run 1	5.90±0.08	0.12±0.01	0.1±0.01	0.00± 0.00	4.06±0.04
	Run 2	7.89±0.08	0.30±0.02	0.06±0.00	0.00±0.00	2.18±0.06
370°C	Run 1	6.12±0.03	0.61±0.01	0.00±0.00	0.00±0.00	0.83±0.02
	Run 2	6.68±0.02	0.29±0.11	0.13±0.05	0.00±0.00	1.92±0.10
Conventional Heating						
290°C	Run 1	13.63±0.01	1.98±0.09	0.07±0.00	0.00±0.00	0.99±0.05
	Run 2	20.25±0.04	1.7±0.10	0.07±0.00	0.00±0.00	0.96±0.03
330°C	Run 1	13.77±0.38	1.19±0.05	0.06±0.00	0.00±0.00	1.37±0.24
	Run 2	11.63±0.13	0.7±0.18	0.04±0.01	0.00±0.00	1.26±0.15
370°C	Run 1	12.83±0.04	0.85±0.09	0.05±0.02	0.00±0.00	1.96±0.06
	Run 2	8.58±0.05	0.36±0.005	0.03±0.02	0.00±0.00	0.99±0.01
Microwave Heating						
290°C	Run 1	5.94±0.02	0.49±0.005	0.02±0.007	0.00±0.00	1.01±0.001
	Run 2	6.68±0.032	0.30±0.06	0.08±0.008	0.00±0.00	1.56±0.021
330°C	Run 1	5.12±0.01	0.36±0.008	0.02±0.008	0.00±0.00	1.18±0.010
	Run 2	4.81±0.04	0.39±0.004	0.005±0.005	0.00±0.00	1.02±0.002
370°C	Run 1	6.12±0.02	0.45±0.009	0.09±0.002	0.00±0.00	1.13±0.036
	Run 2	4.85±0.037	0.31±0.002	0.02±0.003	0.00±0.00	1.31±0.062

Preliminary tests have showed that microwave desorption is an effective technique for the removal of polar adsorbates compared to conventional heating due to the direct volumetric heating achieved in the microwave reactor (Reub et al., 2002; Woodmansee et al., 1995). In this particular case, both coke (the adsorbate) and the HZSM-5 catalyst (the adsorbent) readily heat in the microwave creating a unique situation where desorption with microwave heating is highly plausible (Reub et al., 2002). Moreover, the rigorous molecular rotation of the polar molecules may loosen the coke deposited on the surface. Another prominent effect that microwaves create is occurrence of micro-plasmas and local hot spots that encourage self-gasification of coke (Menendez et al., 2007). The surface area significantly reduced for reused catalyst after run 2.

Table 3.5: BET Surface area and volume of fresh and coked catalyst at 370 $^{\circ}C$

Sample	Run no.	BET surface area (m^2/g)	Micropore area (m^2/g)	Micropore volume (cm^3/g)
HZSM-5	Fresh	247.7	196.4	0.0950
Induction heating	Run 1	210.7	143.4	0.0700
	Run 2	85.5	156.3	0.0690
Conventional heating	Run 1	177.624	105.203	0.047
	Run 2	91.186	50.00	0.022
Microwave heating	Run 1	222.586	97.334	0.043
	Run 2	143.038	66.823	0.031

3.3.3.4 NH_3 -TPD

NH3-TPD analysis was used to determine the extent to which deactivation of catalyst has occurred. NH3-TPD analysis for fresh and used catalyst was conducted. Fresh HZSM-5 catalyst showed two distinct peaks. The peak at the lower temperature (160-190 $^{\circ}C$) represents weak acid sites and the one at the higher temperature (330-360 $^{\circ}C$) represents strong acid sites **(Figure 3.4)**. Our results indicated that coke deposition mainly occurs on the strong acid sites for catalytic upgrading activity. The peak for strong acid site (325 365 $^{\circ}C$) disappears almost entirely for conventionally heated catalyst, marking the high amount

of coke deposition. This peak is still observed for inductively heated catalyst, but with a largely reduced intensity. However, for the microwave heated catalyst, the peak intensity is only slightly reduced compared to the fresh catalyst **(Figure 3.4)**. The highest the peak is at the strong acid site, the greater is the aromatization effect; HZSM-5 has higher concentration of strong acid sites (Viswanathan and Pillai, 1992).

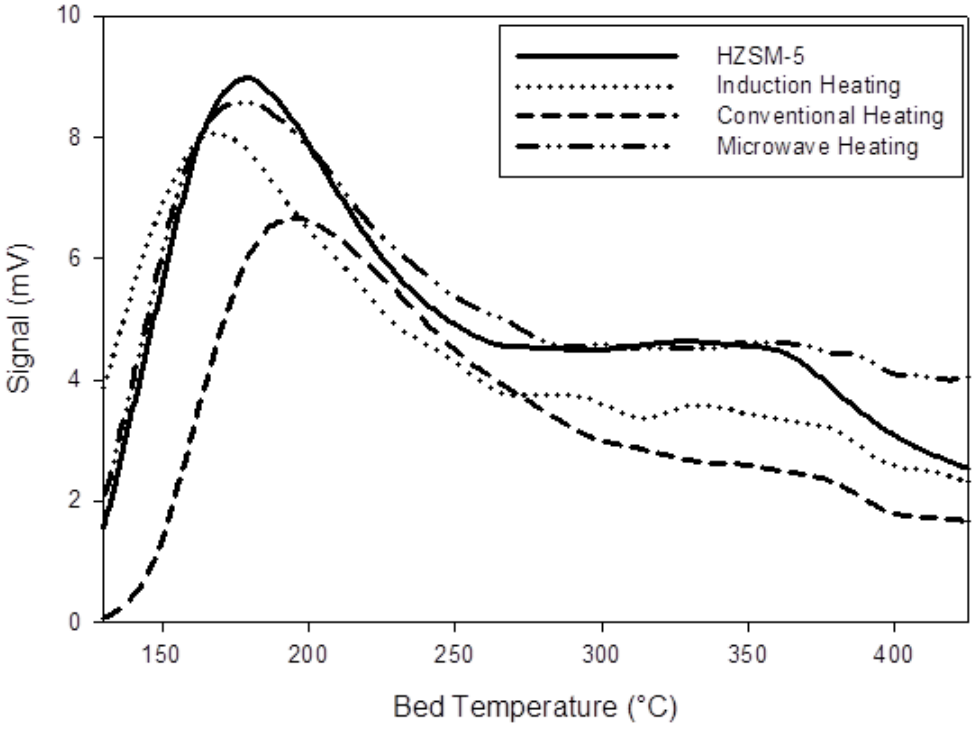

Figure 3.4: NH3-TPD profiles for fresh catalyst and catalyst heated in induction, microwave and conventional reactor

The rate of consumption of weak acid sites is lower compared to that of strong acid sites. These results are consistent with other studies reported in the literature for HZSM-5 catalyst behavior in time (Lin et al., 2007). For the weak acid sites, the peak intensity reduces only slightly for microwave heating followed by inductively heated catalyst; it is decreased the most for conventionally heated catalyst. Slight shift of peak towards left also indicates a decrease in the strength of acid sites due to coke deposition.

3.3.3.5 SEM analysis

SEM images of fresh and used catalyst surface were acquired at 35,000X magnification for catalyst heated at 370 $°C$ for the three different heating methods. A sharp crystalline structure of catalyst is observed in the image of the fresh catalyst **(Figure 3.5)**. The image becomes more granular and loses its crystallinity for catalyst samples after reaction.

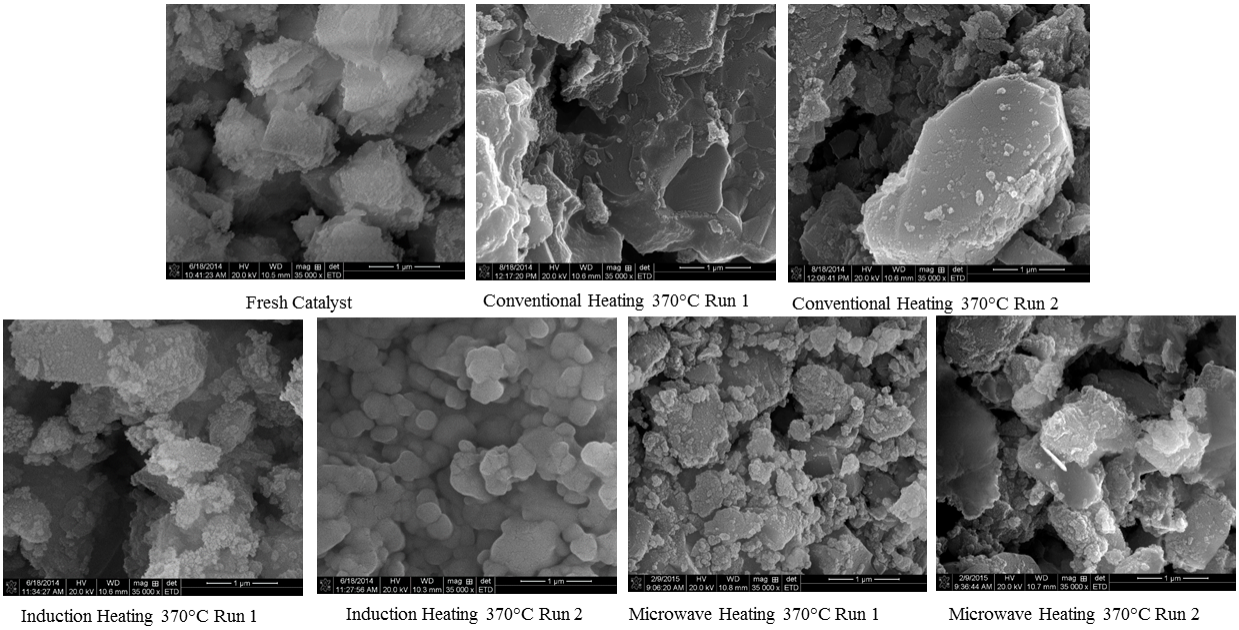

Figure 3.5: SEM imaging of fresh and used catalyst

The effect is higher for reused catalyst for run 2 than run 1. This granular structure could be due to coke deposition on the surface of the catalyst. This crystallinity decreases for the inductively heated catalyst, but does not decrease significantly for the microwave heated catalyst, also indicating that the microwave heating preserved better the initial properties of the fresh catalyst.

3.3.4 Heating value and energy balance

The high heating value of bio-oil was measured using a bomb calorimeter as described in ASTM D200. The high heating values of biomass, char and gas were also calculated based on the CHNSO elemental analysis using Dulongs equation (Scholze and Meier, 2001). The

HHV for raw biomass was measured as 19.56 MJ/kg **(Table 3.6)**. The bio-oil obtained from upgrading of pyrolysis vapors had a high heating value in the range of 15-27 MJ/Kg depending on the catalyst bed temperature. The heating value increased as the catalyst temperature increased. Slightly higher heating values were noted for microwave heating process compared to other two methods **(Table 3.6)**.

Table 3.6: High heating value of bio-oil, char and gas (MJ/kg) for different heating methods

Upgrading temperature ($^{\circ}C$)	Sample	HHV Bio-oil[a] (MJ/kg)	HHV Char (MJ/kg)	HHV Gas (MJ/kg)
		Conventional heating		
290	Run 1	13.75±0.05	31.59±0.09	9.08±0.093
	Run 2	19.59±0.02	32.08±0.03	8.73±0.026
330	Run 1	17.89±0.01	32.93±0.04	10.27±0.05
	Run 2	16.64±0.09	32.33±0.05	9.36±0.09
370	Run 1	18.57±0.09	31.96±0.02	11.73±0.05
	Run 2	17.88±0.01	33.56±0.01	10.21±0.05
		Induction heating		
290	Run 1	13.14±0.09	33.55±0.04	11.32±0.90
	Run 2	14.48±0.20	33.42±0.09	9.04±0.20
330	Run 1	9.06±0.30	33.67±0.07	10.76±0.16
	Run 2	19.12±0.06	31.36±0.06	8.953±0.60
370	Run 1	25.38±0.03	32.67±0.04	11.35±0.60
	Run 2	23.4±0.90	32.22±0.07	9.13±0.09
		Microwave heating		
290	Run 1	17.10±0.08	30.67±0.86	11.75±0.08
	Run 2	17.12±0.83	32.31±0.07	9.65±0.21
330	Run 1	24.09±1.12	31.91±0.16	10.11±0.69
	Run 2	20.96±0.79	32.45±0.49	11.14±0.02
370	Run 1	27.74±0.91	31.90±0.5	10.20±0.03
	Run 2	26.35±0.07	32.14±0.26	11.02±0.75

[a]Not adjusted for water content

The heating value for liquids was higher for run 1 compared to run 2. The highest HHV of 27.74 MJ/kg was obtained for microwave heating at 370 $^{\circ}C$ after 1st run. The typical heating value for non-upgraded pyrolytic bio-oil is 15-17.5 MJ/kg, we observed 25-30%

increase in the heating values of bio-oil obtained, especially at catalyst bed temperature of 370 $°C$. HHV contribution of char was highest ranging from 31-33 MJ/kg; whereas heating value of gas ranged from 9-11 MJ/kg **(Figure 3.6)**.

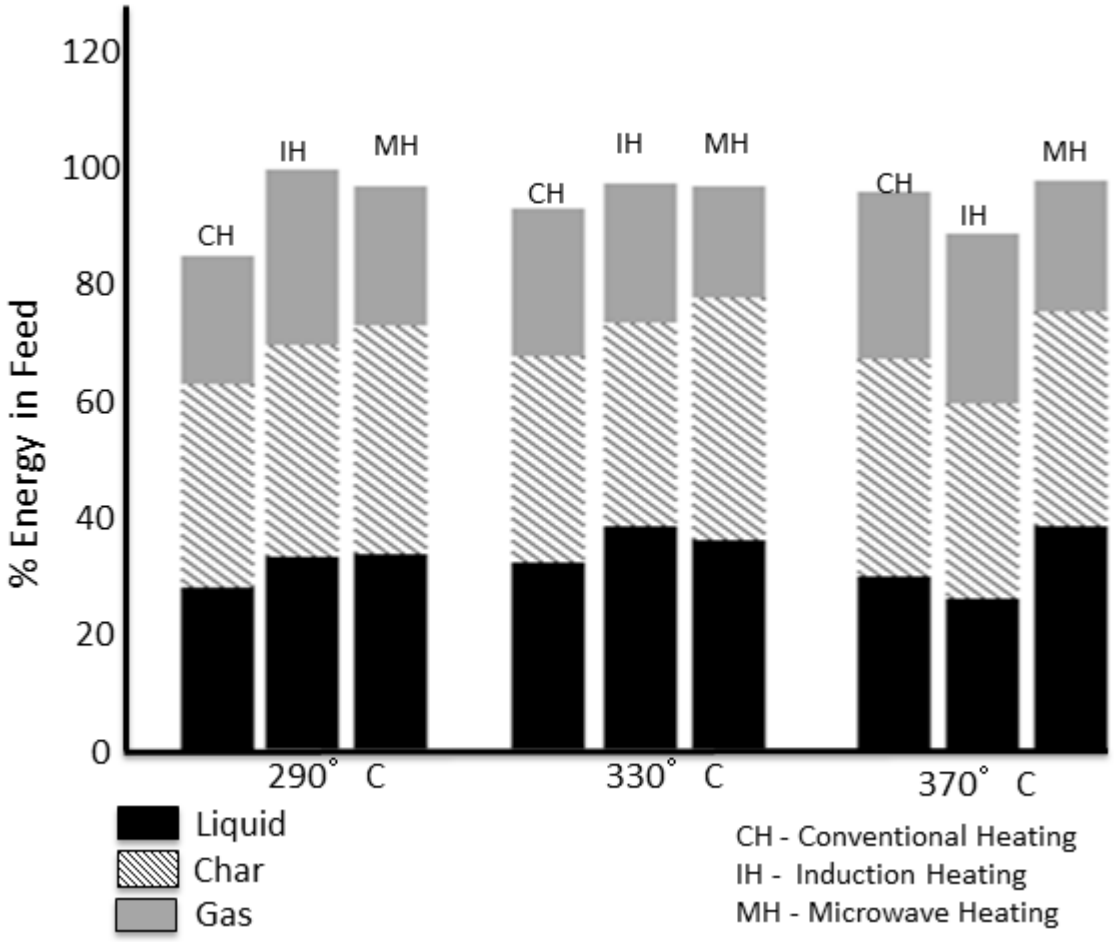

Figure 3.6: Percent energy in feed contribution by liquid, char and gas yields for three heating methods

Although about 50% yield was obtained from gas as it was rich in CO_2. Catalytic upgrading removes oxygen in the form of CO and CO_2 along with water on bio-oil, thus concentration of CO_2 was high, reducing the overall heating value of gas. Highest heating value contribution to gas was from obtained from methane.

Microwave heating mechanism has an advantage of direct heating of material at a molecular level, which reduces heat losses associated with heat transfer between carrier and catalyst.

With proper reactor design, a uniform heating of catalyst bed with minimum temperature gradient can be achieved with microwave reactors. Together with low heat loss and easy temperature control and uniformity, microwave heating is a viable and energy efficient technique for catalyst bed heating. We determined the amount of power consumed for all three catalyst heating methods. Induction heating consumed the most power to heat the catalyst; 1.032 MJ at 290 $^{\circ}C$, 1.29 MJ at 330 $^{\circ}C$ and 1.806 MJ at 370 $^{\circ}C$ **(Table 3.7)**. However the heating rate was higher for induction heating compared to conventional heating.

Table 3.7: Energy input and % efficiency of microwave heating

Upgrading temperature ($^{\circ}C$)	Power input for catalyst bed heating (MJ)			Decrease in energy input by microwave heating (%)	Increase in overall energy efficiency of microwave process (%)
	Conventional heating	Microwave heating	Induction heating		
290	0.6552	0.311	1.032	52.53	29.34
330	0.6552	0.3628	1.290	44.63	31.89
370	0.6552	0.4296	1.806	34.43	30.08

The overall process energy balance was calculated based energy content of biomass and products, energy input for pyrolysis as well as catalyst heating. The energy efficiency of the process was calculated based on the total energy input for the process and the energy output received in the form of energy content of products (HHV values). Microwave heating was the most efficient process of all three. Use of microwave reactor for catalyst heating increased the process efficiency by 30% for all temperatures **(Table 3.7)**. Microwave reactor also consumed least power and the percent energy input for microwave power was 35-50% lower when compared to conventional heating.

3.4 Conclusions

Microwave reactor was designed and operated for thermo-catalytic upgrading of pyrolysis vapors using HZSM-5. Microwave heating was found to be both effective and energy efficient compared to conventional and induction heating methods. Rate of deterioration of catalyst mainly due to coking was lower for microwave heating process. Higher aromatic hydrocarbon yield, lower oxygen content and high HHV value of bio-oil was obtained by microwave heating of catalyst. In principle, this heating technique can be used for thermo-catalytic reactions not limited to pyrolysis, provided the catalyst is a dielectric material. Full capacity of the reactor is yet to be completely realized, however, it holds the potential to improve the catalyst heating efficiency significantly and should be further studied for scale up applications.

Chapter 4
Numerical Modeling of Microwave Heating of Porous Catalyst Bed

4.1 Introduction

The domestic and industrial need for energy can be met either via conversion of fossil fuels or by various renewable resources such as solar energy (Glaser, 1968), wind energy (Karki and Billinton, 2004), hydropower energy (Demirba, 2002), geothermal energy etc. These renewable sources are well developed and have been successfully applied in various fields but mostly as standalone facilities. Production of transportation fuel from renewable biomass as an abundant source of energy has gained momentum in past few decades. However, commercial development of a reliable renewable transportation fuel has several limitations. The fuel has to be in liquid state to be operated in combustion engines (spark ignition gasoline or compression ignition diesel engines). It should have chemical and physical properties such as cetane number, octane number, viscosity, flash point, cloud point etc. similar to those of petroleum derived fuels. It should be competitively priced, and it must be able to operate in the engine without requiring too many modifications.

Thermochemical conversion of biomass by pyrolysis to fuel has potential to overcome many of these limitations. Biomass pyrolysis is a thermochemical decomposition of biomass at elevated temperatures in the absence of oxygen (Bridgwater et al., 1999). Although bio-oil produced from fast pyrolysis of biomass has a potential to be directly used as a liquid fuel, this fuel has certain drawbacks such as high viscosity, acidity, high oxygen content etc. The organic condensate produced from pyrolysis is thermodynamically unstable and its thermo-catalytic treatment could resolve these issues. Since pyrolysis and upgrading are endothermic reactions, it is important to develop an efficient heating mechanism.

There are numerous drawbacks for conventional heating of catalyst bed reactors, amongst the most limiting one is the temperature gradient in radial heat transfer of packed bed reactors. Since most conventional reactors are designed to provide heat at the outer region of the packed bed reactor tubes, most of the energy is rapidly consumed by the outer layers, affecting the rate of reaction in the inner layers. This type of heat profile is especially not recommended for upgrading of pyrolysis vapors as the incoming vapors tend to condense on the relatively cooler catalyst area at the center of the reactor, which causes catalyst fouling and a decrease in yield and quality of bio-oil. Moreover, the catalyst on the outer tubular region may heat to very high temperatures which causes the pyrolysis vapors to break down further into incondensable gases rather than bio-oil. A solution to these issues is providing reheaters in between the layers of the catalyst bed. The modification substantially adds to the cost and also adds extra complexity to the reactor design that could hinder some applications. In spite of improved heat- transfer designs, conventional heating technologies lack efficient and optimum use of imparted energy to achieve desired temperature distribution.

Microwave heating has been well established in society for both residential and industrial uses since its invention in the 1940s. Microwaves are a part of the electromagnetic spectrum, and are generally defined as those waves with wavelengths between 0.001m and 1m, corresponding to the frequencies from 0.3 GHz to 300 GHz (Lam and Chase, 2012). Microwave heating is also known as one of the dielectric heating methods due to its effect on dielectric molecules (the other being RF heating). The electric field component interacts with the dipoles within the material being heated which rotate with high frequency generating friction and heat. As mentioned above, traditional heating methods include external heating via conduction, convection, and radiation. During the transient state of conventional heating, a temperature gradient exists such that the surface temperature is significantly greater than the core temperature. Microwave heating, on the other hand, induces heat at the molecular level by directly converting the electromagnetic field into heat, resulting in a temperature gradient, where the core temperature is greater than the surface temperature (Fernandez

et al., 2011). These properties of microwave heating make it a more efficient heating method compared to conventional heating, with a conversion efficiency of electrical energy to heat that can reach 80%-85% (Lam and Chase, 2012) **(Figure 4.1)**.

Due to these advantages, microwave heating has gained popularity not only in the field of food processing but also in organic chemistry, catalytic reactions and other industrial processes. The effect of microwaves on a material is dependent on the dielectric properties of that material; therefore not all materials are heated equally in a given microwave system. In general, there are three ways in which materials can be categorized in terms of their interaction with the electric field portion of the microwave field: (i) insulator, which are microwave-transparent so that microwave pass through the material with little to no losses, (ii) near perfect conductors where microwave are reflected and (iii) absorber where microwaves penetrate the material and are absorbed (Motasemi and Afzal, 2013).

Although there are few mechanisms that could explain the dielectric response to electromagnetic field, dipolar polarization and ionic conduction (Maxwell-Wagner polarization) effect dominates at the microwave frequencies. A polar molecule when exposed to alternating electromagnetic field, tries to realign itself in the direction of the field at a rate equivalent to the microwave frequency (2.5 billion per second for 2450 MHz). For ionic conduction, some free ions tend to move in the direction of the field and on their way collide with other molecules, this collision converts the molecules kinetic energy into thermal energy, thus generating heat. If these ions are in a space bounded by other molecules and cannot freely couple with the changing electric field, the charge accumulates and the energy is dissipated as heat. Both these responses depend on the dielectric properties of the material (i.e. dielectric permittivity) and hold specifically true for liquids, semi-solids and gases. For dry or partially dry solids without dipoles; such as zeolites, carbon based materials, the theory of dipolar rotation and ionic conduction does not entirely explain the microwave heating mechanism. In order to heat in the microwave environment, these materials should be lossy.

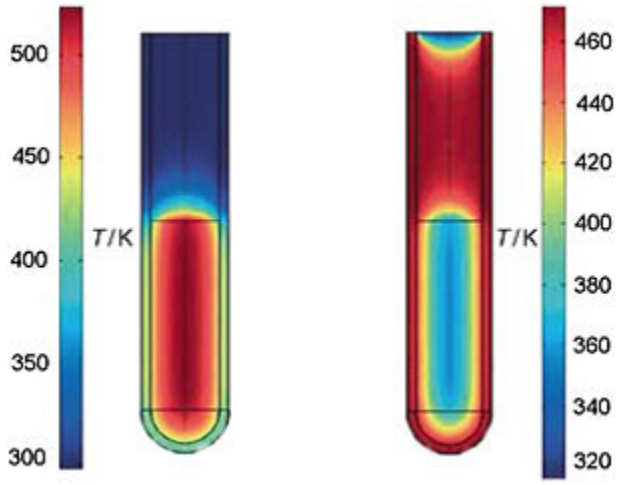

Figure 4.1: Temperature profile of a) microwave heating and b) conventional heating of a dielectric material at same energy input (Schanche 2003)

In other words they should be electrically conductivity ($\sigma > 0$) but not pure conductors ($\sigma \sim \infty$) such as metals that reflect most of the incident microwave radiations. When an electric current flows through a material, some of the energy is converted to heat. This mechanism partially explains the microwave heating of non-polar solids. In certain materials such as carbon, some charged particles such as -electrons that are free to move in the delimited region of the material, a current is induced which produces similar effect as that of ionic conduction. The charged particles vibrate in the constricted region of the material, dissipating heat energy. This effect is also known as the Maxwell-Wagner effect. The microwave heating mechanism in zeolites is not vastly studied. An important study was conducted on microwave heating of zeolites which explains the heating mechanism as ionic rattling effect within the zeolite structure (Komarneni and Roy, 1986). According to the study conducted by OGASHI, the hydrated zeolites when irradiated by microwaves, initially heat due to the moisture present in them. Once the adsorbed moisture is completely desorbed, the dry heated zeolite heats itself directly as zeolites are lossy materials up to 500 $^{\circ}C$ at which point thermal runaway occurs (Ohgushi et al., 2001).

The relation between permittivity and dielectric constant ε' and dielectric loss factor ε'' is given by the complex equation (Gabriel et al., 1998).

$$\varepsilon = \varepsilon' - j\varepsilon'' \tag{4.1}$$

Where the real part (or dielectric constant) ε' is defined as the ability of the material to store imparted microwave energy and the imaginary part (or the dielectric loss factor) ε'' stands for the ability of material to convert the electromagnetic energy into heat. Dependence of dielectric permittivity on frequency and temperature is a complex phenomenon. Frequency dependence of pure polar substances can be expressed using Debyes equation (Hippel, 1954).

$$\varepsilon = \varepsilon'_\infty + \frac{C - \varepsilon'_\infty}{1 + j\omega\tau'} \qquad \varepsilon' = \varepsilon'_\infty + \frac{\varepsilon'_s - \varepsilon'_\infty}{1 + j\omega^2\tau^2} \qquad \varepsilon'' = \frac{(\varepsilon'_s - \varepsilon'_\infty)\omega\tau}{1 + j\omega^2\tau^2} \tag{4.2}$$

Debyes equation can be adapted for non-polar pure materials using Cole-Cole equation (Nelson, 1973),

$$\varepsilon = \varepsilon'_\infty + \frac{\varepsilon'_s - \varepsilon'_\infty}{1 + (j\omega\tau')^{1-\alpha}} \tag{4.3}$$

Where, ε is the complex relative permittivity ε'_∞ stands for relative dielectric constant as ω goes to ∞, ε'_s is the relative static dielectric constant (at $\omega = 0$), τ is relaxation time for a polar molecule in s, ω is the angular frequency, α stands for spread of relaxation times; ($\alpha \in [0, 1]$) and $j = (-1)^1/2$.

Although polar molecules respond to electromagnetic radiation of any given frequency, not all of the responses result in dissipation of energy in the form of heat. At lower frequencies for instance, the electric field components is reversed at a slower pace giving enough time for the molecules to align itself with the changing field, thus little or no energy is dissipated as heat. If the frequency is too high, the field oscillation is too rapid, not giving enough time for the molecules to rotate. The field polarity is reversed before the response of molecules to the previous field is fully received. Hence even the smallest molecule does not respond to the

oscillating field causing a marked decrease in dielectric permittivity. Thus, selecting the right frequency of operation is crucial for efficient heating applications. Other material properties such as viscosity, density, temperature, molecular weight, concentration etc. also affect the response of material to microwave field especially those that are temperature dependent.

Dielectric properties play an important role in calculating energy efficiency of the reaction process. The amount of energy absorbed and dissipated as heat can be given as (Nelson, 1992),

$$P_{abs} = \sigma E^2 = 2\pi f \varepsilon_o \varepsilon'' E^2 \tag{4.4}$$

Where, P_{abs} is volumetric power absorbed (W/m^3), σ is the conductivity (S/m), f is frequency (Hz), ε_0 is the dielectric constant of the vacuum, ε'' 'is relative dielectric loss, E is electric field intensity (V/m).

Apart from increased heating efficiency, microwave heating of catalyst may improve catalyst performance compared to conventional heating. There are reports of increased rate of reaction with the use of microwave heating. One of the explanations of this observation is that microwave heating causes local superheating which in turn increases the molecular activity of the material and subsequent molecular level interaction (Terigar et al., 2010). The lack of adequate measuring techniques for accurate measurement of reaction temperature in the microwave zone could be the cause of hindered growth in this research area (Inoue et al., 2002).

One of the theories explaining the reason for this increase in rate of reaction is related to Arrhenius equation.

$$K = Ae^{\text{-Ea/RT}} \tag{4.5}$$

Where, K is the rate constant, Ea is the activation energy, R is the gas constant, T is temperature and, A pre exponential factor.The ability of microwaves to directly impart energy to the material without conduction or convection via other material can be substan-

tially useful and energy efficient. The frequency factor A represents molecular mobility and depends on the frequency of vibration of reacting molecules at the reaction interface which is directly affected by the microwave irradiation. Increase in frequency factor indicates increased rate of collision, thus, increases the rate of reaction (Lidstrom et al., 2001). Another theory put forth is that the microwave energy affects the activation energy thus affecting the exponential factor increasing the rate of reaction (Lidstrom et al., 2001).

4.1.1 Literature review

Due to the afore mentioned potential advantages of microwave technology applied to chemistry, the technology is now extensively studied to investigate the effect of microwave heating of catalyst in endothermic reactions. (Perry et al., 2002) studied the effect of microwave heating of catalyst in methanol steam reforming reaction both experimentally and numerically (Perry et al., 2002). They developed a 1D heat transfer model in a single pellet and a 2-D model for heat transfer in packed bed tubular reactor. The results were experimentally validated. They concluded that both 1D pellet model and the 2-D tubular reactor model showed elimination of radial heat transfer effects, space gradient and hot spot formation. The experimental results showed improved performance of the catalyst which can be related to uniform heating. (Ioffe et al., 1995) reported improvement in catalyst performance for heterogeneously catalyzed reactions such as conversion of methane (Ioffe et al., 1995). (Bo et al., 2013) studied the effect of microwave heating in catalyzed oxidation of gas phase toluene. They concluded that microwave technology has certain advantages such as rapid heating and steady bed temperature and uniform heating (Bo et al., 2013), which greatly reduce operation cost. (Bolotov et al., 2012) studied the pyrolysis of heavy hydrocarbons under microwave heating of catalysts and estimated the efficiency of microwave power converted to heat energy (Bolotov et al., 2012). (Zhang et al., 2012), studied the catalytic oxygenation of benzene by microwave heating and electric furnace (Zhang et al., 2012) and noted that the catalyst had better catalytic activity under microwave exposure. That study also noted high

oxidation efficiency under microwave heating due to dipolar polarization effects and stable bed temperatures. (Gopalakrishnan et al., 2006) studied the effect of microwave irradiation on oxidation of benzene to phenol over Fe-ZSM-5 catalyst (Gopalakrishnan et al., 2006). They concluded that microwave increases phenol selectivity and decreases catalyst deactivation. However they also noted that microwaves themselves did not seem to play a conclusive role in improvement of the process performance. (Funawatashi and Suzuki, 2003) studied the effect of position on of sample on the electric and temperature fields (Funawatashi and Suzuki, 2003). They observed that the electric field greatly depends on the position of a dielectric material and consequently affect the heating rate. The effect of position was also studied by (Cha-um et al., 2009). They concluded that the rate of heating of dielectric material significantly changes with position of the material in the microwave waveguide (Cha-um et al., 2009).

In order to design an experimental set up for microwave heating of catalyst for pyrolysis vapor upgrading, it is important to understand how the catalyst can be heated in the microwave. Studying the heating patterns of the catalyst bed in the microwave reactor can be helpful for design of the reactor and the operating parameters. For instance, penetration depth of a material is an important parameter to be considered in the design of microwave reactors. Penetration depth is defined as the depth at which 63% ($e^{-}1$) of the incident energy is dissipated (Smith and Hui, 2004). Penetration depth depends on material dielectric properties and frequency of operation and it is given as (Mujumdar, 2007).

$$D_p = \frac{\lambda_0}{\pi \times \sqrt{2\varepsilon'}\sqrt{\sqrt{\left(1+\left(\frac{\varepsilon''}{\varepsilon'}\right)^2\right)}-1}} \tag{4.6}$$

Where, D_p is the penetration depth, λ_0 is the wavelength in free space, ε' is the relative dielectric constant of material, and ε'' is the dielectric loss of material. For cylindrical objects, the penetration depth should be two to three times higher than the diameter of

the material for focused accumulation of electromagnetic density at the center for high Q cavities (Smith and Hui, 2004). If the diameter is much larger than the penetration depth, the material acts as a semi-infinite block where the heating is limited to the surface of the material (Smith and Hui, 2004). The position of the object to be heated with respect to the cavity wall also plays an important role in the efficient heating of the material. Other parameters affecting the heating are frequency and microwave power, single mode or multimode cavity design and flow conditions in the reactor. It is difficult and expensive to optimize these parameters experimentally. For instance, in order to understand which frequency is suitable for a particular catalyst to be heated in a microwave, both 2450 MHz and 915 MHz frequency microwave heaters (allowed by the FCC for ISM use) will have to be tested experimentally. Since each microwave is designed to operate at a particular frequency, completely new microwave reactor and corresponding power supply and magnetron will have to be tested for a new frequency. Thus, a numerical analysis can be employed to understand the effects of these parameters on the process prior to construction of the reactor.

Numerous numerical studies have been conducted to study microwave heating of porous media, with most of them representing food industry applications. (Datta A. and K., 2008), conducted a study to understand the temporal and spatial temperature and moisture patterns in food cooked in a combination of microwaves and hot air (Datta A. and K., 2008). (V. Nicolas et al., 2010) studied the heat and mass transfer in bread baking using COMSOL multiphysics (V. Nicolas et al., 2010). For the non food industry related applications, (Chen et al., 2013) numerically studied the effect of microwave power on catalyst bed heating and methane decomposition reaction (Chen et al., 2013).

4.1.2 Dielectric properties of HZSM-5 catalyst at different temperatures

As mentioned earlier, the dielectric properties play an important role in the microwave heating of material. Knowledge of dielectric properties of material under treatment gives a clear understanding of how a particular material will heat under the influence of elec-

tromagnetic waves. Depending on the material, dielectric properties may be temperature and frequency dependent. The dielectric properties of HZSM-5 powder was measured using an Agilent ENA series E5071C Network Analyzer and Agilent 85070E dielectric probe kit (Agilent Technologies, Inc. Santa Carla, CA) using a slim form open-ended probe method in a 201-point frequency sweep from 280MHz to 4500 MHz. The network analyzer was controlled by Agilent 85070E dielectric kit software (Agilent Technologies, Inc. Santa Carla, CA) and calibrated using the 3-point method (short-circuit, air and water at 25 $^{\circ}C$). The NaZSM-5 catalyst was calcined in air at 550 $^{\circ}C$ for 5 hours. The powder was then filled in a tube surrounded with a heating tape. Dielectric properties were measured at nine different temperatures ranging from 250 $^{\circ}$ - 700 $^{\circ}C$. **Figure 4.2** shows change in dielectric constant and dielectric loss with frequencies and temperatures.

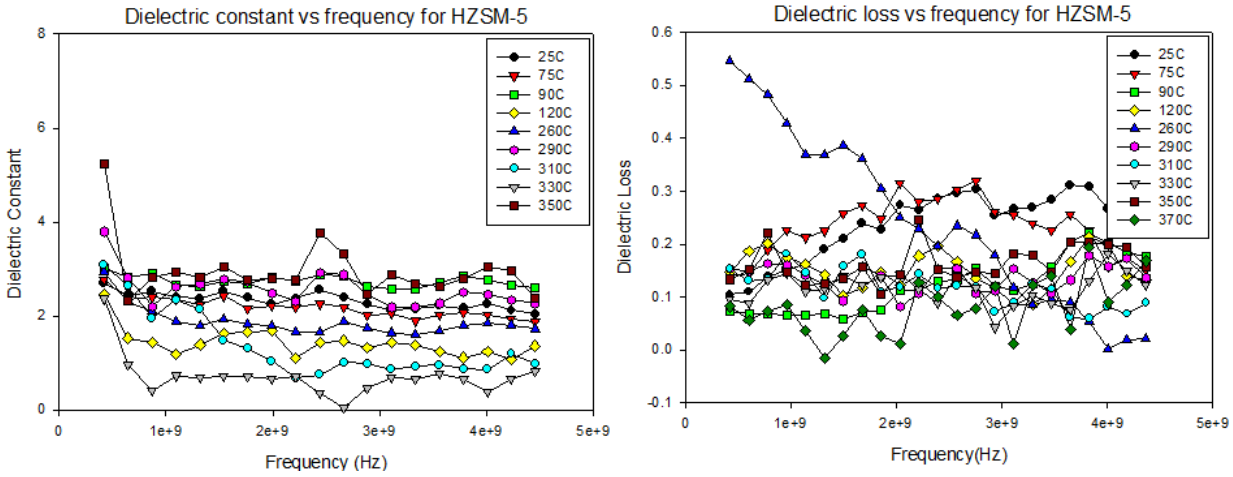

Figure 4.2: Dielectric properties of HZSM-5 powder at different temperatures and frequencies

No significant difference was observed with the change in frequency or temperature. **Figure 4.3** shows the electrical conductivity, dielectric loss and dielectric constant values at the 2450 MHz frequency of interest for different temperatures. The dielectric constant values for all temperatures were between 1.0- 3.0 S/m. Electrical conductivity of the catalyst was calculated for different temperatures.

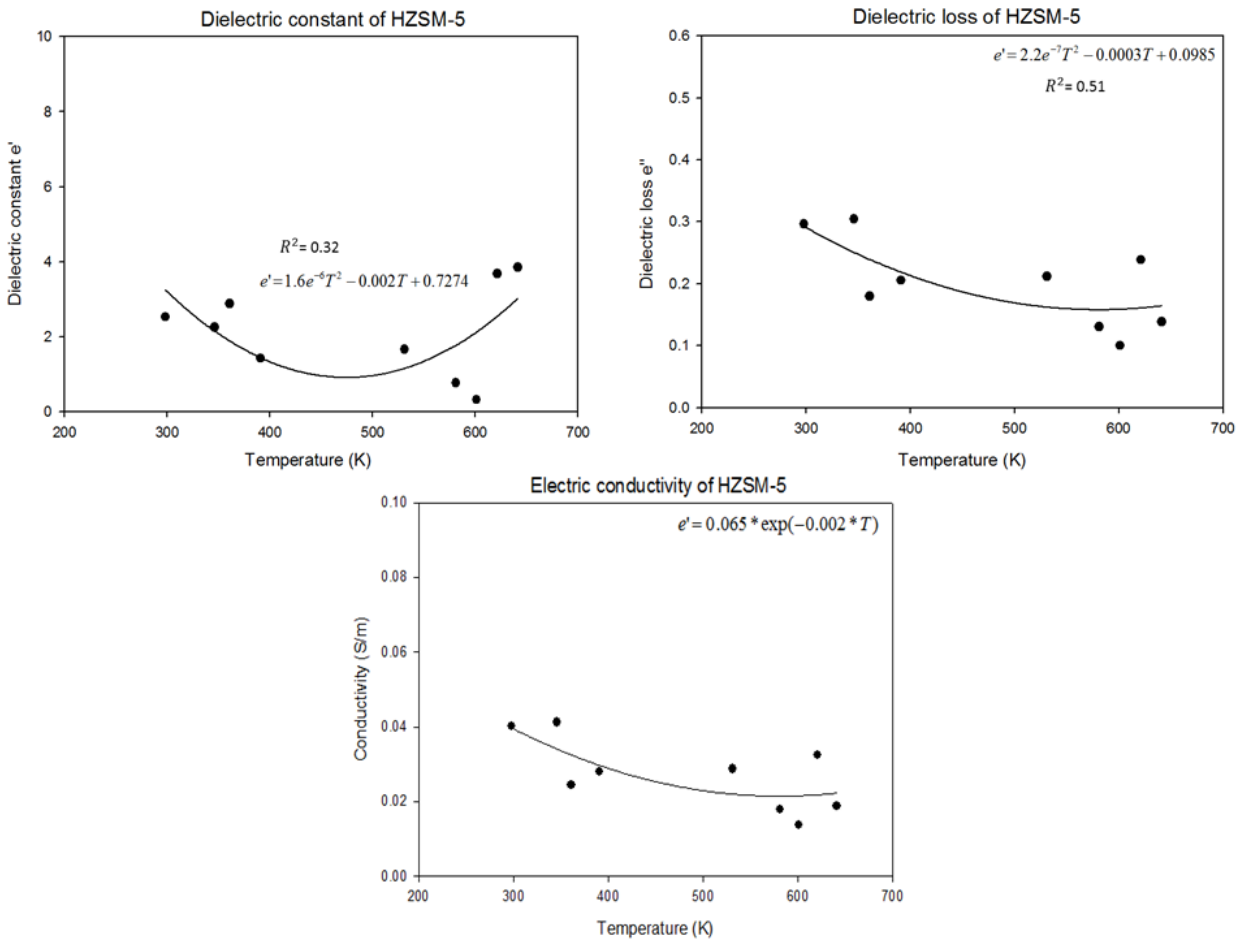

Figure 4.3: Electric conductivity, dielectric loss and dielectric constant of HZSM-5 at 2450MHz frequency at varying temperatures

Electric conductivity is given by,

$$\sigma = 2\pi f \varepsilon_0 \varepsilon'' \tag{4.7}$$

Where, f is frequency (Hz), ε_0 is the dielectric constant of the vacuum, ε'' is relative dielectric loss of material. For a material to undergo dielectric heating under microwave radiation, the conductivity of the material should be higher that 0; i.e. the electric field flows through the material. When electric field flows through the material, some of the energy is converted to heat. Materials with conductivity $\sigma = 0$ are called lossless material (air, vacuum). Material with very high conductivities $\sigma >> 0$, are called conductors (Metals)

and materials with medium range conductivities $\sigma > 0$ are called lossy materials; materials that readily heat in a microwave. Since the conductivity of catalyst is slightly greater than 0, it is categorized as a lossy material **(Figure 4.3)**

4.2 Objective

The objective of this study was to investigate the microwave and conventional heating of a porous catalyst bed in order to understand the heat and flow profiles within the reactor. The effect of size, shape and position of catalyst bed inside the microwave on the temperature attained and the overall heating profile was investigated.

4.3 Model development

COMSOL 5.1 multiphysics software was used to solve the multiphysics numerical problem. The heat transfer and flow through porous media was coupled with RF electromagnetics module by extracting the heat source term Q for the heat transfer problem from the electromagnetics. Main steps in model development were geometry generation, defining boundary and subdomain settings, mesh generation, solver definition, solving and post processing.

4.3.1 Governing equations

4.3.1.1 Electromagnetics

The governing equation for electromagnetic wave propagation in a medium is given by Maxwells equations.

$$\nabla \cdot \vec{D} = \rho \tag{4.8}$$

$$\nabla \times \vec{E} = -\frac{\partial \vec{B}}{\partial t} \tag{4.9}$$

$$\nabla \cdot \vec{B} = 0 \tag{4.10}$$

$$\nabla \times \vec{H} = \vec{j} + \frac{\partial \vec{D}}{\partial t} \tag{4.11}$$

$$\vec{d} = \varepsilon' \varepsilon_0 \vec{E} \tag{4.12}$$

$$\vec{B} = \mu' \mu_0 \vec{H} \tag{4.13}$$

$$\vec{j} = \sigma_e \vec{E} \tag{4.14}$$

Where, E is the electric field; B is the magnetic flux density; ρ is electric charge density; j is the electric current; σ_e is electrical conductivity; D is electric displacement; ε_0 is the permittivity of free space $(8.854x10^{-12})$ F/m; H is magnetic field intensity; ε' is the relative dielectric constant; t is time (s); μ' is relative permeability of material; μ_0 is magnetic permeability of vacuum $(4\pi \times 10^{-7})$ N/A^2.

To determine the electric field distribution in a TE10 rectangular waveguide, a wave equation derived from Maxwells equations is solved,

$$\nabla \times \left(\frac{1}{\mu'} \nabla \times \vec{E} \right) - \frac{\omega^2}{c} (\varepsilon' - j\varepsilon'') \vec{E} = 0 \tag{4.15}$$

Total volumetric power generation due to microwave is calculated by the following equation,

$$Q_{gen} = \sigma_e E^2 = 2\pi f \varepsilon_0 \varepsilon'' E_{rms}^2 \tag{4.16}$$

Q_{gen} is power absorbed from microwave, which is used as a heat generation term in Fourier equation (W/m^3), σ_e is the conductivity (S/m), f is the frequency (Hz),

4.3.1.2 Heat transfer

The source of heat was direct heating of catalyst bed due to electromagnetic heating. Generally, heat transfer in porous media is given by the following equation;

$$(\rho C_p)_{eq}\frac{\partial T}{\partial t} + \rho C_p u \cdot \nabla T = \nabla \cdot \left(k_{eq}\nabla T\right) + Q \tag{4.17}$$

Where ρ and C_p are the fluid density and heat capacity of the fluid. Whereas $(\rho C_p)_{eq}$ is defined as the equivalent volumetric heat capacity at constant pressure. k_eq is the equivalent thermal conductivity, u is defined as the Darcys velocity expressed as volume flow rate per unit cross sectional area; Q is the heat source. The equivalent terms are related to the respective property of the solid and the fluid. Thus, k_eq is the equivalent solid-fluid conductivity given by,

$$k_{eq} = \theta_s k_s + \theta_L k \tag{4.18}$$

And the volumetric heat capacity for solid-fluid system is given by

$$(\rho C_p)_{eq} = \theta_s \rho C_p + \theta_L \rho C_p \tag{4.19}$$

where $\theta_s + \theta_L = 1$

Where, θ_s and θ_L are volume fractions of solid and fluid material respectively. However, these equations assume Local Thermal Equilibrium within the solid and fluid material within the porous body. As the heat is generated within the porous material, this assumption is no more valid and the solid and fluid temperatures in the porous domain are not in equilibrium. The problem then needs to be formulated by coupling the heat equations in the solid and fluid subdomains through a transfer term proportional to the temperature difference between the fluid and the solid.

The Local Thermal Non-Equilibrium (LTNE) Equations are given as follows;

For solid phase;

$$(1-\theta_s)(\rho C_p)_s \frac{\partial T_s}{\partial t} = (1-\theta_s)\nabla \cdot (k_s \nabla T_s) + (1-\theta_s)q_s + h(T_L - T_s) \tag{4.20}$$

For fluid phase;

$$\theta_s(\rho C_p)_f \frac{\partial T_f}{\partial t} + (\rho C_p)_f u \cdot \nabla T_f = \theta_s \nabla \cdot (k_f \nabla T_f) + \theta_s Q_f + h(T_s - T_f) \tag{4.21}$$

Where, θ_s is the solid volume fraction, ρ is the density, C_p is the heat capacity, k_s and k_f are solid and fluid thermal conductivities, q_s is the interstitial convective heat transfer coefficient, u is the velocity and h is the heat transfer coefficient. The critical step in solving this equation is the determination of heat transfer co-efficient h. There are numerous studies reported which have established a correlation for appropriate value of h (Alazmi and Vafai, 1999; Bejan, 1995; Minkowycz et al., 1999; Saito and de Lemos, 2005). In general heat transfer coefficient is given by $h = a_{fs}h^*$, where a_{fs} is the specific surface area given by $a_{fs} = 6(1-\varphi)/d_p$, and h^* is given as;

$$\frac{1}{h^*} = \frac{d_p}{Nu_{fs}k_f} + \frac{d_p}{\beta k_s} \tag{4.22}$$

Where d_p is the particle diameter, Nu_{fs} is the fluid to solid Nusselt number. β is 10 for spherical particles. Nusselt number for the solid to fluid interface is dependent on Reynolds number. For $R_e > 100$ an expression for Nusselt number is given by (Handley and Heggs, 1968);

$$Nu_{fs} = \left(\frac{0.255}{\varphi}\right) P_r^{1/3} Re_p^{2/3} \tag{4.23}$$

This equation is valid for catalyst bed packing of various shapes including spherical, cylindrical and flat plate. COMSOL calculates the Reynolds number based on the velocity in porous region. There are various other parameters that affect the heat transfer between

solid and fluid in the porous region such as effect of turbulent and transient flows, variable porosity, thermal dispersion and effect of pressure and viscous dissipation. These effects will not be considered in the given study. The heat transfer in open regions was solved using regular conduction convection equations as applicable.

4.3.1.3 Free and porous media flow

The flow of gases through the free and porous region of the tube was solved using their respective equations (Navier-Stokes and Brinkmans equation) as follows. The flow of gases through open regions in described by Navier-Stokes equation;

$$\rho_m\left(\frac{\partial u}{\partial t} + u \cdot \nabla u\right) = -\nabla P + \mu\nabla^2 u + F \tag{4.24}$$

Continuity equation is given as;

$$\nabla \cdot \vec{u} = 0 \tag{4.25}$$

Where; u is velocity of fluid in (m/s); μ is viscosity in $(P_a \cdot s)$; P is pressure (P_a); F is other forces such as gravity or centrifugal force per unit volume (N/m^3)

Whereas, Brinkman equation is used to describe the flow of gases through porous matrix and is given by;

$$\frac{\rho}{\theta}\left(\frac{du}{dt} + (u \cdot \nabla)\frac{u}{\theta}\right) = \left[-\nabla P + \frac{\mu}{\theta}\nabla^2 u - \frac{2\mu}{3\theta}\nabla^2 u\right] - \left[\mu k^{-1} u + \beta_F |u|^2 + \frac{Q_{br}}{\theta^2} u\right] + F \tag{4.26}$$

Where, θ is the porosity, k is the relative permeability, β is the effective viscosity and Q is the total discharge.

4.3.2 Assumptions

High frequency electromagnetism module was coupled with heat transfer in porous medium and flow through porous media using COMSOL Multiphysics 5.1. To reduce the complexity

of the model, certain assumptions were made for the model development.

- The porous media was considered uniformly porous throughout the catalyst bed
- Thermal properties were constant with changing temperature
- No chemical reaction or phase change is taking place.
- The quartz tube with catalyst bed placed inside the microwave was considered completely transparent to the microwaves.
- Waveguide walls are perfect conductors
- Average inlet velocity was 0.1 m/s

4.3.3 Geometry

A 3-D geometry of a pilot scale microwave waveguide was built in COMSOL 5.1 **(Figure 4.4)** corresponding to the physical construct existent at LSU. The microwave system was powered by a 1.2 kW, 2450 MHz continuous generator with a reactor in a traveling wave configuration. The physical construct was a travelling waveguide manufactured by Industrial Microwave Systems (IMS), Inc., Morrisville, NC. The design consisted of an aluminum waveguide of dimensions 1.37 m long, 0.106 m wide and 0.053 m deep. The porous catalyst bed was placed inside a quartz tube with 0.014 m radius and 0.49 m length sitting at the center of the waveguide. The catalyst bed has a 0.014 m radius and is 0.25 m long, initially placed at the geometrical center of the quartz tube **(Figure 4.4)**.

4.3.4 Boundary conditions

4.3.4.1 Electromagnetic Waves

The microwave power was set at 400 W for all combinations investigated. The electromagnetics wave module was active in all domains. The microwave energy was supplied to the

cavity through the rectangular waveguide at port one in TE10 mode electric. The dielectric properties of the catalyst bed were measured as described above and defined in the model, the dielectric properties were temperature dependent and the electrical conductivity was given by equation $\sigma = 0.065 * exp(-0.002 * T)$. Scattering boundary conditions were defined at the outlet and inlet of the quartz tube in order to avoid undesired reflections and perturbations in the field caused by sudden discontinuity in the waveguide. A continuity boundary condition was applied to all the internal boundaries of the domains.

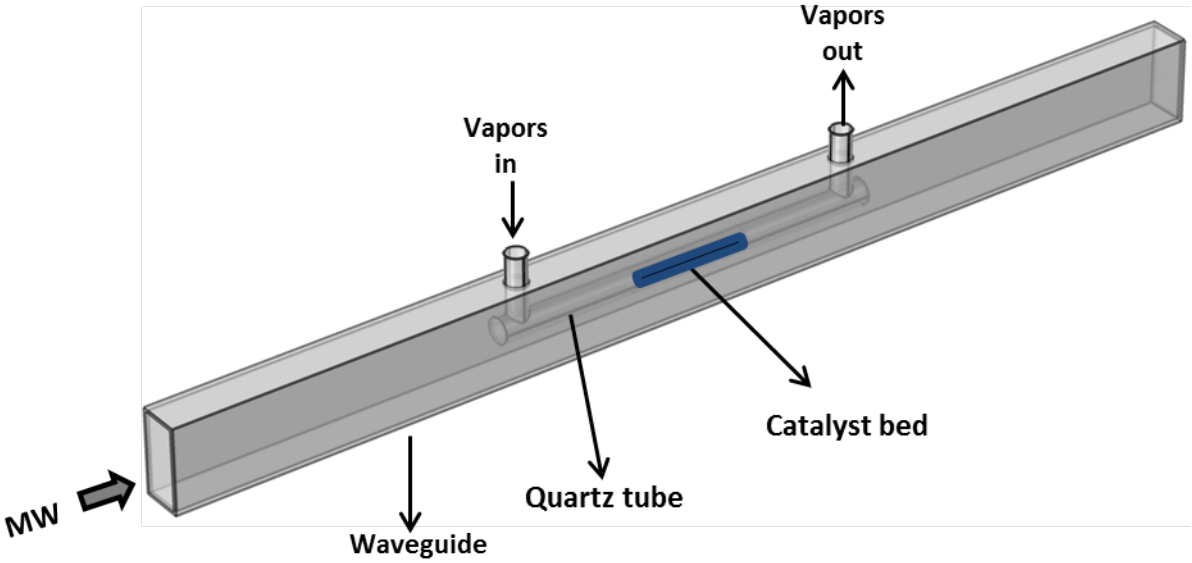

Figure 4.4: Geometry of microwave system used to heat porous catalyst bed

4.3.4.2 Heat transfer in porous media

Heat transfer in porous media module was coupled with the electromagnetics and flow module. The porous matrix was the catalyst bed whose porosity was measured in lab to be 0.67. The density, thermal conductivity and specific heat of the material were obtained for material properties from Zeolyst International. The density of the catalyst was 720 kg/m^3, the thermal conductivity was 0.12 W/m^2K and the specific heat was 1369 $J/(kg^\circ K)$. Heat source Q was set as the electromagnetic power loss density calculated from the electromagnetics module.

Convective cooling was defined for the outer walls of the waveguide and quartz tube walls. Conjugate heat transfer was active in all domains.

4.3.4.3 Free and porous media flow

The laminar flow module was active in the quartz tube only. The inlet velocity of the fluid was measured as 0.1 m/s, and the inlet temperature was 100 $°C$. The porosity was determined to be 0.67 and was assumed to be uniform throughout the catalyst bed.

4.3.5 Mesh generation

The element size requirement for solving the electromagnetic problem is that the maximum grid element size (S_max) should be less than half the wavelength. This requirement, known as the Nyquist criterion is defined as,

$$S_{max} < \frac{\lambda}{2} = \frac{c}{2f\sqrt{\varepsilon'\mu'}} \tag{4.27}$$

Where, λ is the wavelength in m, f is the frequency in Hz, c is the speed of light in vacuum (m/s), ε' is the relative dielectric constant, and μ' is the relative permeability. Based on this criterion, the default fine mesh size was used where the maximum element size was set conservatively at 0.00614m in the waveguide and the maximum element size was set to 0.00116 m for quartz tube and porous media. The models were tested at 3 different mesh sizes of (cavity element number, reaction tube element number) = (243599, 32229), (306159, 41004), (490640, 81895) and the mesh independence for both microwave and conventional heating models was established.

4.3.6 Solver used

The frequency domain was used to solve the wave equation in the radio frequency module. The frequency was set to 2.45GHz, which is the operating frequency of the microwave. The

stationary solver was used to solve heat transfer and fluid flow equations in porous media to obtain the temperature profiles.

4.3.7 Methods

A preliminary study was conducted to study the effect of sample size, shape and position inside the microwave cavity. A numerical model was developed using COMSOL Multiphysics 5.1 studying the effect of electromagnetic irradiation on porous catalyst bed for this purpose. Gas flow through the porous media was not considered for the preliminary study. The catalyst used is a dielectric material and readily heats up in a microwave reactor. Two shapes of catalyst bed were investigated to study the effect of shape on the temperature profile block and cylindrical. Since the position of catalyst bed inside the reactor plays a crucial role in the uniform heating of catalyst, five different positions were studied;

- center of the waveguide
- base of the waveguide (z=-0.03 m),
- upper edge of the waveguide z=0.03 m,
- z=-0.01 m and 0.02 m

The effect of size of the catalyst bed was also tested by designing a smaller diameter tube while maintaining the volume of the catalyst bed. The new design was also tested for 3 different positions: center of the waveguide z=0,) z=-0.01 and, z=-0.02.

A more thorough secondary study was performed where the flow of gas through the quartz tube was taken in to account. The conjugate heat transfer equation was solved for porous domain where the solid and fluid temperatures are not in equilibrium. The average velocity of the incoming gas was 0.1 m/s. The incoming gas temperature was 100 $^{\circ}C$ and external atmospheric temperature was 25 $^{\circ}C$. A conventional heating model was also developed for comparison. Experimental temperatures at three locations were also matched for model

validation. Due to limitations with temperature measurements within the microwave cavity, only two locations were chosen for temperature measurement using IR pyroprobe sensors. The IR probes were calibrated for quartz glass transparency and emissivity. To test the grid independence (sensitivity analysis with respect to mesh size) of the models, the models were tested at 3 different mesh sizes of (cavity element number, reaction tube element number) = (243599, 32229), (306159, 41004), (490640, 81895). The distribution of temperature along the centerline of the catalyst bed in x direction is plotted in **(Figure 4.5)**.

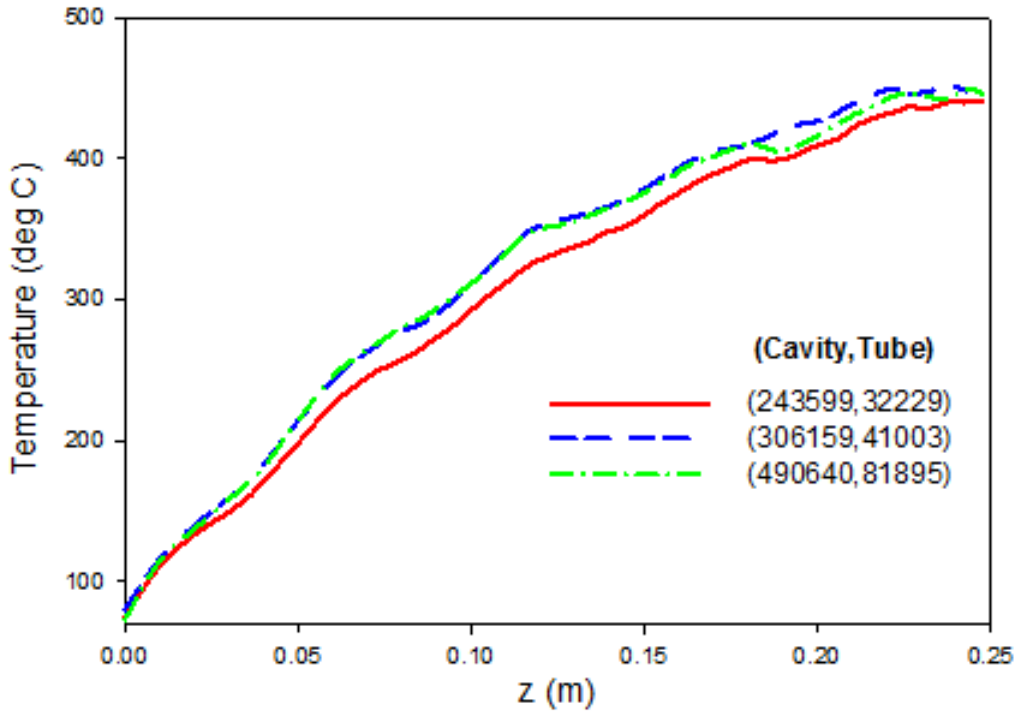

Figure 4.5: Temperature distribution along the centerline of the reaction tube at three different grid systems

The difference in temperature distribution between all three grid sizes is low, but it is especially negligible between the second (306159, 41003) and third grid size (490640, 81895) and satisfies the grid independence.

4.4 Results and discussion

4.4.1 Priliminary study

4.4.2 Effect of position of catalyst bed

We studied three different locations of dielectric material when inserted into the existing quartz reactor a) center of the cavity (z=0), b) base of the waveguide z=-0.03m) and, c) top of the waveguide z = 0.03m. **(Figure 4.6)(Figure 4.7)**.

If the catalyst bed is moved close to the base of the waveguide by 3 cm, most of the electric field is concentrated only in the upper region of the catalyst bed, leaving the base of the catalyst bed unheated **(Figure 4.8)**. The maximum electric field intensity in the catalyst bed was about 10000 V/m, similar to the case when the catalyst bed is placed in the center of the cavity, but now the corresponding highest temperature achieved is 654.46 $^{\circ}C$, because only a fraction of the catalyst is absorbing the energy. However, for the same incident power, higher temperature is achieved when the bed is close to the base of the waveguide compared to the center. This could be because, since some of the catalyst material is outside the electric field area, the energy absorbed is limited to the upper part of the catalyst bed. Only the top fraction of the catalyst bed, the part closer to the center of the waveguide absorbs most of the incident power and higher temperature is achieved (Vadivambal and Jayas, 2010).
In the case where the dielectric catalyst bed in placed at the center of the cavity, the electric field intensity is observed to decrease as the microwaves travel through the dielectric material. The electric field is weaker inside the dielectric material than in the empty cavity. The temperature distribution is consistent with the distribution of the electric field; the heating rate of dielectric in a microwave field is proportional to the square of the electric field. The maximum electric field intensity in the catalyst bed was approximately 10,000 V/m and the corresponding temperature was 472.47 $^{\circ}C$ **(Figure 4.8)**.

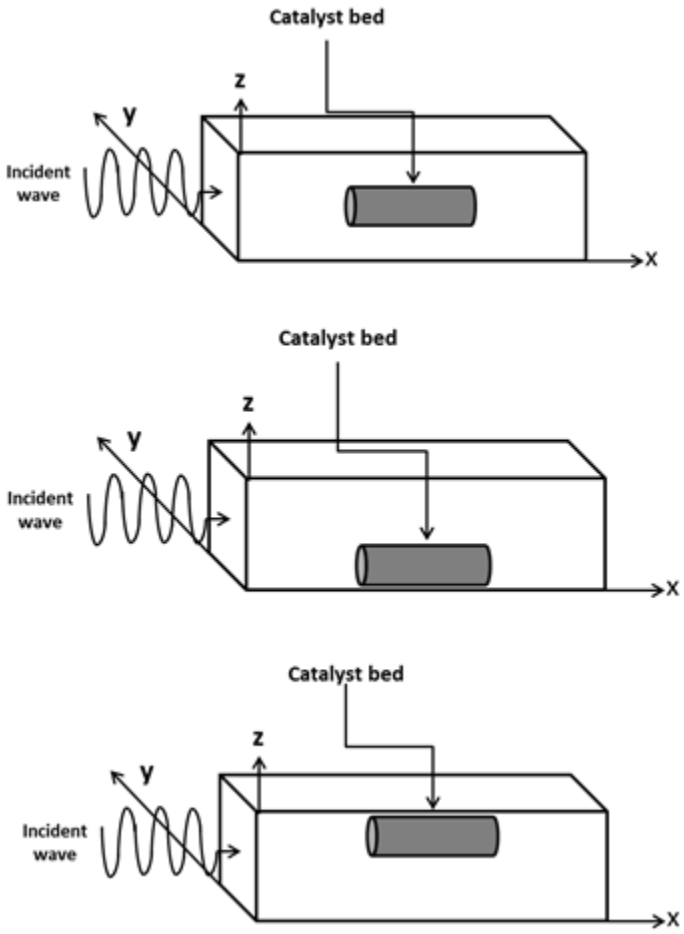

Figure 4.6: Position of catalyst bed within the waveguide a) center (z=0), b) base (z = -0.03) and, c) top (z = 0.03)

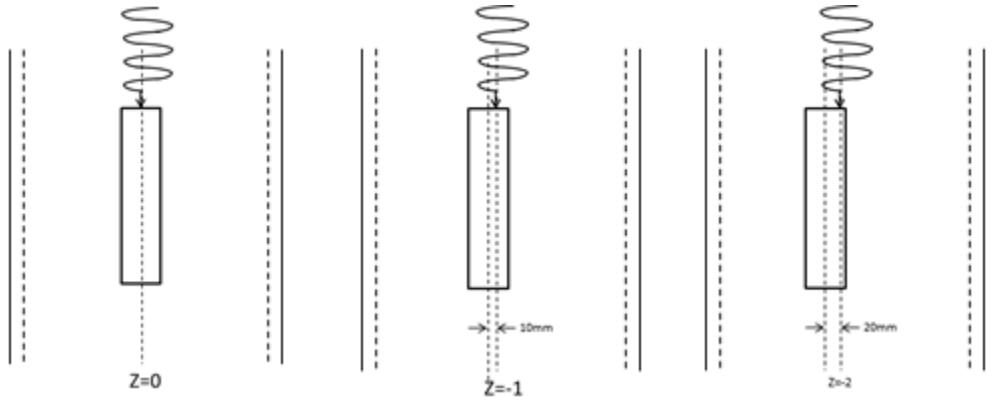

Figure 4.7: Position of narrow catalyst bed inside the cavity a) center (z = 0), b) 10 mm away from center and , c) 20 mm away from center

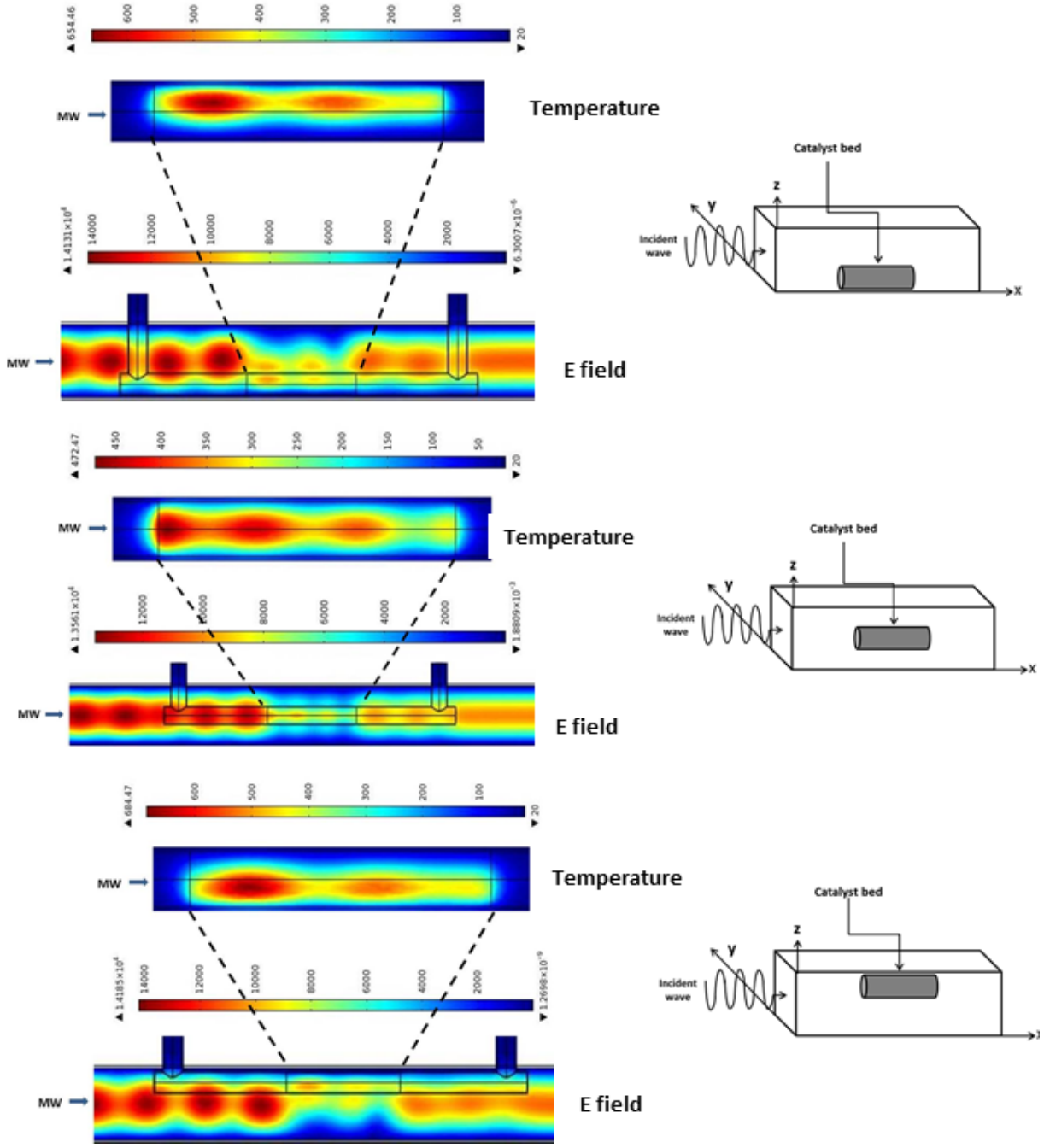

Figure 4.8: Electric field (V/m) and temperature profile for catalyst bed at a) base of the cavity (z =-0.03), b) center and c) top of the cavity (z =0.03)

It is also observed that most of the energy is absorbed at the side of the catalyst bed located towards the incident wave and that the temperature decreases further down the bed **(Figure 4.8)**. This can be explained by the fact that most of the power is absorbed by the highly lossy catalyst bed, as the thickness of the bed increases, power decreases faster, resulting in lower temperatures, since more volume of dielectric is available at the front end (towards the incident wave) which reduces the electric field intensity downstream.

Similar electric field distribution and temperature profile is observed when the catalyst bed is positioned close to the top of the waveguide (z=0.03 m) **(Figure 4.8)**. Since most of the energy is concentrated in the lower part of the catalyst bed, the upper catalyst area is not heated. The maximum electric field intensity in the catalyst bed was about 10000 V/m and the corresponding maximum temperature achieved is 684.47 $°C$. Higher temperature is achieved when the catalyst bed is placed away from the center. The uneven heating in the microwave is a result of two phenomena; one due to the occurrence of a standing wave and second due to rapid decay of microwaves and uneven exposure of the catalyst mass to the incident microwaves (Cha-um et al., 2009; Vadivambal and Jayas, 2010).

Figure 4.9 shows the temperature profile of the catalyst bed in YZ direction at the center of the catalyst bed. It can be clearly observed that the hot spot is at the center when the position of the catalyst bed is in the center of the waveguide. However, as the position of the catalyst bed is changed, the hot spot position changes.

For the bed position base and top, a significant part of the catalyst bed remains cooler creating a larger temperature gradient which is highly undesirable. However, the temperature gradient greatly reduces when the catalyst bed position is 20 mm off from the center.

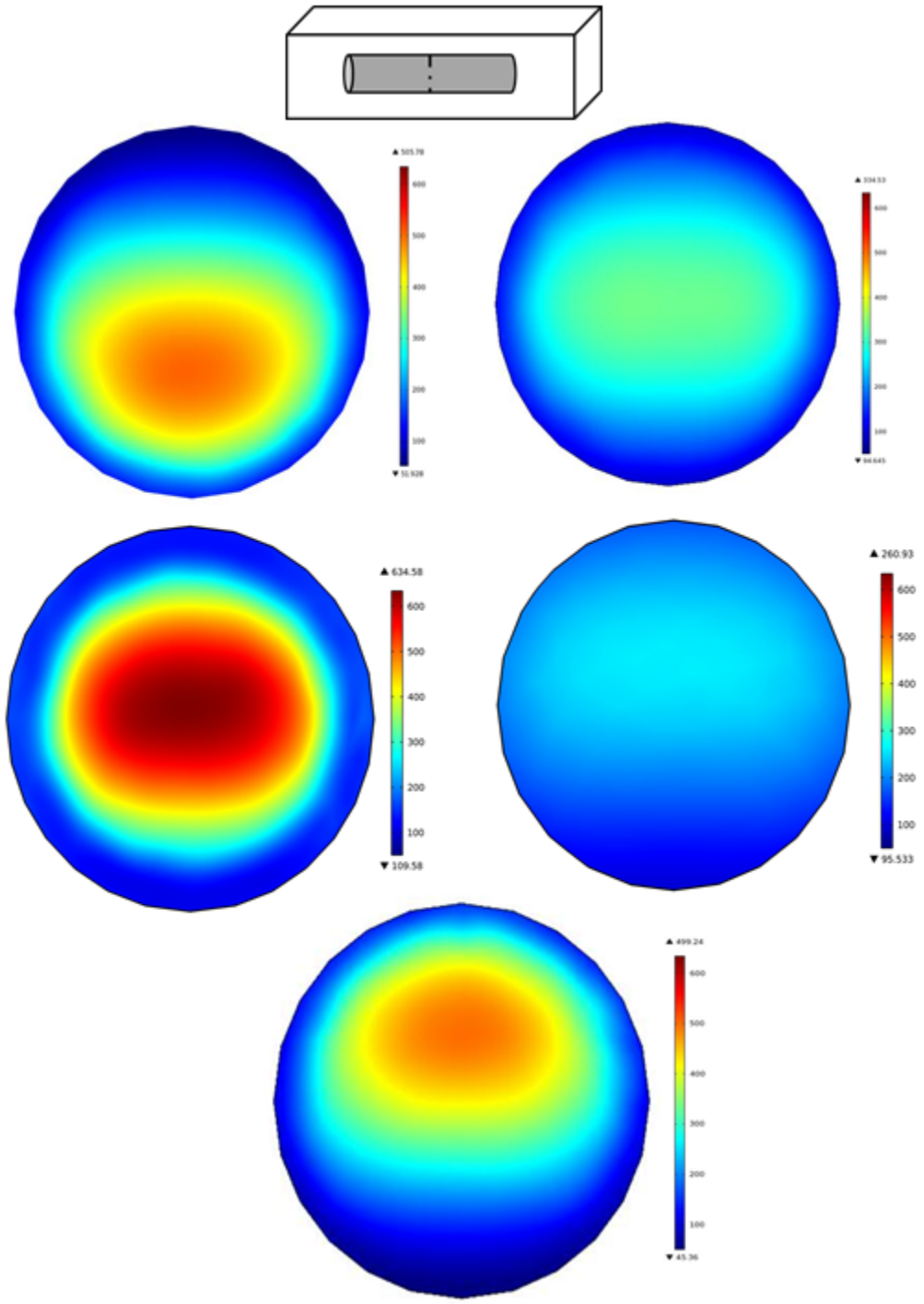

Figure 4.9: Temperature profile in YZ-direction at the center of the catalyst bed. The catalyst bed position is a) top of the waveguide z=0.03m, b) center of the waveguide z=0, c) 10 mm off from the center z = -0.01m, d) 20mm off from the center of the waveguide z = -0.02m and, e) base of the waveguide z=-0.03m

4.4.3 Effect of catalyst bed dimensions

We studied the effect of dimension of sample on microwave heating. The catalyst bed was diameter was reduced while keeping the volume constant by increasing the length of the bed. As opposed to the earlier model with higher diameter catalyst bed, no cold spots were observed for the new geometry **(Figure 4.10)**. Higher temperature observed at the surface where the microwaves enter the catalyst bed, but this temperature was lower (about half) than that observed in the thicker catalyst bed.

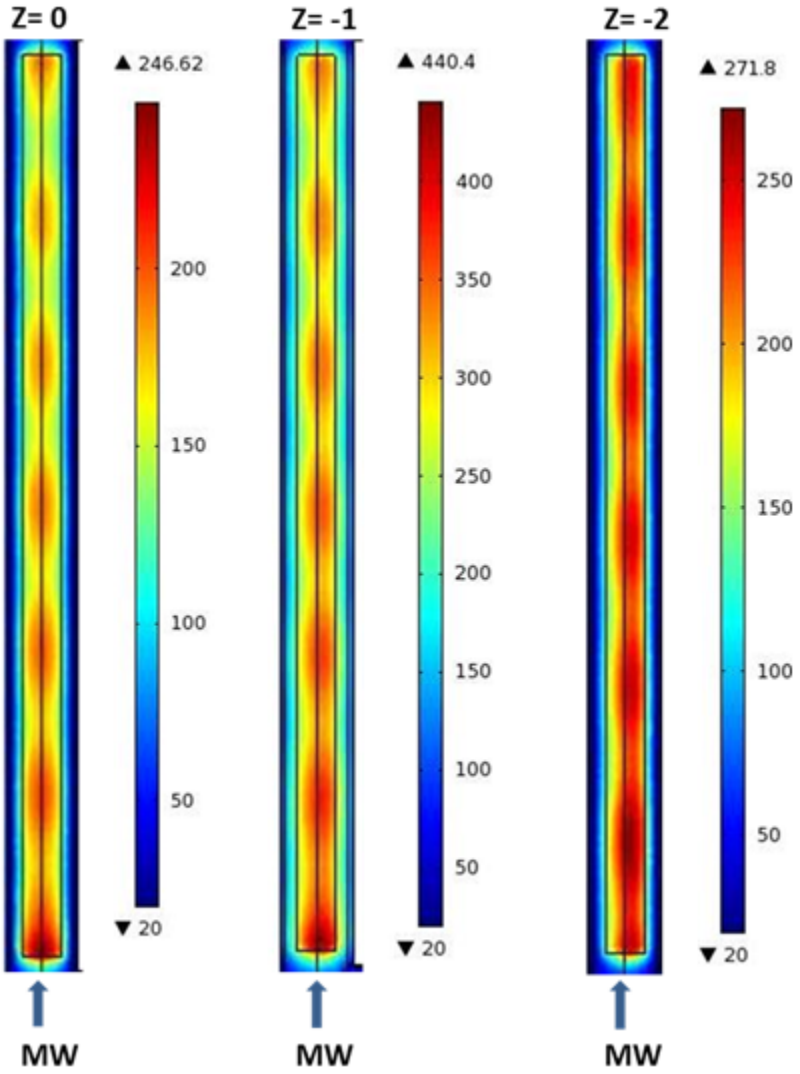

Figure 4.10: Temperature profile for narrow catalyst bed at different positions a) center (z=0), b) 10 mm away from center (z=-0.01) and 20 mm away from center (z=-0.02)

Moreover, no catalyst bed part was left unheated **(Figure 4.10)**. This could be because, since the thickness of the sample decreased, catalyst bed length increased and microwave absorption was evenly distributed along the length of the bed as opposed to being absorbed all upfront in the thicker catalyst bed, the ratio of penetration depth to the bed diameter changed and microwaves were absorbed along the complete length of the catalyst bed. The non-uniform heating of microwave that is attributed to rapid decay of microwaves can be controlled by changing the dimensions of the dielectric sample. A general trend is that as the sample volume increases, the rate of temperature rise decreases. However, if the thickness of the sample is smaller than the penetration depth of the sample, even with larger volume, a higher rate of temperature rise can be obtained **(Figure 4.11)**.

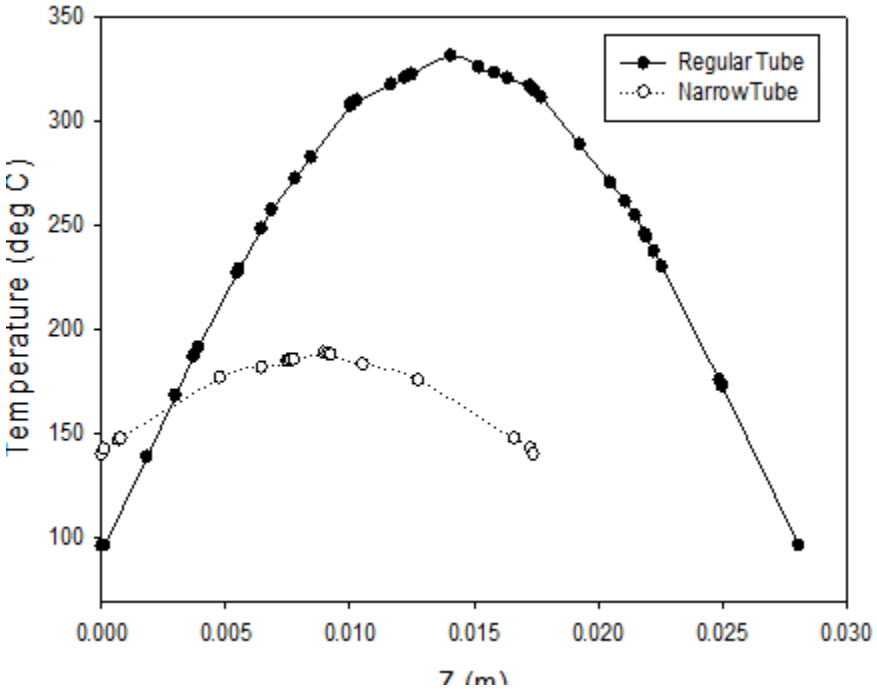

Figure 4.11: Change in temperature at the center of the catalyst bed in z-direction for regular sized and narrow catalyst bed

If the penetration depth of the sample is greater than the thickness of the sample, it causes interference to the waves that are reflected from sample-air interface due to the difference in air and sample dielectric properties. This reflection and transmission at the interfaces

contribute to the resonance of standing waves inside the porous sample and the electric field distribution does not possess exponential decay from the surface, eventually decreasing the rate of temperature rise (Cha-um et al., 2009). It is also noted that the temperature distribution was more uniform when the sample was placed 20mm away from the center **(Figure 4.10)**.

4.4.4 Effect of sample shape

We investigated different shaped catalyst tubes **(Figure 4.12)**. We studied the effect of brick shaped sample and compared the results with the cylindrical sample of same volume **(Figure 4.12)**. More uniform temperature distribution was observed for bricked shaped sample compared to cylindrical sample **(Figure 4.12)**.

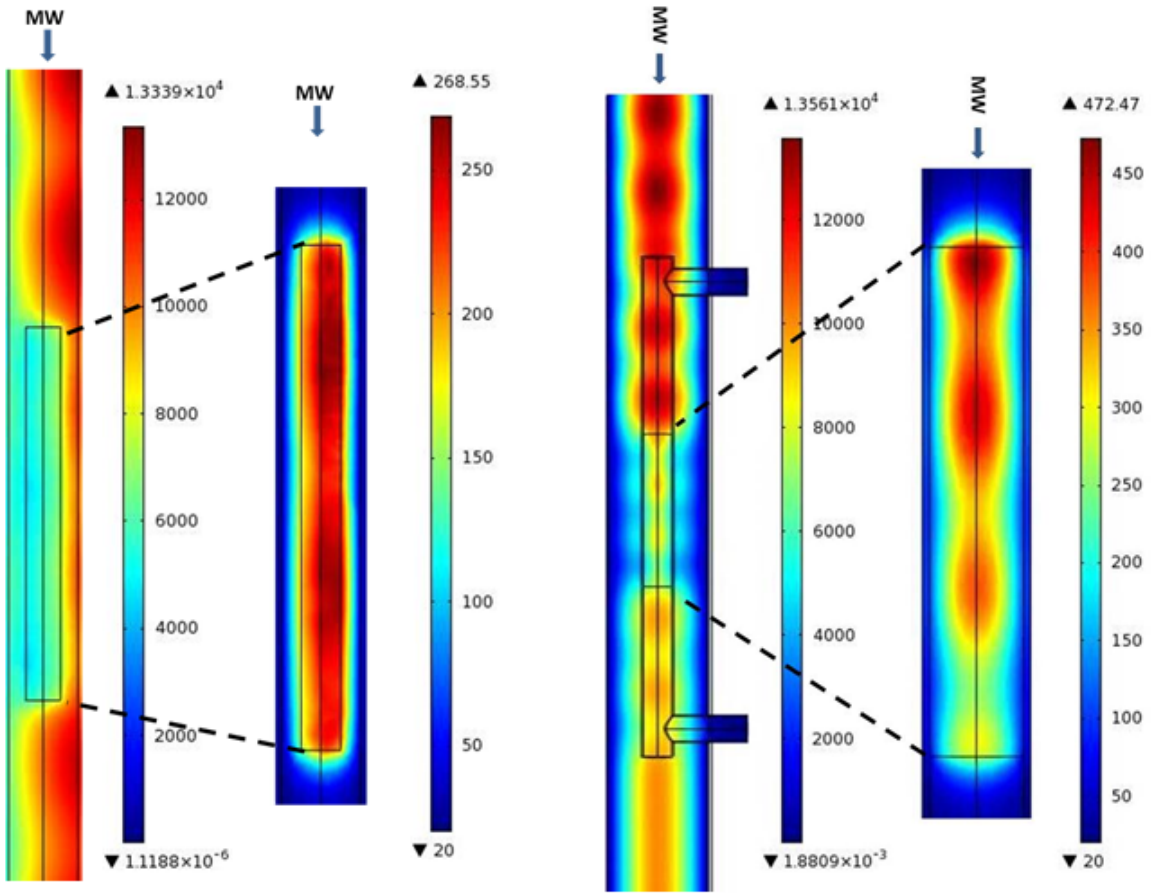

Figure 4.12: Electric field (V/m) and temperature ($°C$) in a) brick shaped catalyst bed and, b) cylindrical catalyst bed both placed in the center of the cavity

A sharp rise in temperature was observed in the z direction at the center of the sample. The effect of sample shape is studied by many researchers (Vadivambal and Jayas, 2010; Vilayannur et al., 1998). (Vilayannur et al., 1998) studied three different shapes; cylindrical, brick and hexagonal prism. They concluded that for a brick shaped sample, the heating is mostly concentrated on the corners of the samples as opposed to the center in case of cylindrical samples (Vilayannur et al., 1998).This effect was also observed in the presented study where a cylindrical sample showed higher temperature at the center and cooler temperature zones at the corners.

4.4.5 Secondary study

The thorough secondary study included the free flow and flow through porous media of pyrolysis gases entering at 100 $^{\circ}C$. **Figure 4.13** shows the temperature profiles for microwave and conventionally heated catalyst bed. The temperature of the entering fluid was 100C. For the conventional heating model, the walls of catalyst bed were maintained at a constant temperature of 370 $^{\circ}C$. The temperature along the x-axis is plotted **(Figure 4.14)**. The temperature at the core of the catalyst bed is higher for microwave heating and lower towards the wall. However, for conventional heating, higher temperature is obtained at the walls of the catalyst bed and the temperature reduces towards the center.

Due to the local thermal non-equilibrium condition, the heat is carried by the fluid and the exit temperature of the fluid is higher than the inlet temperature. The highest temperature achieved by microwave heating was 430 $^{\circ}C$ towards the end of the catalyst bed. The numerically predicted temperature was compared the experimental data obtained during microwave pyrolysis runs. The temperature was measured at three different locations in the x-direction along the quartz tube. An IR probe and a thermal camera were used for temperature measurement.

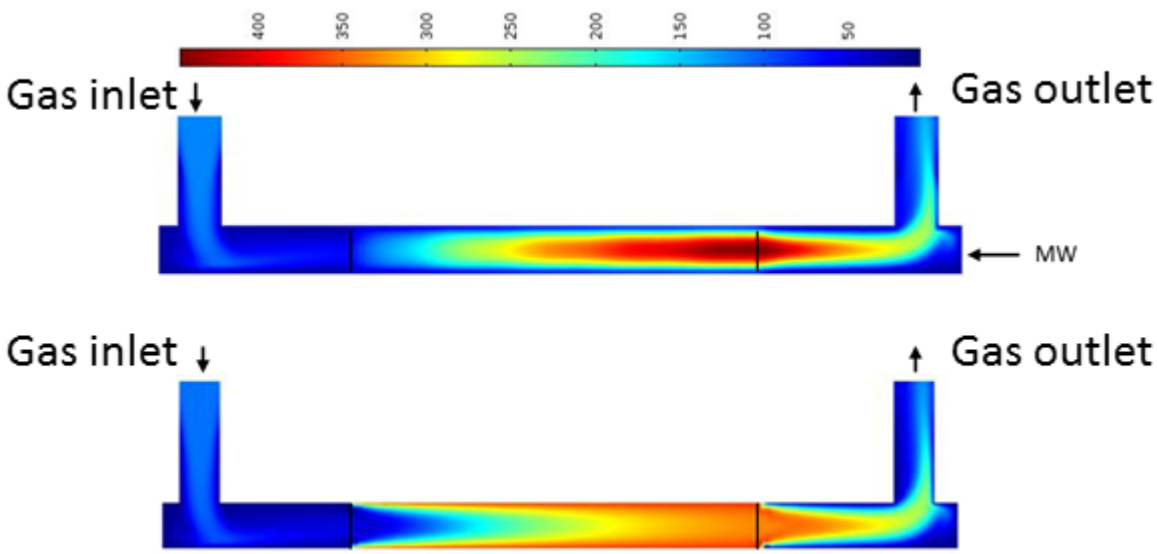

Figure 4.13: Longitudinal (xz-axis) temperature profile for microwave and conventional heating methods

The numerical predictions were within 20% to the experimental temperature results. The numerical model over-predicted the temperature of the catalyst bed. This could be mainly due to average flow rate assumed in the model. In reality, due to gas generation within the system, the flow rate varies in the system over the time. Moreover, other external factors such as convective cooling, local super-heating caused within the microwave field, effect of coke deposition and poisoning of catalyst bed was not precisely modeled.

A steady rise of temperature is observed for both microwave and conventional heating in X-direction **(Figure 4.14)**. The temperature profile in z-direction shows a wall to wall temperature gradient within the catalyst bed for microwave and conventional heating **(Figure 4.15)**. An effect of reaction kinetics should also be modeled for predicting the temperature profiles within the microwave system accurately. The changes in thermal conductivity and other thermodynamic parameters due to formation of new products and intermediates should be accurately modeled for precision.

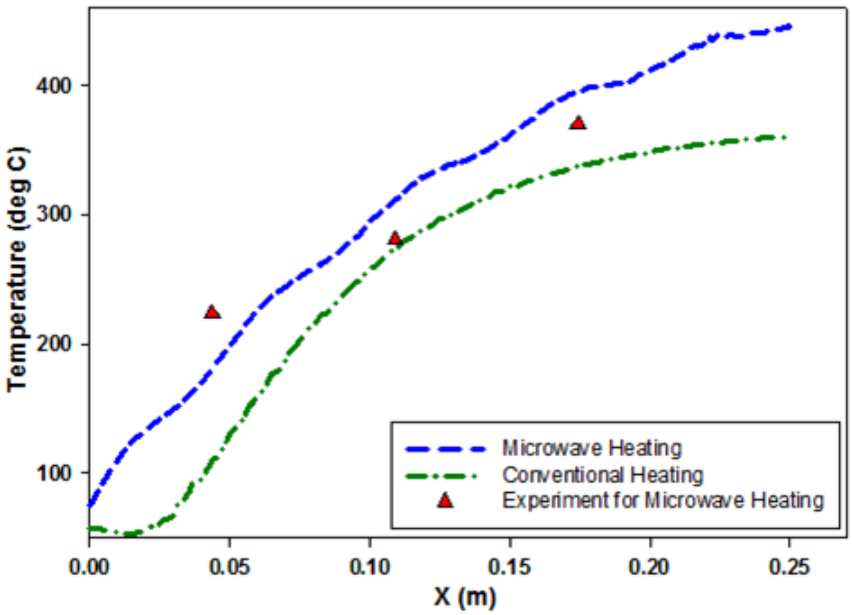

Figure 4.14: Temperature distribution along the centerline in x-axis for microwave heating, conventional heating and experimental data

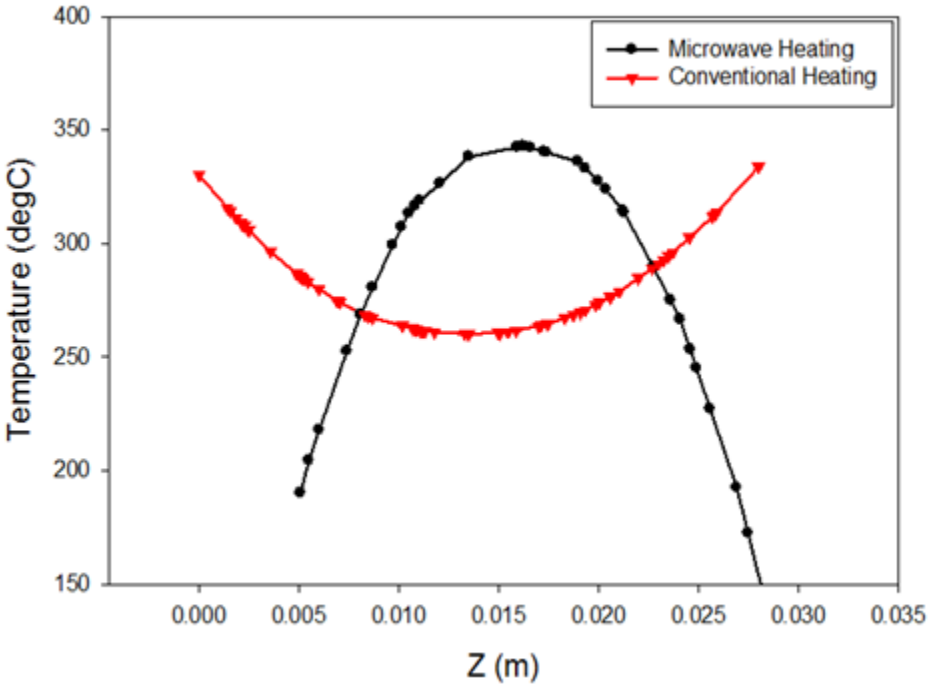

Figure 4.15: Temperature distribution along the centerline in z-axis for microwave heating and conventional heating

4.4.5.1 Velocity profile

The laminar flow was modeled across the porous catalyst bed. The gas inlet velocity was 0.1 m/s. The velocity profile in longitudinal direction (xz- direction) was plotted. The velocity profile was consistent with the boundary conditions. The porous bed was defined as uniformly porous and a drop in velocity was observed in this region. A small recirculation region was also observed at the back ends of the geometry where the vertical tubes meet the horizontal tube. The highest velocity obtained was 0.18 m/s **(Figure 4.16)**.

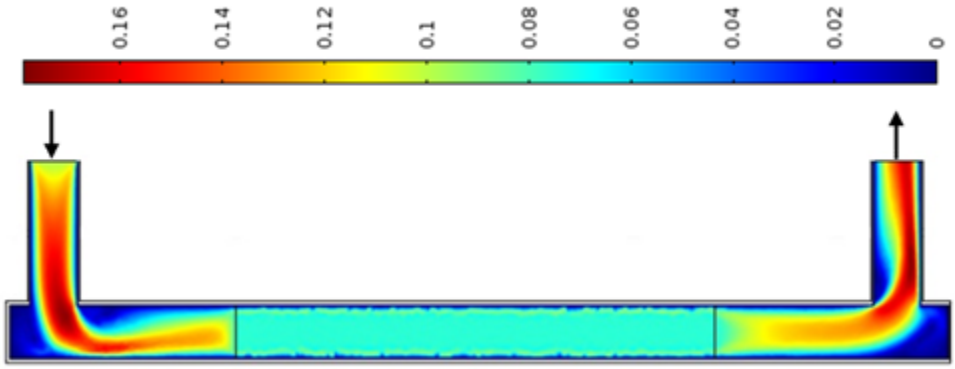

Figure 4.16: Velocity profile along the zx-axis

4.4.6 Effect of tube diameter

Similar to the no flow conditions, when the diameter of the tube was reduced to 0.02 m for narrow tube from 0.028 m for regular tube and the length was increased from 0.25 m to 0.4 m, more uniform temperature distribution was observed **(Figure 4.17)**. The overall temperature was lower for the narrow tube (20 $°C$ to 300 $°C$) compared to that for the bigger diameter shorter tube (20 $°C$ to 390 $°C$). A temperature plot across x axis was plotted for both tubes **(Figure 4.18)**. The temperature within the narrow, long tube increases to 280C in about 0.1 m of the tube length and remains steady at that temperature for the remainder of the length, whereas a steady increase is observed for the shorter tube. The microwaves for the shorter tube absorbed all upfront in the thicker catalyst bed.

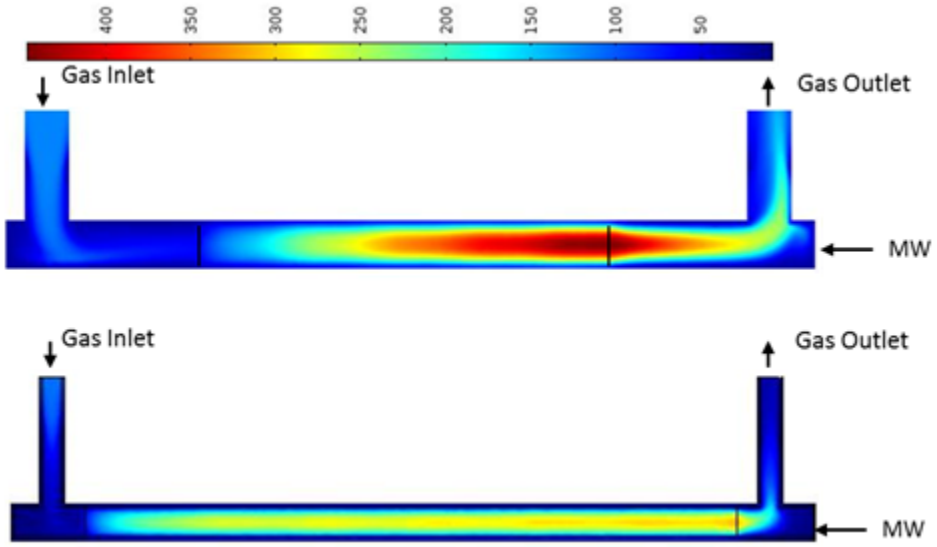

Figure 4.17: Longitudinal (XZ-axis) temperature profile for microwave heated tubes a) regular tube and b) narrow tube

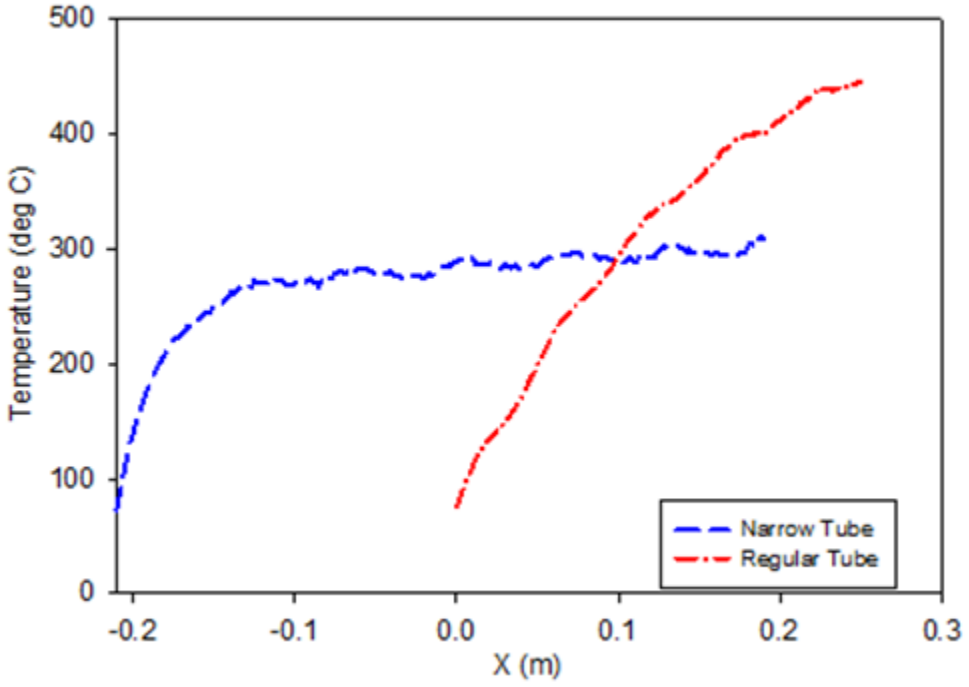

Figure 4.18: Temperature distributions along the centerline in x-axis for microwave heating of regular sized and narrow tube

4.4.7 Effect of sample position

We also studied the effect of position of sample in z-direction (z= 10 mm and 20 mm off center) based on the primary study results. However, there was no change in the temperature distribution for secondary study, mainly because of high inlet gas velocity **(Figure 4.19)**. For inlet gas velocity lower than 0.04 m/s, the effect of position of sample still hold true as established in the primary study. However, as the velocity is increased beyond 0.04 m/s, the temperature distribution changes as some of the heat is swept away by flow contributing to the convective cooling. The effect of shape of sample was not studied for the secondary study as building a brick shaped tube can be practically unfeasible.

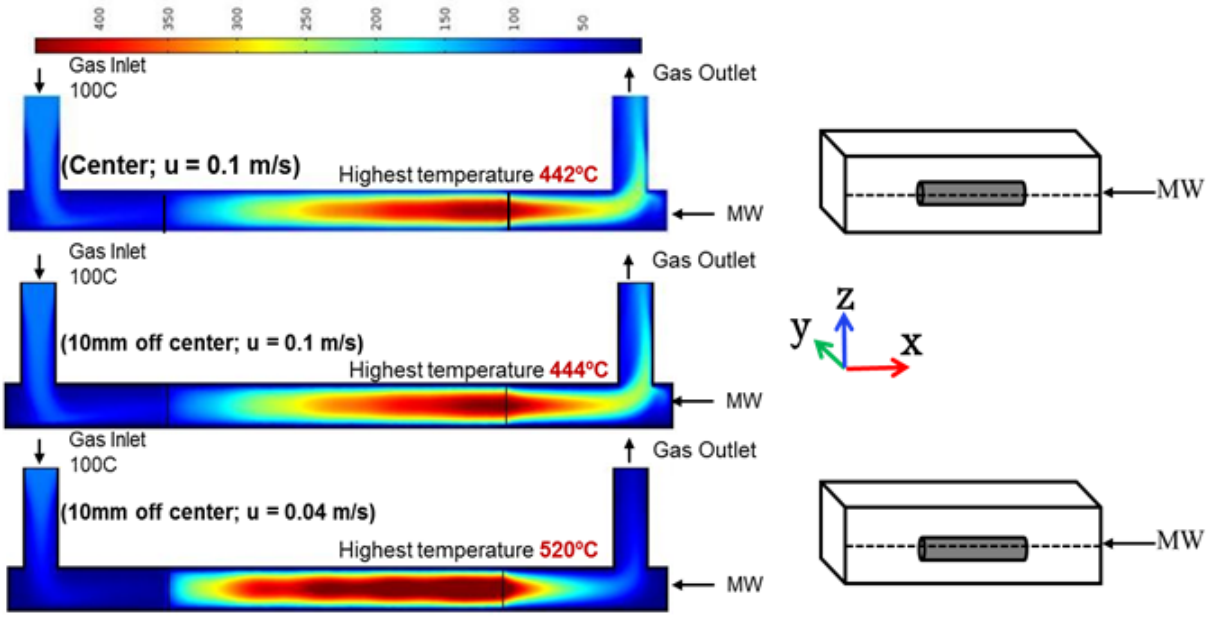

Figure 4.19: Longitudinal (XZ-axis) temperature profile for microwave heated catalyst bed at different locations in z-direction

This study gives a good understanding about the distribution of temperature within the catalyst bed when heated in a microwave reactor.

4.5 Conclusions

A numerical model studying the microwave heating of porous catalyst bed was developed using COMSOL Multiphysics 5.1. The model was validated against the experimental data. The temperature profiles obtained from microwave heating were compared to those obtained from conventional heating. A solid-fluid thermal non-equilibrium condition was modeled as the heat is generated within the catalyst. The experimental results and the predicted temperatures were a good match. Microwave heating had higher total internal energy but conventional heating had lower temperature gradient after reaching steady state. The effect of sample shape, size and position on microwave heating of porous catalyst bed was studied. It was observed that sample position, shape and size of sample all significantly affect the heating profile and temperature gradient inside the sample. Brick shaped sample heats more uniformly compared to cylindrical sample. If the radius of the sample is decreased, while maintaining the volume of the sample, the microwaves penetrate deeper inside the sample, and more uniform heating is observed throughout the length of the sample. The design of the catalyst bed also depends on the ease of operation and manufacturing and the cost efficiency.

Chapter 5
Conclusions and Future Work

5.1 Conclusions

The objective of this study was to develop an efficient catalytic upgrading technique for enhanced biofuel production from pyrolysis of biomass. We investigated the application of advanced electromagnetic heating for pyrolysis and catalytic upgrading. Pyrolysis of pinewood sawdust was carried out at 600 $^{\circ}C$ using radio frequency induction heater. Two separate catalytic reactors were designed for upgrading the pyrolysis vapors exiting the induction heater and their performance was tested against conventional catalytic bed reactor.

The first catalytic reactor was a high frequency induction heating reactor designed to effectively heat the metallic reactor walls. Different reaction parameters were tested for optimization. The ratio of biomass to catalyst was studied and the effect of different catalyst bed temperatures was also investigated. The quality of bio-oil was compared to that obtained without upgrading reaction. It was observed that temperature plays an important role in the quality and yield of product. As the temperature increased, higher concentration of aromatic compounds was obtained but the liquid yield decreased. As the B/C ratio increases, the quality of oil gets better with more aromatic compounds. However, the water content of the bio-oil also increases. Higher gas yield is achieved with higher catalyst bed temperatures. From the catalyst characterization, high coke deposition, lower BET surface area and lower acid sites are observed for conventionally heated catalyst compared to induction heated catalyst which can be attributed to high thermal gradient which causes condensation of molecules on catalyst surface and incomplete reactions due to uneven heating.

The second catalytic reactor was a microwave based reactor operated at a frequency of 2450 MHz and maximum power of 1.2 kW. The catalyst bed was directly heated by the imparted electromagnetic irradiation. Microwave heating was found to be both effective

and energy efficient compared to conventional and induction heating methods. Rate of deterioration of catalyst mainly due to coking was lower for microwave heating process. Higher aromatic hydrocarbon yield, lower oxygen content and high HHV value of bio-oil was obtained by microwave heating of catalyst.

Since microwave based catalytic reactor showed promising results, a numerical model was developed to study the thermal and flow profiles across the catalytic bed and to investigate the effect of size, shape and position of the catalyst bed on microwave heating. Dielectric properties of the HZSM-5 catalyst was measured at different frequencies and temperatures. The model was developed in COMSOL Multiphysics 5.1. The model was validated against the experimental data. The temperature profiles obtained from microwave heating were compared to those obtained from conventional heating. A solid-fluid thermal non-equilibrium condition was modeled as the heat is generated within the catalyst.Microwave heating had higher total internal energy but conventional heating had lower temperature gradient after reaching steady state. The effect of sample shape, size and position on microwave heating of porous catalyst bed was significant for microwave heating method. A smaller diameter cylindrical sample heated more uniformly as the microwaves penetrate deeper inside the sample. The experimental results were in good agreement with the predicted temperatures.

5.2 Future Work

The study compares the performance of a novel electromagnetic heating technique with conventional catalytic reactors. Preliminary bench scale studies show that the microwave reactor is more energy efficient as well as effective in production of higher grade biofuel as it increases the overall rate of reaction.In principle, this heating technique can be used for thermo-catalytic reactions not limited to pyrolysis, provided the catalyst is a dielectric material. However further studies should be carried out to test this reactor at a pilot scale. Full capacity of the reactor is yet to be completely realized, however, it holds a potential to improve the catalyst heating efficiency and should be further studied for scale up applications.

The numerical studies presented here should also be expanded to include reaction kinetics for product selectivity. Addition of reaction kinetics to the model will help in obtaining the optimum operation temperatures. The effect of geometry of the waveguide should also be studied to optimize the performance of the reactor. Microwave reactors holds a promise for energy efficient production of high quality bio-oil from pyrolysis of biomass so as to replace petroleum fuel in the future.

Bibliography

Judit Adam, Marianne Blazsa, Erika Maszaros, Michael Stacker, Merete H. Nilsen, Aud Bouzga, Johan E. Hustad, Morten Granli, and Gisle Aye. Pyrolysis of biomass in the presence of al-mcm-41 type catalysts. *Fuel*, 84(1213):1494–1502, 2005.

J. D. Adjaye and N. N. Bakhshi. Production of hydrocarbons by catalytic upgrading of a fast pyrolysis bio-oil. part ii: Comparative catalyst performance and reaction pathways. *Fuel Processing Technology*, 45(3):185–202, 1995.

Roberto Aguado, Martin Olazar, Mara Jos San Jos, Gorka Aguirre, and Javier Bilbao. Pyrolysis of sawdust in a conical spouted bed reactor. yields and product composition. *Industrial & Engineering Chemistry Research*, 39(6):1925–1933, 2000.

S. Al-Khattaf, C. D'Agostino, M. N. Akhtar, N. Al-Yassir, N. Y. Tan, and L. F. Gladden. The effect of coke deposition on the activity and selectivity of the hzsm-5 zeolite during ethylbenzene alkylation reaction in the presence of ethanol. *Catalysis Science & Technology*, 4(4):1017–1027, 2014.

B. Alazmi and K. Vafai. Analysis of variants within the porous media transport models. *Journal of Heat Transfer*, 122(2):303–326, 1999. 10.1115/1.521468.

M. Amutio, G. Lopez, M. Artetxe, G. Elordi, M. Olazar, and J. Bilbao. Influence of temperature on biomass pyrolysis in a conical spouted bed reactor. *Resources, Conservation and Recycling*, 59(0):23–31, 2012.

W. G. Appleby, J. W. Gibson, and G. M. Good. Coke formation in catalytic cracking. *Industrial & Engineering Chemistry Process Design and Development*, 1(2):102–110, 1962.

A. Bejan. *Convection heat transfer*. John Wiley & Sons, Incorporated, 1995. ISBN 9780471579724.

Longli Bo, Jianbo Liao, Yucai Zhang, Xiaohui Wang, and Quan Yang. Cuo/zeolite catalyzed oxidation of gaseous toluene under microwave heating. *Frontiers of Environmental Science & Engineering*, 7(3):395–402, 2013.

Vasily A. Bolotov, Evgeny I. Udalov, Valentin N. Parmon, Yuriy Yu Tanashev, and Yuriy D. Chernousov. Pyrolysis of heavy hydrocarbons under microwave heating of catalysts and adsorbents. *The Journal of microwave power and electromagnetic energy : a publication of the International Microwave Power Institute*, 46(1):39–46, 2012.

Fernanda Cabral Borges, Zhenyi Du, Qinglong Xie, Jorge Otvio Trierweiler, Yanling Cheng, Yiqin Wan, Yuhuan Liu, Rongbi Zhu, Xiangyang Lin, Paul Chen, and Roger Ruan. Fast microwave assisted pyrolysis of biomass using microwave absorbent. *Bioresource Technology*, 156(0):267–274, 2014.

A. V. Bridgwater. Review of fast pyrolysis of biomass and product upgrading. *Biomass and Bioenergy*, 38(0):68–94, 2012.

A. V. Bridgwater, D. Meier, and D. Radlein. An overview of fast pyrolysis of biomass. *Organic Geochemistry*, 30(12):1479–1493, 1999.

David George Briggs. *Forest Products Measurements and Conversion Factors: with special emphasis on the US Pacific Northwest*. College of Forest Resources, University of Washington, 1994. ISBN 9994995685.

Waraporn Cha-um, Phadungsak Rattanadecho, and Watit Pakdee. Experimental analysis of microwave heating of dielectric materials using a rectangular wave guide (mode: Te10) (case study: Water layer and saturated porous medium). *Experimental Thermal and Fluid Science*, 33(3):472–481, 2009.

Wei-Hsin Chen, Hong-Jyu Liou, and Chen-I. Hung. A numerical approach of interaction of methane thermocatalytic decomposition and microwave irradiation. *International Journal of Hydrogen Energy*, 38(30):13260–13271, 2013.

D. Chiaramonti, M. Bonini, E. Fratini, G. Tondi, K. Gartner, A. V. Bridgwater, H. P. Grimm, I. Soldaini, A. Webster, and P. Baglioni. Development of emulsions from biomass pyrolysis liquid and diesel and their use in enginespart 1 : emulsion production. *Biomass and Bioenergy*, 25(1):85–99, 2003.

A. Cimino, D. Gazzoli, and M. Valigi. Xps quantitative analysis and models of supported oxide catalysts. *Journal of Electron Spectroscopy and Related Phenomena*, 104(13):1–29, 1999.

S. Czernik and A. V. Bridgwater. Overview of applications of biomass fast pyrolysis oil. *Energy & Fuels*, 18(2):590–598, 2004.

Vineet Rakesh Datta A. and Ashim K. Coupled electromagnetics- multiphase porous media model for microwave combination heating. *Excerpt from the Proceedings of the COMSOL Conference Boston 2008*, 2008.

Ayhan Demirba. Turkey's geothermal energy potential. *Energy Sources*, 24(12):1107–1115, 2002.

A. Demirbas. Relationship between initial moisture content and the liquid yield from pyrolysis of sawdust. *Energy Sources, Part A: Recovery, Utilization, and Environmental Effects*, 27(9):823, 2005.

D. C. Elliott and G. G. Neuenschwander. *Liquid Fuels by Low-Severity Hydrotreating of Biocrude*, book section 48, pages 611–621. Springer Netherlands, 1997. ISBN 978-94-010-7196-3.

Yolanda Fernandez, Ana Arenillas, and J. Angel Menendez. *Microwave Heating Applied to Pyrolysis, Advances in Induction and Microwave Heating of Mineral and Organic Materials, Stanislaw Grundas (Ed.), ISBN: 978-953-307-522-8, InTech*, volume 31. 2011.

Andrew J. Foster, Jungho Jae, Yu-Ting Cheng, George W. Huber, and Raul F. Lobo. Optimizing the aromatic yield and distribution from catalytic fast pyrolysis of biomass over zsm-5. *Applied Catalysis A: General*, 423424:154–161, 2012.

Yuichi Funawatashi and Tateyuki Suzuki. Numerical analysis of microwave heating of a dielectric. *Heat Transfer Asian Research*, 32(3):227–236, 2003.

C. Gabriel, S. Gabriel, E. H. Grant, B. S. J. Halstead, and D. M. P. Mingos. Dielectric parameters relevant to microwave dielectric heating. *Chemical Society Reviews*, 27(3): 213–223, 1998.

Peter E Glaser. Power from the sun: its future. *Science*, 162(3856):857–861, 1968.

S. Gopalakrishnan, J. Mnch, R. Herrmann, and W. Schwieger. Effects of microwave radiation on one-step oxidation of benzene to phenol with nitrous oxide over fe-zsm-5 catalyst. *Chemical Engineering Journal*, 120(1):99–105, 2006.

M. Guisnet and P. Magnoux. Organic chemistry of coke formation. *Applied Catalysis A: General*, 212(12):83–96, 2001.

D. Handley and P. J. Heggs. Momentum and heat transfer mechanisms in regular shaped packings. *Transactions of the Institution of Chemical Engineers and the Chemical Engineer*, 46(9):T251–&, 1968.

C. Henkel. *A Study of Induction Pyrolysis of Lignocellulosic Biomass for the Production of Bio-oil*. Thesis, 2014.

A.R.V. Hippel. *Dielectric materials and applications: papers by twenty-two contributors*. published jointly by the Technology Press of M.I.T. and Wiley, 1954.

Michio Ikura, Maria Stanciulescu, and Ed Hogan. Emulsification of pyrolysis derived bio-oil in diesel fuel. *Biomass and Bioenergy*, 24(3):221–232, 2003.

C. Inoue, Y. Hagura, M. Ishikawa, and K. Suzuki. The dielectric property of soybean oil in deep-fat frying and the effect of frequency. *Journal of Food Science*, 67(3):1126–1129, 2002.

ASTM International. *Standard Test Method for Heat of Combustion of Liquid Hydrocarbon Fuels by Bomb Calorimeter*. 2009.

M. S. Ioffe, S. D. Pollington, and J. K. S. Wan. High-power pulsed radio-frequency and microwave catalytic processes: Selective production of acetylene from the reaction of methane over carbon. *Journal of Catalysis*, 151(2):349–355, 1995.

Jungho Jae, Robert Coolman, T. J. Mountziaris, and George W. Huber. Catalytic fast pyrolysis of lignocellulosic biomass in a process development unit with continual catalyst addition and removal. *Chemical Engineering Science*, 108:33–46, 2014.

Pranav U. Karanjkar, Robert J. Coolman, George W. Huber, Michael T. Blatnik, Saba Almalkie, Stephen M. de Bruyn Kops, Triantafillos J. Mountziaris, and William C. Conner. Production of aromatics by catalytic fast pyrolysis of cellulose in a bubbling fluidized bed reactor. *AIChE Journal*, 60(4):1320–1335, 2014.

Rajesh Karki and Roy Billinton. Cost-effective wind energy utilization for reliable power supply. *Energy Conversion, IEEE Transactions on*, 19(2):435–440, 2004.

Sridhar Komarneni and Rustum Roy. Anomalous microwave melting of zeolites. *Materials Letters*, 4(2):107–110, 1986.

Su Shiung Lam and Howard A. Chase. A review on waste to energy processes using microwave pyrolysis. *Energies (19961073)*, 5(10):4209–4232, 2012.

Mohammad Latifi, Franco Berruti, and Cedric Briens. A novel fluidized and induction heated microreactor for catalyst testing. *AIChE Journal*, 60(9):3107–3122, 2014.

Ki-Yong Lee, Min-Young Kang, and Son-Ki Ihm. Deactivation by coke deposition on the hzsm-5 catalysts in the methanol-to-hydrocarbon conversion. *Journal of Physics and Chemistry of Solids*, 73(12):1542–1545, 2012.

P. Lidstrom, J. Tierney, B. Wathey, and J. Westman. Microwave assisted organic synthesis - a review. *Tetrahedron*, 57(45):9225–9283, 2001.

Xiuying Lin, Yu Fan, Gang Shi, Haiyan Liu, and Xiaojun Bao. Coking and deactivation behavior of hzsm-5 zeolite-based fcc gasoline hydro-upgrading catalyst. *Energy & Fuels*, 21(5):2517–2524, 2007.

Oscar Lucia, Pascal Maussion, Enrique J. Dede, and Jose M. Burdio. Induction heating technology and its applications: Past developments, current technology, and future challenges. *IEEE Transactions on Industrial Electronics*, 61(5):2509–2520, 2014.

Peter McKendry. Energy production from biomass: overview of biomass conversion technologies. *Bioresource Technology*, 83(1):37–46, 2002.

J. A. Menendez, J. Andez, A. Domanguez, Y. Fernandez, and J. J. Pis. Evidence of self-gasification during the microwave-induced pyrolysis of coffee hulls. *Energy & Fuels*, 21(1): 373–378, 2007.

A. C. Metaxas and R. J. Meredith. *Industrial Microwave Heating*. P. Peregrinus, 1983. ISBN 9780906048894.

W. J. Minkowycz, A. Haji-Sheikh, and K. Vafai. On departure from local thermal equilibrium in porous media due to a rapidly changing heat source: the sparrow number. *International Journal of Heat and Mass Transfer*, 42(18):3373–3385, 1999.

F. Motasemi and Muhammad T. Afzal. A review on the microwave-assisted pyrolysis technique. *Renewable and Sustainable Energy Reviews*, 28(0):317–330, 2013.

A. S. Mujumdar. *Handbook of industrial drying*. CRC/Taylor & Francis, 2007. ISBN 9781574446685.

Charles A. Mullen and Akwasi A. Boateng. Catalytic pyrolysis-gc/ms of lignin from several sources. *Fuel Processing Technology*, 91(11):1446–1458, 2010.

Charles A. Mullen, Akwasi A. Boateng, Neil M. Goldberg, Isabel M. Lima, David A. Laird, and Kevin B. Hicks. Bio-oil and bio-char production from corn cobs and stover by fast pyrolysis. *Biomass and Bioenergy*, 34(1):67–74, 2010.

S. O. Nelson. Electrical properties of agricultural products - critical review. *Transactions of the Asae*, 16(2):384–400, 1973.

S. O. Nelson. Correlating dielectric properties of solids and particulate samples through mixture relationships. *Transactions of the Asae*, 35(2):625–629, 1992.

T. S. Nguyen, M. Zabeti, L. Lefferts, G. Brem, and K. Seshan. Catalytic upgrading of biomass pyrolysis vapours using faujasite zeolite catalysts. *Biomass and Bioenergy*, 48(0): 100–110, 2013.

Tatsuo Ohgushi, Sridhar Komarneni, and AmarS Bhalla. Mechanism of microwave heating of zeolite a. *Journal of Porous Materials*, 8(1):23–35, 2001.

Annual Energy Outlook et al. Energy information administration annual energy review, 2011.

K. K. Abdollahi D. Boldor P. D. Muley, C. Henkel. Pyrolysis and catalyti upgrading of pinewood sawdust using induction heating reactor - unpublished manuscript submitted to journal. 2015.

Boontham Paweewan, Patrick J. Barrie, and Lynn F. Gladden. Coking and deactivation during n-hexane cracking in ultrastable zeolite y. *Applied Catalysis A: General*, 185(2): 259–268, 1999.

Robert D Perlack, Laurence M Eaton, Anthony F Turhollow Jr, Matt H Langholtz, Craig C Brandt, Mark E Downing, Robin L Graham, Lynn L Wright, Jacob M Kavkewitz, Anna M Shamey, et al. Us billion-ton update: biomass supply for a bioenergy and bioproducts industry, 2011.

W. Lee Perry, Abhaya K. Datye, Anil K. Prinja, Lee F. Brown, and Joel D. Katz. Microwave heating of endothermic catalytic reactions: Reforming of methanol. *AIChE Journal*, 48 (4):820–831, 2002.

Zhang Qi, Chang Jie, Wang Tiejun, and Xu Ying. Review of biomass pyrolysis oil properties and upgrading research. *Energy Conversion and Management*, 48:87–92, 2007.

J. Reub, D. Bathen, and H. Schmidt-Traub. Desorption by microwaves: Mechanisms of multicomponent mixtures. *Chemical Engineering & Technology*, 25(4):381–384, 2002.

Frederik Ronsse, Sven van Hecke, Dane Dickinson, and Wolter Prins. Production and characterization of slow pyrolysis biochar: influence of feedstock type and pyrolysis conditions. *GCB Bioenergy*, 5(2):104–115, 2013.

Marcelo B. Saito and Marcelo J. S. de Lemos. A correlation for interfacial heat transfer coefficient for turbulent flow over an array of square rods. *Journal of Heat Transfer*, 128 (5):444–452, 2005. 10.1115/1.2175150.

B. Scholze and D. Meier. Characterization of the water-insoluble fraction from pyrolysis oil (pyrolytic lignin). part i. py–gc/ms, ftir, and functional groups. *Journal of Analytical and Applied Pyrolysis*, 60(1):41–54, 2001.

Dong Kyun Seo, Sang Shin Park, Jungho Hwang, and Tae-U. Yu. Study of the pyrolysis of biomass using thermo-gravimetric analysis (tga) and concentration measurements of the evolved species. *Journal of Analytical and Applied Pyrolysis*, 89(1):66–73, 2010.

F. Shafizadeh. Introduction to pyrolysis of biomass. *Journal of Analytical and Applied Pyrolysis*, 3(4):283–305, 1982.

J. S. Smith and Y. H. Hui. *Food processing: principles and applications*. Blackwell Pub., 2004. ISBN 9780813819426.

S. Stefanidis, K. Kalogiannis, E. F. Iliopoulou, A. A. Lappas, J. Martinez Triguero, M. T. Navarro, A. Chica, and F. Rey. Mesopore-modified mordenites as catalysts for catalytic pyrolysis of biomass and cracking of vacuum gasoil processes. *Green Chemistry*, 15(6): 1647–1658, 2013.

BeatriceG Terigar, Sundar Balasubramanian, and Dorin Boldor. Effect of storage conditions on the oil quality of chinese tallow tree seeds. *Journal of the American Oil Chemists' Society*, 87(5):573–582, 2010.

W. T. Tsai, M. K. Lee, and Y. M. Chang. Fast pyrolysis of rice husk: Product yields and compositions. *Bioresource Technology*, 98(1):22–28, 2006a.

W. T. Tsai, M. K. Lee, and Y. M. Chang. Fast pyrolysis of rice straw, sugarcane bagasse and coconut shell in an induction-heating reactor. *Journal of Analytical and Applied Pyrolysis*, 76(12):230–237, 2006b.

Wen-Tien Tsai, Mei-Kuei Lee, Jeng-Hung Chang, Ting-Yi Su, and Yuan-Ming Chang. Characterization of bio-oil from induction-heating pyrolysis of food-processing sewage sludges using chromatographic analysis. *Bioresource Technology*, 100(9):2650–2654, 2009a.

Wen-Tien Tsai, Hsiao-Hsuan Mi, Jeng-Hung Chang, and Yuan-Ming Chang. Levels of polycyclic aromatic hydrocarbons in the bio-oils from induction-heating pyrolysis of food-processing sewage sludges. *Journal of Analytical & Applied Pyrolysis*, 86(2):364–368, 2009b.

P. Salagnac V. Nicolas, P. Glouannec , V. Jury , L. Boillereaux , and J.P. Ploteau . Modeling heat and mass transfer in bread during baking. *Excerpt from the Proceedings of the COMSOL Conference 2010 Paris*, 2010.

R. Vadivambal and D. S. Jayas. Non-uniform temperature distribution during microwave heating of food materialsa review. *Food and Bioprocess Technology*, 3(2):161–171, 2010.

R. S. Vilayannur, V. M. Puri, and R. C. Anantheswaran. Size and shape effect on nonuniformity of temperature and moisture distributions in microwave heated food materials: Part i simulation. *Journal of Food Process Engineering*, 21(3):209–233, 1998.

B. Viswanathan and C.N. Pillai. *Recent Developments in Catalysis: Theory and Practice*. Editions Technip, 1992. ISBN 9782710806264.

Yiqin Wan, Paul Chen, Bo Zhang, Changyang Yang, Yuhuan Liu, Xiangyang Lin, and Roger Ruan. Microwave-assisted pyrolysis of biomass: Catalysts to improve product selectivity. *Journal of Analytical and Applied Pyrolysis*, 86(1):161–167, 2009.

D.E. Woodmansee, P.J. Caliendo, and A.P. Shapiro. Batch system for microwave desorption of adsorbents, 1995.

Qinglong Xie, Fernanda Cabral Borges, Yanling Cheng, Yiqin Wan, Yun Li, Xiangyang Lin, Yuhuan Liu, Fida Hussain, Paul Chen, and Roger Ruan. Fast microwave-assisted catalytic gasification of biomass for syngas production and tar removal. *Bioresource Technology*, 156(0):291–296, 2014.

Linghong Zhang, Chunbao Xu, and Pascale Champagne. Overview of recent advances in thermo-chemical conversion of biomass. *Energy Conversion and Management*, 51(5):969–982, 2010. (Charles).

Qi Zhang, Jie Chang, Wang, and Ying Xu. Upgrading bio-oil over different solid catalysts. *Energy & Fuels*, 20(6):2717–2720, 2006.

Qi Zhang, Jie Chang, Tiejun Wang, and Ying Xu. Review of biomass pyrolysis oil properties and upgrading research. *Energy Conversion and Management*, 48(1):87–92, 2007.

Suping Zhang, Yongjie Yan, Tingchen Li, and Zhengwei Ren. Upgrading of liquid fuel from the pyrolysis of biomass. *Bioresource Technology*, 96(5):545–550, 2005.

Y. C. Zhang, L. L. Bo, X. H. Wang, H. N. Liu, and H. Zhang. Study on catalytic oxidation of benzene by microwave heating. *Huan Jing Ke Xue*, 33(8):2759–65, 2012. Zhang, Yu-cai Bo, Long-li Wang, Xiao-hui Liu, Hai-nan Zhang, Hao English Abstract Journal Article Research Support, Non-U.S. Gov't China Huan Jing Ke Xue. 2012 Aug;33(8):2759-65.

Rui Zhou, Hanwu Lei, and James Julson. The effects of pyrolytic conditions on microwave pyrolysis of prairie cordgrass and kinetics. *Journal of Analytical and Applied Pyrolysis*, 101(0):172–176, 2013.

Appendix A
Chapter 2: Comparison of bio-oil properties obtained from conventional and induction catalyst bed reactor

Property	Conventional heating		Induction heating	
	% Composition		% Composition	
	Run 1	Run 2	Run 1	Run 2
Char	21.33±1.20	20.43±0.85	21.13±1.74	21.37±1.65
Gas	43.13±2.01	40.18±1.89	47.84±1.23	39.14±1.52
Water	21.08±0.74	20.23±0.52	17.47±1.61	24.21±1.33
Bio-oil	10.37±0.44	13.11±0.86	9.76±1.38	12.92±0.75
Coke	4.09±1.01	6.05±0.96	3.80±1.03	2.36±0.39
Total	100	100	100	100
CHN analysis of liquid fraction				
Carbon	62.35±0.54	60.33±0.54	65.8±0.20	61.49±0.2
Hydrogen	3.004±0.20	3.35±1.27	2.067±0.07	1.57±0.10
Nitrogen	traces			
Oxygen[1]	34.64±0.7	36.32±0.75	32.13±0.52	36.94±1.2
Total	100	100	100	100
Temperature 330 $^{\circ}C$				
Char	20.93±1.53	22.7±1.66	20.17±2.0	21.97±1.33
Gas	44.3±2.03	40.73±3.02	41.76±1.68	39.93±1.00
Water	20.29±1.26	17.59±1.52	15.65±1.11	21.36±1.06
Bio-oil	10.44±0.96	15.48±1.02	21.29±1.07	14.08±1.03
Coke	4.04±0.92	3.50±0.8	1.13±0.64	2.66±0.32
Total	100	100	100	100
CHN analysis of liquid fraction				
Carbon	69.18±1.49	62.82±0.39	67.2±0.4	66.711.1
Hydrogen	3.15±0.53	3.65±0.84	2.88±0.4	2.13±0.7

[1]Determined by difference

Nitrogen		traces		
Oxygen[2]	27.67±2.14	33.52±2.33	30.92±0.77	31.16±0.74
Total	100	100	100	100
Temperature 370 $^{\circ}C$				
Char	22.7±1.85	23.57±2.0	19.87±1.06	21.4±1.05
Gas	45.56±1.57	46.56±1.43	48.40±1.26	44.72±1.09
Water	19.41±0.97	15.37±0.68	20.21±1.01	18.41±1.07
Bio-oil	9.91±1.02	11.00±0.78	9.69±1.02	13.72±0.99
Coke	2.42±0.01	3.50±0.23	1.83±0.26	1.75±0.25
Total	100	100	100	100
CHN analysis of liquid fraction				
Carbon	69.16±0.01	68.41±0.62	69.46±0.1	65.4±0.8
Hydrogen	69.16±0.01	68.41±0.62	69.46±0.1	65.4±0.8
Nitrogen		traces		
Oxygen[3]	28.38±1.98	27.66±1.38	28.6±0.34	31.97±0.8
Total	100	100	100	100

[2]Determined by difference
[3]Determined by difference

Appendix B
List of Symbols

A	pre-exponential factor s-1
α	spread of relaxation times $\alpha \in [0, 1]$
B	magnetic flux density $V - s$
c	speed of light in vacuum m/s
C_p	specific heat J/kgK
D	electric displacement C/m^2
D_p	penetration depth m
δ	loss angle
E	electric field intensity V/m
E_a	activation energy $kj/mole$
ε'	relative dielectric constant S/m
ε''	relative dielectric loss factor
ε	complex relative permittivity
ε_∞'	relative dielectric constant as $\omega \to \infty$
ε'_s	relative static dielectric constant (at $\omega = 0$)
ε'_0	dielectric constant of the vacuum ($value = 8.85410^12S/m$)
F	force; N
f	frequency Hz
g	acceleration due to gravity m/s^2
H	magnetic field intensity A/m
J	electric current A
k	rate constant
K	thermal conductivity W/mK
k_b	Boltzmanns constant $1.3806504x10 - 23J/K$
λ	wavelength m
λ_0	wavelength in free space m
μ	viscosity Pas
μ'	relative permeability of material H/m
μ_0	magnetic permeability of material $4\pi \times 10^-7N/A^2$
P	pressure Pa

P_{abs}	power absorbed W/m^3
Q_{gen}	power generated W/m^3
R	gas constant $8.314 J/mole.K$
r	radius m
ρ	electric charge density
ρ_m	density of material kg/m^3
σ	conductivity S/m
σ_e	electrical conductivity S/m
T	absolute temperature $^\circ K$
t	time s
τ	relaxation time s
u	fluid velocity m/s
v_2	volume fraction of dispersed phase
ω	angular frequency rad/sec

Vita

Pranjali D. Muley was born in India. She received her Bachelor of Technology degree in Petrochemical Engineering from Dr. Babasaheb Ambedkar Technological University, India and M.S from Louisiana State University in 2012. She is expected to receive her PhD in December 2015 from Louisiana State University.